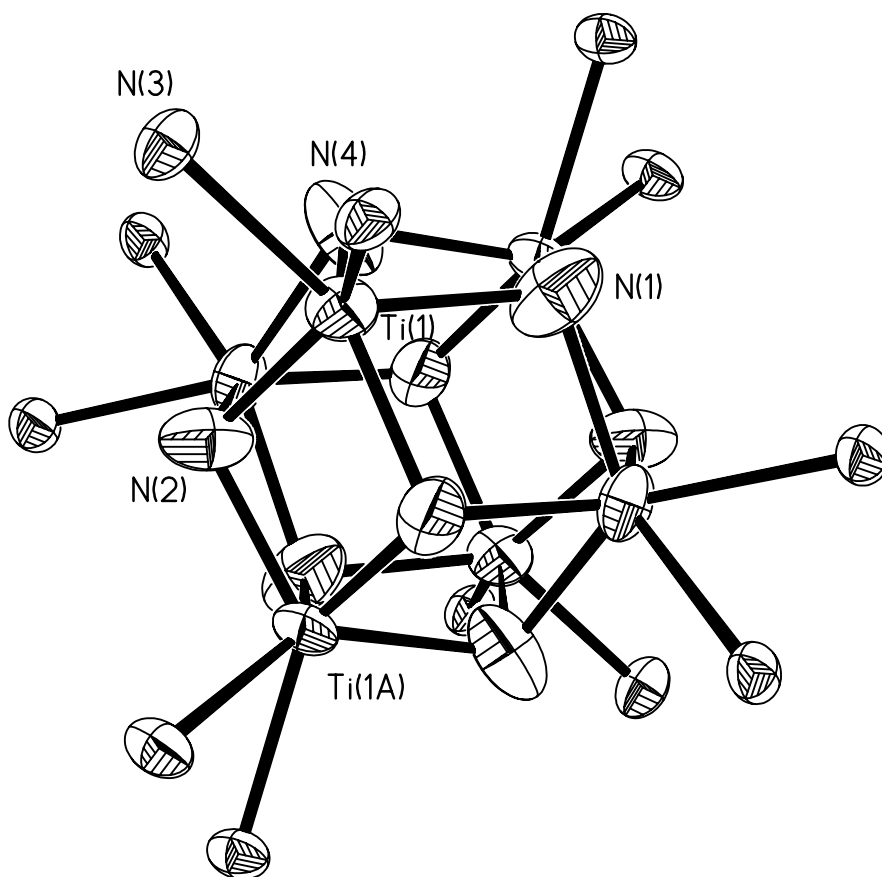Guangcai Bai

New Methods for the Syntheses of Amido, Imido, Nitrido and Dinitrogen Metal Complexes and Organometallic Hydrides and Oxides

New Methods for the Syntheses of Amido, Imido, Nitrido and Dinitrogen Metal Complexes and Organometallic Hydrides and Oxides

Dissertation

zur Erlangung des Doktorgrades

der Mathematisch-Naturwissenschaftlichen Fakultäten

der Georg-August-Universität zu Göttingen

vorgelegt von

Guangcai Bai

aus Guangdong (China)

Göttingen 2001

D 7

Dedicated to my parents,
my wife and son
for their love and affection

Acknowledgement

Abbreviations

Ar	2,6-di-*iso*-propylphenyl
Ar′	4-*tert*-butylphenyl
av	average
b	bridging
br	broad
*t*Bu	*tert*-butyl
C	Celsius
calcd	calculated
Cp	cyclopentadienyl
Cp′	cyclopentadienyl ligands with various substituents
Cp*	pentamethylcyclopentadienyl
d	doublet
dec	decomposition
δ	chemical shift
EI	electron impact ionization
eq(s)	equation(s)
equiv(s)	equivalent(s)
Et	ethyl
EtMe$_4$C$_5$	ethyltetramethylcyclopentadienyl
extr	extract
IR	infrared
J	coupling constant
h	hour(s)
η	hapto
Hz	Hertz
λ	wavelength
L	bis(*tert*-butylamido)cyclodiphosph(III)azane
L′	N,N′-bis(trimethylsilyl)-*p*-toluamidinato
L″	N,N′-bis(trimethylsilyl)benzamidinato

liq	liquid
M	metal
M^+	molecular ion
m	multiplet
m/z	mass/charge
Me	methyl
MeC_5H_4	methylcyclopentadienyl
mes	mesitylene or 2,4, 6-trimethylphenyl
mp	melting point
MS	mass spectrometry
μ	bridging
NMR	nuclear magnetic resonance
$\tilde{\nu}$	wave number
Ph	phenyl
ppm	parts per million
*i*Pr	*iso*-propyl
q	quartet
R	organic substituents
RT	room temperature
s	singlet
t	triplet
t	terminal
tert	tertiary
THF	tetrahydrofuran
Z	number of molecules in the unit cell

1. Introduction

1.1. Reactions of Alkali Metal Ammonia Solutions with Metal Compounds

The first investigations of sodium and potassium ammonia solutions were carried out by Weyl[1] over a century ago. He postulated that such solutions could be regarded as combinations of metal with ammonia and called them 'metal ammoniums'. In 1908, Kraus[2] suggested that alkali metals dissolved in ammonia give solvated cations and solvated electrons, the latter being responsible for the intense blue color of the solutions.

In very dilute solutions, there is complete dissociation to give alkali metal cations and electrons both of which are solvated by ammonia molecules (Scheme 1). It is common to regard the electron to exist in a cavity in the ammonia, loosely solvated by the surrounding molecules.[3]

$$M(s) \xrightleftharpoons[\text{in } NH_3]{\text{dissolve}} M(NH_3)_x \xrightleftharpoons{} [M(NH_3)_y]^+ + [e(NH_3)_z]^-$$
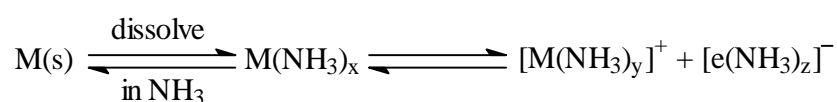
Scheme 1

At higher concentrations, there are insufficient solvent molecules to coordinate both the metal ions and the electrons. Solvated electrons begin to pair up and are removed by the formation of solvated alkalide anions (Scheme 2).

$$M(NH_3)_x + [e(NH_3)_z]^- \xrightleftharpoons{} [M(NH_3)_m]^-$$
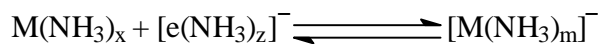
Scheme 2

These bronze solutions have properties which are consistent with a model describing the solution as a 'dilute metal' or 'alloy' in which the electrons behave essentially as in a metal, but the metal atoms have been moved apart by interspersed molecules of ammonia.

Alkali metal ammonia solutions are stable over long periods of time, but decomposition to hydrogen and metal amide occurs slowly if impurities are present but rapidly with suitable catalysts such as transition metals (Scheme 3).

$$[e(NH_3)_z]^- \underset{}{\overset{cat}{\rightleftharpoons}} NH_2^- + 1/2\ H_2 + (z-1)\ NH_3$$

Scheme 3

In view of the powerful reducing properties of metal ammonia solutions, they are often regarded as convenient electron producing reagents and have been used extensively for the reduction of inorganic and organic compounds.[4]

The reactions of many ionic metal salts (e.g. CuI,[5] InI$_3$, GaI$_3$,[6] AgBr,[7] Pt(NH$_3$)$_4$Br$_2$,[8] and [Ir(NH$_3$)$_5$Br]Br$_2$[9]) with solutions of alkali metals in liquid ammonia typically result in rapid reduction to the elements, in some cases the metals react with excess alkali metal to form insoluble intermetallic compounds (e. g. NaZn$_4$, NaCd, Na$_4$Sn[10] and NaAu[5]).

In reactions of the more ionic transition metal halides with alkali metal ammonia solutions, the finely divided metal initially produced is almost invariably an excellent catalyst for the decomposition of the alkali metal ammonia solutions yielding alkali amides, the final products from these reactions contain varying amounts of transition metal amides, imides and/or nitrides. The reduction of nickel(II) bromide with ammonia solutions of potassium results in the formation of elemental nickel, nickel(II) amide diammoniacate, and one or more potassium containing products.[11] Similarly, the reactions of iron(II) bromide with potassium in liquid ammonia leads to the formation of elemental iron, iron(I) nitride, and one or more amide products.[12] The dihalides of manganese[13] and cobalt[14] are reduced to the metallic state by solutions of potassium in ammonia, although the metals are normally contaminated by amide.

The effect of the alkali metal ammonia solutions on the more covalent transition metal compounds leads to ammonolysis with the formation of metal amido or imido complexes. These products are amphoteric so that the ultimate product is a alkali metal salt. The reduction of vanadium(III) bromide with potassium ammonia solution results in the formation of the

imidovanadate(III) (V(NH)(NK)).[15] Indeed, the same product would be obtained if the halide had been treated with an alkali metal amide ammonia solution.

Aluminum iodide ammonia solutions contain $[Al(NH_3)_6]^{3+}$ ions as seen from the ^{1}H NMR spectra.[16] However, ammonolysis occurs when the ammoniacates are treated with potassium amide or alkali metal ammonia solutions. Alkali metal ammonia solutions react vigorously with suspensions of aluminum iodide hexammoniacate[17] in ammonia at –78 °C. A series of acid/base equilibria has been proposed and it is believed that the rapid initial reaction occurs between the metal and the ammonium ion which results from the ammonolysis of the aluminum ion. The final products are $Al(NH_2)_2I$, $Al(NH_2)_3$, and $[Al(NH_2)_4]^-$, respectively, depending on the equivs of metal (or ammonia) consumed. Treatment of aluminum iodide with potassium amide ammonia solutions[6] leads to $Al(NH_2)_3$ and $K[Al(NH_2)_4]$.

The reaction of tetramethyllead with alkali metal solutions has been investigated in detail, and it has been shown that with alkali metals (Li, Na, K) the first stage of the reaction is the formation of methyl radicals and the anion $[PbMe_3]^-$. With excess potassium, progressive ammonolysis of the anion finally produces lead imide. Yet when lithium or sodium is used in the reaction, the product is dimethyl lead. The different reaction behavior is believed to lie in the relative insolubility of the lithium and sodium amides.[18]

Relatively little work has been reported on the reduction of π-bonded organometallic compounds in ammonia. Both Cp_2Fe and Cp_2Ni are unreactive toward ammonia solutions of potassium amide, but Cp_2Cr reacts to form CrN. All three metallocenes Cp_2M (M = Fe, Cr, Ni)[19] are reduced to the metals by potassium ammonia solutions.

1.2. Amido (NH_2^-), Imido (NH^{2-}), and Nitrido (N^{3-}) Transition Metal Compounds

Main group elements and transition metal fragments interact with each other in interesting and often unexpected fashions.   The unexpected situations result from the differing orbital requirements of the p-block vs d-block elements, as well as mismatches in size, electronegativities, substituent properties, etc.[20]

The nitrogen atom has five valence electrons that may be involved in bonding to the metals. It may provide three or four electrons for bonding when serving as a cluster vertex. It is also possible for N to adopt an interstitial arrangement, in which case it is considered to donate all five electrons to cluster bonding. The simplest N-M compounds can be viewed as derivatives of NR_3 (**I**, Figure

1) in which the R groups are successively replaced by metal fragments. These complexes are represented by $R_{3-x}N^{x-}$ (x = 1, amide **II**; x = 2, imide **III**; x = 3, nitride **IV**) bonded to one and up to three M^+ units. Higher coordination numbers at N produce complexes in which N may be considered as occupying an interstitial site. The metal atoms arrange around the centering atoms in many different structural geometries, including **V−VII** coordination modes. The centering atoms prove to be important in stabilizing such structures by forming strong interstitial N−M bonds.[21]
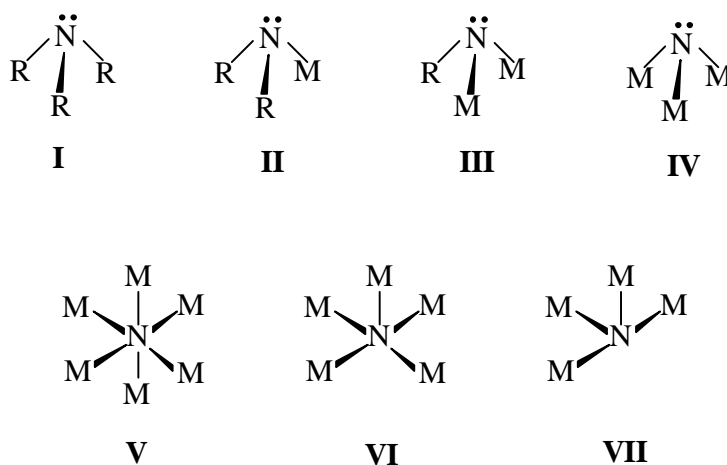
Figure 1. Coordination modes of N to metals

There are many similarities, but also important differences, between the behavior of the group 15 elements and those of the other main groups. Compounds may have very similar structural arrangements for different main group elements, but the synthetic routes that are necessary to make them may be completely different. A series of oxygen-containing organometallic clusters have been prepared.[22] But isoelectronic or isostructural nitrogen-based analogues containing amido (NH_2^-), imido (NH^{2-}) and nitrido (N^{3-}) ligands are very rare.

Nitrogen monoxide, which is usually coordinated to a transition metal, can be used as the source of the nitrogen atoms in amido, imido, and nitrido carbonyl clusters. The first carbonyl clusters containing an interstitial nitrogen atom $[Co_6N(CO)_{15}]^-$ and $[Rh_6N(CO)_{15}]^-$ were prepared by Martinengo and co-workers in 1979.[23] There are numerous examples of reactions involving the conversion of a coordinated nitrosyl ligand into a nitrido cluster.[24]

Nitrido bridged transition metal complexes like $[Cp^*V(\mu\text{-}N)Cl]_2$,[25] $[(dmpe)_2BrV\equiv N-VBr_2(N_3)(dmpe)]$ (dmpe = 1,2-bis(dimethylphosphino)ethane),[26] and $[(TMEDA)Cl_2V\equiv$

N−VCl$_3$(TMEDA)] (N,N,N′,N′-tetramethylethylenediamine),[27] have been obtained via the reactions of trimethylsilyl azide (Me$_3$SiN$_3$) with the corresponding metal containing precursors. The reaction of [Cp*V(μ-N)Cl]$_2$ with sodium amalgam gave the cubane [Cp*V(μ_3-N)]$_4$.[28]

Heterobimetallic complexes [(Me$_3$SiO)$_3$V≡N−Pt(Me)(PEt$_3$)$_2$][29] and [(Me$_3$SiO)$_3$V≡N−Re(CO)$_3$(PPh$_3$)$_2$][30] were obtained by condensation of a trimethylsilylimido vanadium complex with corresponding metal halide derivatives. A series of vanadium(V) nitrido complexes of formula [V(μ-N)Cl$_2$L$_2$]$_n$[31] has been prepared by net loss of chlorotrimethylsilane from Cl$_3$V≡NSiMe$_3$ on reaction with substituted pyridines or an amine.

The stable cyclic complex (Cp*TaNCl)$_3$,[32] postulated to be a benzene analogue,[33] was prepared by the reaction of Cp*TaCl$_4$ with N(SnMe$_3$)$_3$. Thermal ring opening of (Cp*TaNCl)$_3$ yielded the first soluble organometallic polymer of high stability (Cp*TaNCl)$_n$.[34]

The ready availability and high reactivity of ammonia renders this small molecule attractive as a nitrogen source. The propensity of early transition metal centers to form extremely strong bonds with nitrogen donors often results in an important driving force in the ammonolysis of organometallic derivatives. Early transition metal alkyl bonds are polarized and probable functionalities for ammonolysis. Coordinated NH$_3$ is considered to possess an acidic hydrogen atom, the 1,2-elimination maybe viewed as a deprotonation by an anionic alkyl. The formation of strong metal-nitrogen bonds from coordinated ammonia and the entropically favorable release of alkane molecule lead to the formation of metal nitrogen-containing compounds (Scheme 4).[35]

$$L_nM^{\delta-}-R^{\delta+} + NH_3 \rightleftharpoons L_nM-R \longrightarrow L_nMNH_2 + RH$$

Scheme 4
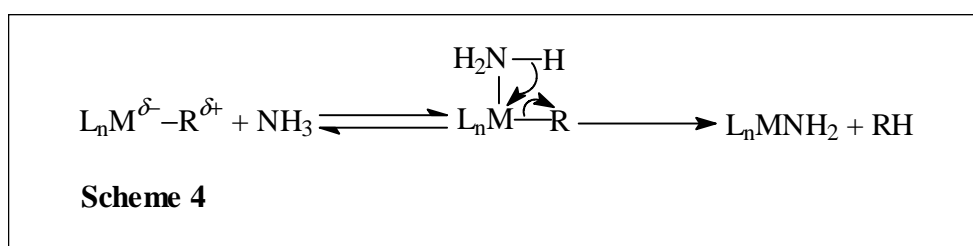
The early transition metal nitrides with the stoichiometry MN have many properties including extreme hardness, high melting points, excellent chemical resistance, interesting optical properties and good chemical conductivity.[36] Thin films of MN compounds have many applications as technologically important materials because of the their unique combination of properties.[37] Traditional synthetic methods for metal nitrides involve high temperature treatment of anhydrous

metal halides with nitrogen and hydrogen, or ammonia. Recent synthetic strategies to new and known metal nitrides involve the use of molecular precursors, especially amido complexes.[38] For example, multiprecursor systems include the chemical vapor deposition (CVD) reaction between titanium tetrachloride, nitrogen, and hydrogen at $\geq$ 1000 °C,[39] titanium tetrachloride and ammonia at 550 °C,[40] or tetrakis(dialkylamido)titanium(IV) complexes and ammonia at temperatures between 200 and 450 °C.[41] Gas-phase studies on the reaction of $Ti(NR_2)_4$ and NH_3 suggested that the intermediates contain amido NH_2^- ($Ti(NR_2)_{4-n}(NH_2)_n$) and imido NH^{2-} ($\{(NR)_2Ti(\mu\text{-NH})\}_n$) groups.[42] The reaction between $Ti(NMe_2)_4$ and liquid ammonia produced an brick-red insoluble polymeric material formulated as $[Ti_3(NMe_2)(NH_2)_2N_3]$ on the basis of analytical and IR data.[43]

A burgeoning discipline of inorganic and organometallic transition metal chemistry involves the preparation of solid-state materials via solution methods using molecular precursors.[44] In recent years several polynuclear early transition metal complexes containing nitrogen have been obtained via solution ammonolysis of precursor alkyl or dialkylamido organometallic derivatives. When Cp^*TaMe_4 was exposed to excess NH_3, $(Cp^*MeTaN)_3$[35] was isolated in good yield. Ammonolysis of $(tBuCH_2)_3Ta=CH(tBu)$ produced a pentamer $[(tBuCH_2)_2TaN]_5$.[45] Treatment of $ROZr(CH_2Ph)_3$ (RO = tBu_3CO) with NH_3 in benzene at 25 °C provided the square pyramidal $(ROZr)_5(\mu_5\text{-N})(\mu_3\text{-NH})_4(\mu\text{-NH}_2)_4$ complex.[46] Meanwhile, the pseudooctahedral $[(ROZr)_6(\mu_5\text{-N})(\mu_3\text{-NH})_6(\mu\text{-NH}_2)_3]$ and square pyramidal dodecaamido $[(ROZr)_5(\mu_5\text{-N})(\mu\text{-NH}_2)_{12}]$ clusters have been postulated on the basis of ^1H, $^{13}C\{1H\}$, and ^{15}N NMR investigations. The structural characterization of these complexes revealed the presence of amido (NH_2^-), imido (NH^{2-}), and nitrido (N^{3-}) ligands bridging and capping the metal centers or as interstitial nitride. More important, some of them contain NH_2, NH, and N ligands, interconversions among each other and with NH_3 may provide insight into the interplay of cluster electronic requirements and reactivity.

1.3. Group 4 Organometallic Imido (RN^{2-}) Complexes

Particular attention has been focused on the chemistry of group 4 metal imido complexes since the discovery of the C–H bond activation by zirconium imido compounds in 1988.[47] In recent years considerable progress has been achieved using metal imido compounds in C–H bond activation,[48] catalytic hydroamination of alkynes and allenes,[49] dihydrogen activation,[50] [2+2] cycloaddition,[51] addition or imido/oxo exchange reactions of carbonyl compounds,[52] synthesis and new reactions of heterometallic complexes,[53] and in metal nitride film deposition,[54]

respectively. A variety of group 4 metal imido complexes supported by ligands like cyclopentadienyl, bulky amides, bis(amidophosphines), amidinates, tetraazaanulenates, chloro, siloxy, and alkoxy has been successfully prepared.[55] Imido bridged dinuclear complexes, such as $[Cp_2Zr(\mu\text{-}NAr')]_2$ $(Ar' = 4\text{-}tBuC_6H_4)$,[47a,52b] $[(Me_2N)_2Zr(\mu\text{-}NtBu)]_2$,[56] $[CpTiCl(\mu\text{-}NPh)]_2$, $[CpTiCl(\mu\text{-}NPh)_2TiCp_2]$,[57] $[(\eta^8\text{-}C_8H_8)M(\mu\text{-}NAr)]_2$ $(M = Zr, Hf, Ar = 2,6\text{-}iPr_2C_6H_3)$, $[(MeC_5H_4)ZrCl(\mu\text{-}NAr)]_2$[58] are available with sterically less demanding ligands, and thus steric bulk often prevents the formation of imido bridged dinuclear compounds. Consequently under these conditions the terminal imido monomers are formed, such as $R_2M=NAr$ $(M = Zr, Hf, R_2 = $ *meso*-tetra-*p*-tolylporphyrinato, tetramethyldibenzotetraaza[14]-annulenate),[59] and $(P_2N_2)Zr=NtBu$ $(P_2N_2 = PhP(CH_2SiMe_2NSiMe_2CH_2)_2PPh)$.[60] NH bridged dinuclear titanium compound $[Cp^*TiMe(\mu\text{-}NH)]_2$[61] and amidoimidonitrido zirconium clusters[46] with $(\mu_3\text{-}NH)$ groups have been reported. However, so far no imido NH bridged dinuclear zirconium complex has been detected or isolated.

In recent years, some group 4 metal imido complexes were prepared in our group. In 1990 the first terminal titanium imido complex $Cl_2Ti=N(S)PPh_2\cdot3(C_5H_5N)$ was structurally characterized.[62] Moreover, the imido complexes $(Cl_2Ti=NPPh_2O)_2\cdot4MeCN$,[63] $Cl_2Ti=N(S)PiPr_2\cdot3(C_5H_5N)$, $[iPr_2P(S)NTiCl_2\cdot(MeCN)]_2$,[64] $[(Me_3SiC_5H_4)TiCl(\mu\text{-}NtBu)]_2$, $[Cp'TiCl(\mu\text{-}NSnMe_3)]_2$ $(Cp' = Cp^*, Me_3SiC_5H_4)$,[65] $[CpTiCl(\mu\text{-}NtBu)]_2$, $[CpTi(NHtBu)(\mu\text{-}NtBu)]_2$,[66] $[(MeC_5H_4)TiF(\mu\text{-}NPh)]_2$, $[(Me_3SiC_5H_4)TiF(\mu\text{-}NtBu)]_2$,[67] $[(tBuNH)_2M(\mu\text{-}NtBu)]_2$, $[Cp^*M(NHPh)(\mu\text{-}NPh)]_2(M = Zr, Hf)$, and $Cp^*Zr=NAr(NHAr)\cdot(C_5H_5N)$[68] have been prepared.

1.4. Hydrolysis of Group 4 Organometallic Compounds

Early transition metal oxides have long been used extensively as useful catalysts for a variety of inorganic and organic reactions.[69] In recent years the chemistry of polyoxo organometallic aggregates has attracted great interest in regard to their catalytic properties, their size in the nanometer range, and as modeling system for the reactions and properties of metal oxides in solution.[70] In general, hydrolysis of early transition metal halides (or other derivatives) results in the facile formation of several types of μ-oxo metal complexes depending upon the nature of the metals, the substituents, and the reaction conditions.

The representative oxo group 4 metal complexes which were obtained by hydrolysis of appropriate metal precursors include bridged dinuclear complexes $([(Cp_2MX)_2(\mu\text{-}O)]$ (M = Ti, Zr,

Hf; X = Cl, Me),[71] [(Cp′TiX$_2$)$_2$(μ-O)] (Cp′ = Cp, Cp*, Me$_4$PhC$_5$; Cp* = Me$_5$C$_5$; X = Cl, Me),[72] and [(Cp$^*_2$MH)$_2$(μ-O)] (M = Zr, Hf)[73]), trimers([{Cp′TiX(μ-O)}$_3$] (Cp′ = Cp*, Me$_4$PhC$_5$; X = Br, Cl, Me),[72a,74] [Cp$_2$TiCl(μ-O)CpTiCl(μ-O)Cp$_2$TiCl·CHCl$_3$],[75] [{(Cp*ZrCl)(μ-OH)}$_3$(μ_3-OH)(μ_3-O)·2THF],[76] [{(Cp*MCl)(μ-OH)}$_3$(μ_3-O)(μ-Cl)](M = Zr, Hf), and [{(Cp*HfCl)(μ-OH)}$_3$(μ_3-O)(μ-OH)][77]), and tetramers ([(Cp′Ti)$_4$(μ-O)$_6$][72a,78] and [{(Cp*TiX)(μ-O)}$_4$] (X = Br, Cl)[79]).

The larger polyoxotitanium clusters [{(MeC$_5$H$_4$)Ti}$_6$(μ_3-Cl)$_4$(μ_3-O)$_4$], [(CpTi)$_6$(μ_3-Cl)$_2$(μ_3-O)$_6$][80] and [(CpTi)$_6$(μ_3-O)$_8$][81] have been prepared by reduction of corresponding cyclopentadienyloxochloro titanium complexes and by treatment of Cp$_2$Ti(CO)$_2$ with H$_2$ and CO or with H$_2$O, respectively. CO$_2$ converts Cp$_2$Zr(CO)$_2$ to the cyclic trimer [{Cp$_2$Zr(μ-O)}$_3$].[82]

Several organic modified zirconium oxo/hydroxo clusters, such as [Zr$_6$(OH)$_4$O$_4$(OMc)$_{12}$] (OMc = methacrylate),[83] [Zr$_6$(OH)$_4$O$_4$(OOCR)$_{12}$]·(PrOH) (R = Ph, C(Me)=CH$_2$), [{Zr$_6$(OH)$_4$O$_4$(OOCCH=CH$_2$)$_{10}$}$_2$(μ-OOCCH=CH$_2$)$_4$],[84] and [Zr$_{10}$O$_6$(OH)$_4$(OOCC$_6$H$_4$OH)$_8$ (OOCC$_6$H$_4$O)$_8$]·6PrOH,[85] have been obtained from the reaction of zirconium alkoxides with carboxylic acids.

1.5. Reactions of Diazomethane Derivatives with Group 4 Organometallic Compounds

Diazoalkanes have been attracting wide interest as versatile reagents in synthetic organic and organometallic chemistry due to their high reactivity and variety of coordination modes possible for metal complexes.[86] Complexes containing the diazoalkyl ligand C−bonded to a metal are obtained by the reaction of a lithiated diazomethane with metal halides.[87] The α-metalated diazoalkanes are potential precursors for metal carbene or carbyne complexes.[88] Early transition metals, especially in their higher oxidation states, have the ability to form extremely strong bonds with N donors.[89] η^2-N$_2$- and terminal bonded η^1-N-metal diazoalkane complexes[90] are known. Another well-defined coordination mode of the CN$_2$ ligand as a dinuclear center is the μ-η^1 bond through the terminal N atom only.[91]

Boche and co-workers[92] calculated the energies of lithiated CH$_2$N$_2$ derivatives **1a-d**, and found that the N-lithiated N-isocyanamide (C≡N−NHLi) **1d** is the most stable isomer. Under basic conditions, **1d** should be in equilibrium with **1a** via **1b** and/or **1c** (Scheme 5).

Scheme 5
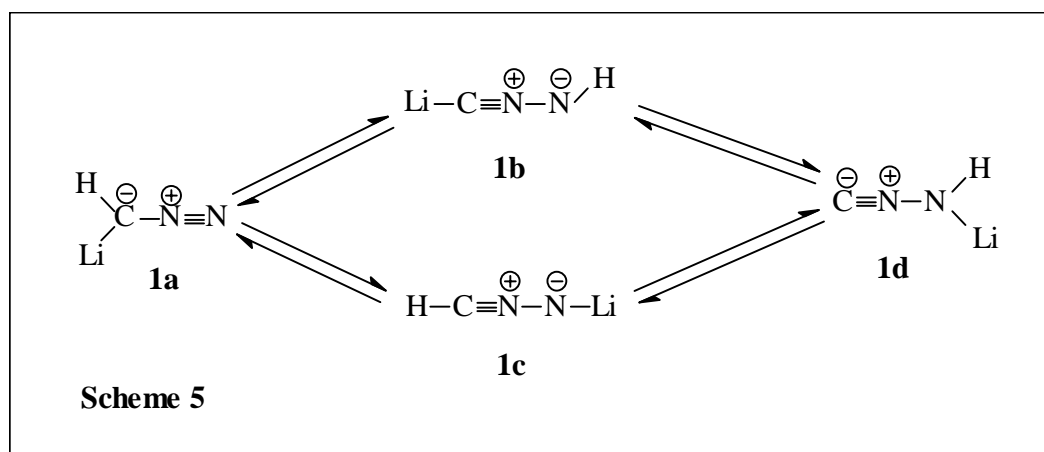
However, in the case of trimethylsilyl diazomethane the most stable isomer (in the crystalline state obtained from ether solutions) is the N-lithiated nitrile imide (Me$_3$SiC≡N−NLi) **2c** (Figure 2) cocrystallizing with Li-1,2,3-triazolide.[93] However, only the C−Li isomer **2a** was found in the solid state structure of the THF complex of lithiated trimethylsilyl diazomethane.[94] Interestingly, so far no evidence has been found that the trimethylsilyl group migrates to the terminal N atom to form LiC≡N−NSiMe$_3$ (**2b**) or C≡N−NLiSiMe$_3$ (**2d**).
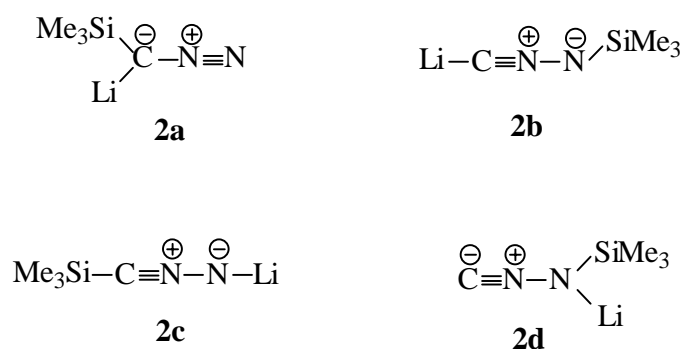
Figure 2. Possible trimethylsilyl diazomethane isomers

1.6. Scope and Aim of the Present Work

Based on the aforementioned background material, nitrogen containing transition metal compounds and metal oxides have been extensively prepared via different methods. These compounds are important in scientific and technological developments. In recent years, the interest in using transition metal nitrides and oxides has promoted studies on the ammonolysis and hydrolysis of transition metal compounds. The products with amido, imido and nitrido groups

formed during the ammonolysis of transition metal compounds and organometallic transition metal oxides have attracted considerable attention. However, there have been only very few attempts to investigate the reactions of transition metal organometallic compounds with alkali metal ammonia solutions and to prepare transition metal nitrides via ammonolysis of the organometallic chlorides. Meanwhile, there have been almost no attempts to prepare nitrogen containing transition metal compounds via ammonolysis of organometallic chlorides or to synthesize transition metal oxides in a liquid ammonia/toluene two phase system.

Hence, the objectives of the present work have been (1) to investigate the reactions of the organometallic early transition metal chlorides with alkali metals in a liquid ammonia/toluene two phase system, (2) to investigate the ammonolysis of the organic early transition metal chlorides in the presence of MNH_2 (M = K, Na) or KH in a liquid ammonia/toluene two phase system and in other solvents, (3) to investigate the base-assisted hydrolysis of organometallic early transition metal chlorides in a liquid ammonia/toluene two phase system, and (4) to investigate alternative methods for the preparation of nitrogen-containing group 4 metal compounds.

2. Results and Discussion

2.1. Syntheses of Amido (NH_2^-), Imido (NH^{2-}), and Nitrido (N^{3-}) Group 4 Metal Compounds in a Liquid Ammonia/Toluene Two Phase System

As aforementioned, significant progress has been made towards the ammonolysis of transition metal compounds. However, complete ammonolysis of early transition metal halides in liquid ammonia is very difficult to achieve.[95] It is fairly certain that the first step of the ammonolysis of the covalent transition metal halides (e.g. $TiCl_4$, Scheme 6) involves the formation of simple adducts (eq 1) which can be isolated.[96] The acidic nature of the hydrogen from the coordinated ammonia due to the higher positive charge on the titanium leads to hydrogen chloride elimination as ammonium chloride (eq 2) in the presence of an excess of ammonia. The process repeats as in eqs 3 and 4 with the eventual formation of the amide until a stage is reached at which the positive charge on the central titanium has been largely neutralized by the electron density delivered by the nitrogen atoms. The partially ammonolysed product is a poorer Lewis acid and will not attract ammonia molecules as well as the tetrachloride. Excess ammonia will not result in complete ammonolysis, the last step (eq 5) does not take place.

$$TiCl_4 + 2\ NH_3 \longrightarrow TiCl_4(NH_3)_2 \tag{1}$$

$$(2)$$

$$TiCl_3(NH_2)(NH_3)_2 + 2\ NH_3 \longrightarrow TiCl_2(NH_2)_2(NH_3)_2 + NH_4Cl \tag{3}$$

$$TiCl_2(NH_2)_2(NH_3)_2 + 2\ NH_3 \longrightarrow TiCl(NH_2)_3(NH_3)_2 + NH_4Cl \tag{4}$$

$$TiCl(NH_2)_3(NH_3)_2 + 2\ NH_3 \longrightarrow\!\!\!/\!\!\!\longrightarrow Ti(NH_2)_4(NH_3)_2 + NH_4Cl \tag{5}$$

Scheme 6
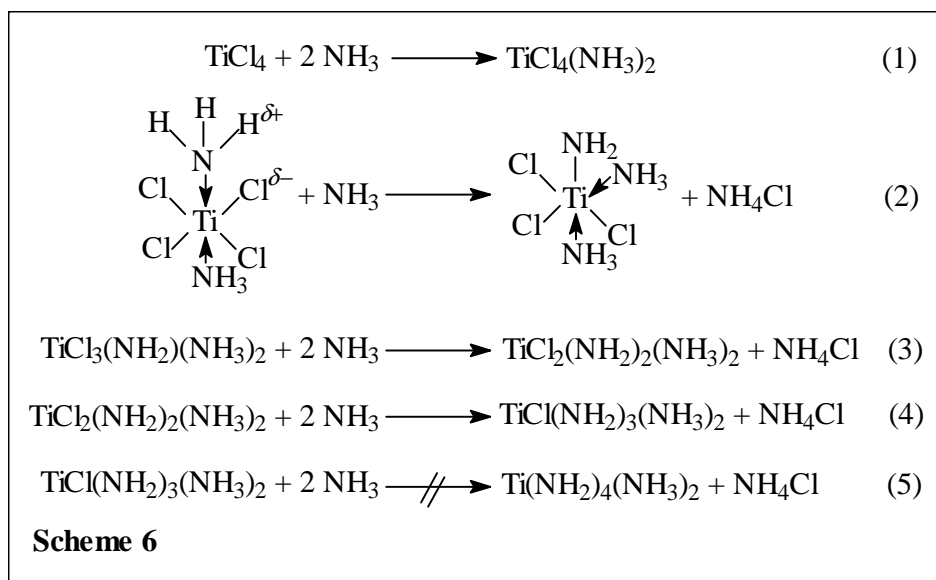
It seems likely that polymerization occurs at the same time as ammonolysis, as evidenced by the formation of insoluble ammonobasic products in all solvents except those which decompose

then completely. The nature of such a polymer is uncertain, but it is likely to involve bridging of the titanium atoms by either NH_2 or NH groups (Figure 3).[97]
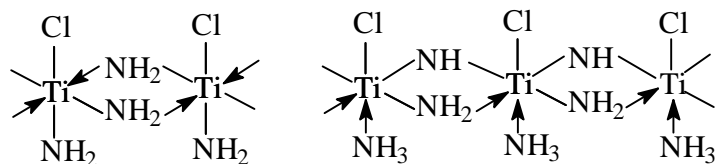
Figure 3. Polymeric structure of amido imido titanium chloride

The addition of alkali metal amides or alkali metals results in the further ammonolysis due to the reactions of amides or alkali metals with the protons of ammonium and the coordinated ammonia or amide. Table 1 shows that complete ammonolysis occurs upon treatment of group 4 to 6 metal halides with potassium amide in liquid ammonia. But the isolation of the amide products is extremely difficult due to the concomitant formation of potassium salts.

Table 1. Reactions of Some Group 4 to 6 Transition Metal Halides with Potassium Amide Ammonia Solutions

Compound	Product	Ref.
$TiBr_4$	$Ti(NH)(NK)$	98
$ZrBr_4$	$Zr(NH_2)_2 + K_2[Zr(NH_2)_2]$	99
$ZrNI$	$ZrN(NH_2)$	100
VBr_3	$V_2(NH)_3 + KV(NH)_2$	101
VCl_4	$V(NH)_2 + K_2[V(NH)_3]$	101
$TaBr_5$	$K_2[Ta(NH)_2(NH_2)_3]$	102
$MoBr_3$	$Mo(NH_2)_2NHK$	103
$MoCl_5$	$Mo(NH_2)(NK)_2$	103
WBr_5	$W(NH_2)(NK)_2$	103

The alkali metal amides are the only important bases in liquid ammonia. Potassium amide has good solubility, while sodium amide is almost insoluble in liquid ammonia and can be used as a suspension when a low concentration of amide ions is required. In addition, very strong bases

produce the amide ion in liquid ammonia, KH yields the amide and hydrogen, and sodium oxide forms a mixture of the amide and hydroxide.

In the last few years, some groups have been focusing on the ammonolysis of organometallic derivatives, which resulted in a few nitrogen-containing polynuclear transition metal complexes.[58] These compounds are promising precursors to solid-state metal nitride materials via solution methods. Some years ago, in our research group, ammonolysis of Cp^*TiMe_3 was shown to yield $[(Cp^*Ti)(\mu\text{-}NH)]_3(\mu_3\text{-}N)$[104] via the intermediate $[(Cp^*Ti)Me]_2(\mu\text{-}NH)_2$ which was proved by us[105] two years ago and others[61] recently, respectively.

One of the objectives of the present work is to investigate the intermediates with amido (NH_2^-), imido (NH^{2-}), and nitrido (N^{3-}) groups formed during the ammonolysis of early transition metal halides in a liquid ammonia/toluene two phase system in the presence of alkali metals, alkali metal amides and potassium hydride.

2.1.1. Syntheses and Characterization of Polyamidoimidonitrido Square Pyramidal Zirconium Cluster $[\{(MeC_5H_4)Zr\}_5(\mu_5\text{-}N)(\mu_3\text{-}NH)_4(\mu\text{-}NH_2)_4]$ (3) and Organopotassium Polymer $[(MeC_5H_4)K]_n$ (4)

Treatment of $(MeC_5H_4)_2ZrCl_2$ in a nitrogen atmosphere with 3 equivs of K (Na) in liquid ammonia/toluene at -78 °C results in the loss of two chloride ligands and one MeC_5H_4 group per Zr, and the formation of an unusual pentanuclear zirconium cluster $[\{(MeC_5H_4)Zr\}_5(\mu_5\text{-}N)(\mu_3\text{-}NH)_4(\mu\text{-}NH_2)_4]$ (3) in a yield of 35 % (Scheme 7).[106] Extraction of the residue with THF leads to $[(MeC_5H_4)K]_n$ (4) in 40 % yield.[107] Treatment of $(MeC_5H_4)_2ZrCl_2$ with $NaNH_2$ in liquid ammonia/toluene at -78 °C or alternatively with $NaNH_2$ in THF at room temperature in 1 : 3 molar ratio leads also to the formation of 3 with elimination of the MeC_5H_4 group as the sodium salt $[(MeC_5H_4)Na]_n$. The loss of MeC_5H_4 during the preparation of 3 is similar to the situation observed for the preparation of $[(CpTi)_6(\mu_3\text{-}O)_8]$,[108] $[(CpTi)_5(\mu_3\text{-}S)_6]$,[109] and $[(CpTi)_6(\mu_3\text{-}Te)_6(\mu_3\text{-}O)_2]$,[110] respectively.

Reduction of organometallic zirconium compounds under N_2 may result in zirconium dinitrogen complexes.[111] Alkali metal ammonia solutions are strong reducing agents, the formation of zirconium dinitrogen intermediates from the reaction of $(MeC_5H_4)_2ZrCl_2$ with alkali metal ammonia solution may be taken into consideration. The resulting intermediates can be turned to imido or nitrido complexes in liquid ammonia. In order to get some more information

about the mechanism for the formation of **3**, $(MeC_5H_4)_2ZrCl_2$ was reacted with K (Na) in liquid ammonia/toluene at -78 °C under argon gas resulting also in the formation of **3**, indicating that all the nitrogen atoms stem from NH_3.

$$5\ (MeC_5H_4)_2ZrCl_2 \xrightarrow{\begin{array}{c} 15\ K \\ \text{liq.}NH_3,\ \text{toluene},\ -78\ ^{o}C \\ 15\ NaNH_2 \\ \text{liq.}NH_3,\ \text{toluene},\ -78\ ^{o}C \\ 15\ NaNH_2 \\ \text{THF, RT} \end{array}} [\{(MeC_5H_4)Zr\}_5(\mu_5\text{-}N)(\mu_3\text{-}NH)_4(\mu\text{-}NH_2)_4]$$

$$\textbf{3}$$

$$+\ 5/n\ (MeC_5H_4M)_n + 10\ MCl$$

M = K or Na, **4** = $[(MeC_5H_4)K]_n$
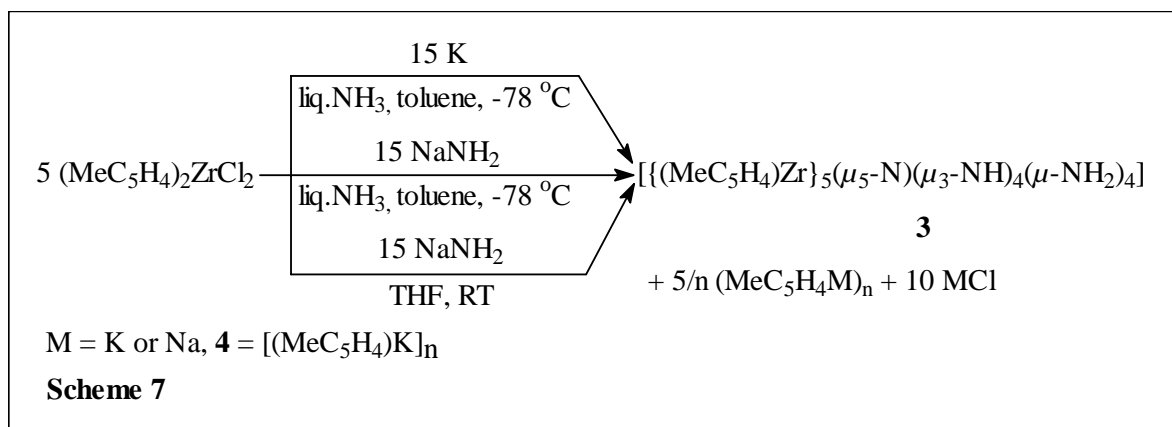
Scheme 7

A possible mechanism for the formation of **3** is shown in Scheme 8.

$$(MeC_5H_4)_2ZrCl_2 \underset{}{\overset{2\ NH_3}{\rightleftharpoons}} [(MeC_5H_4)_2ZrCl_2(NH_3)_2] \qquad (6)$$
$$\textbf{5}$$

$$[(MeC_5H_4)_2ZrCl_2(NH_3)_2] \xrightarrow[-MCl,\ -1/2\ H_2]{+\ M} [(MeC_5H_4)_2ZrCl(NH_2)(NH_3)] \qquad (7)$$
$$\textbf{5} \qquad\qquad\qquad\qquad\qquad\qquad\qquad\qquad\qquad\qquad \textbf{6}$$

$$[(MeC_5H_4)_2ZrCl(NH_2)(NH_3)] \xrightarrow[-MCl,\ -1/2\ H_2]{+\ M} [(MeC_5H_4)_2Zr(NH_2)_2] \qquad (8)$$
$$\textbf{6} \qquad\qquad\qquad\qquad\qquad\qquad\qquad\qquad\qquad\qquad \textbf{7}$$

$$[(MeC_5H_4)_2Zr(NH_2)_2] \xrightarrow[-1/2\ H_2]{+\ M} \left[(MeC_5H_4)Zr\substack{NH_2 \\ \diagdown NH}\right] + 1/n\ [(MeC_5H_4)M]_n \quad (9)$$
$$\textbf{7} \qquad\qquad\qquad\qquad\qquad\qquad\qquad\qquad\qquad\qquad \textbf{8}$$

$$5\left[(MeC_5H_4)Zr\substack{NH_2 \\ \diagdown NH}\right] \xrightarrow[-NH_3]{} [\{(MeC_5H_4)Zr\}_5(\mu_5\text{-}N)(\mu_3\text{-}NH)_4(\mu\text{-}NH_2)_4] \quad (10)$$
$$\textbf{8} \qquad\qquad\qquad\qquad\qquad\qquad\qquad\qquad\qquad\qquad \textbf{3}$$

M = K or Na, **4** = $[(MeC_5H_4)K]_n$

Scheme 8
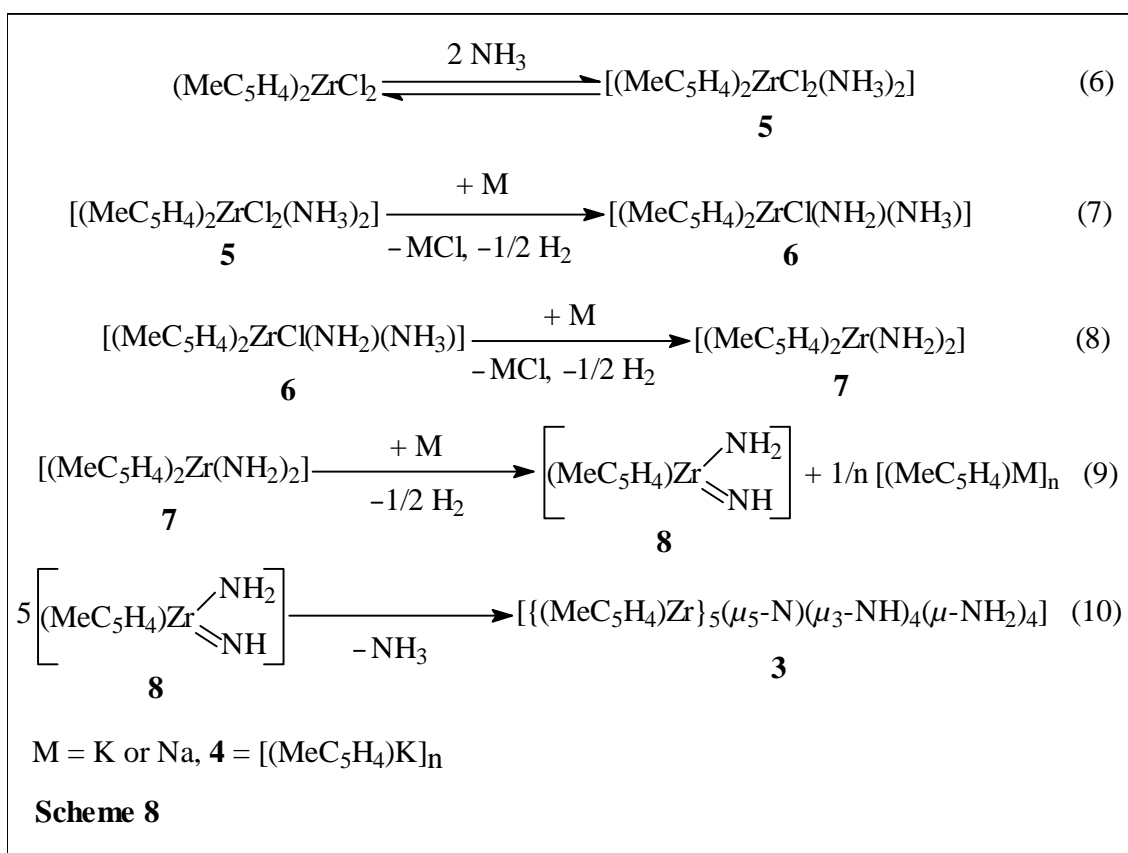
When NH_3 was condensed into a solution of $(MeC_5H_4)_2ZrCl_2$ in toluene, a white precipitate was formed immediately. Equation (6) represents the initial coordination of ammonia molecules to form ammonobasic zirconium chloride **5**. Removal of the solvents *in vacuo*, no ammoniation or ammonolysis product was obtained (only the organozirconium dichloride was isolated). Therefore, equation (6) is an equilibrium. The zirconium atom withdraws electron density from the nitrogen atom leading to a more acidic hydrogen from the coordinated ammonia. The addition of alkali metal results in the displacement of a chlorine atom from the individual zirconium unit of the ammonobasic zirconium chloride and the formation of zirconium amides **6** and **7** (eqs 7 and 8), and subsequently leads to amidoimidozirconium intermediate **8** with concomitant loss of a MeC_5H_4 group from the zirconium amide as $(MeC_5H_4)M$ which polymerizes leading to stable $[(MeC_5H_4)M]_n$ (eq 9). The amidoimidozirconium intermediate **8** is unstable and very easily forms the pentamer under simultaneously elimination of one molecule of NH_3 (eq 10). Treatment of $(MeC_5H_4)_2ZrCl_2$ with $NaNH_2$ in liquid ammonia and toluene leads also to **3** and $[(MeC_5H_4)Na]_n$ via the same intermediates, while NH_3 is formed instead of H_2 in eqs 7, 8, and 9. When $(MeC_5H_4)_2ZrCl_2$ reacts with $NaNH_2$ in THF, the first step can be assumed to be the coordination of THF to zirconium. The amide ion displaces chloride from the zirconium atom are the second and third steps of the reaction.

Attempts to detect or isolate any intermediate in the formation of **3** failed. Treatment of $(MeC_5H_4)_2ZrCl_2$ with 1, 1.5, and 2 equivs of K (Na) in liquid ammonia/toluene at -78 °C leads also to the formation of **3** in relatively low yields of 5 %, 12 %, and 14 %, respectively. Furthermore, light yellow liquid products were formed in the reactions of $(MeC_5H_4)_2ZrCl_2$ with K (Na) in liquid ammonia/toluene in a 1 : 0. 5 molar ratio at -78 °C.

Treatment of $(MeC_5H_4)_2ZrCl_2$ with $NaNH_2$ in toluene at room temperature for 72 h did not lead to any reaction. The reason for that is believed to be due to the insolubility of $NaNH_2$ in toluene. The two phase system liquid ammonia/toluene and polar solvents like THF are very essential for the formation of **3**.

Compound **3** is a colorless crystalline solid melting at 302 °C. In solution (toluene or THF) no decomposition is observed for **3** over a period of one year. The IR spectrum of **3** shows broad absorptions at 3299 and 3371 cm^{-1}, assignable to the NH and NH_2 stretching frequencies, respectively. The most intense peak in the EI mass spectrum of **3** is at m/z 910 [$M^+ − MeC_5H_4$] and the fragment of highest mass is at m/z 989 (62 %) [M^+]. The ^1H NMR spectrum of **3** shows a

multiplet in the region δ 5.73 − 5.56 ppm attributed to the protons of the C_5H_4 groups and two singlet resonances at δ 2.13 and 2.11 ppm assigned to the protons of the Me groups attached to the cyclopentadienyl rings. The protons of the NH groups resonate at δ 6.56 ppm as a broad singlet and the protons of NH_2 groups at relatively high field at δ 0.69 ppm (a broad doublet, ^2J(H, H) = 8.3 Hz) and δ 0.14 ppm (a broad doublet, ^2J(H, H) = 8.3 Hz).

The molecular structure and the central inorganic core of **3** are shown in Figures 4 and 5. The selected bond lengths and angles for **3** are presented in Table 2.
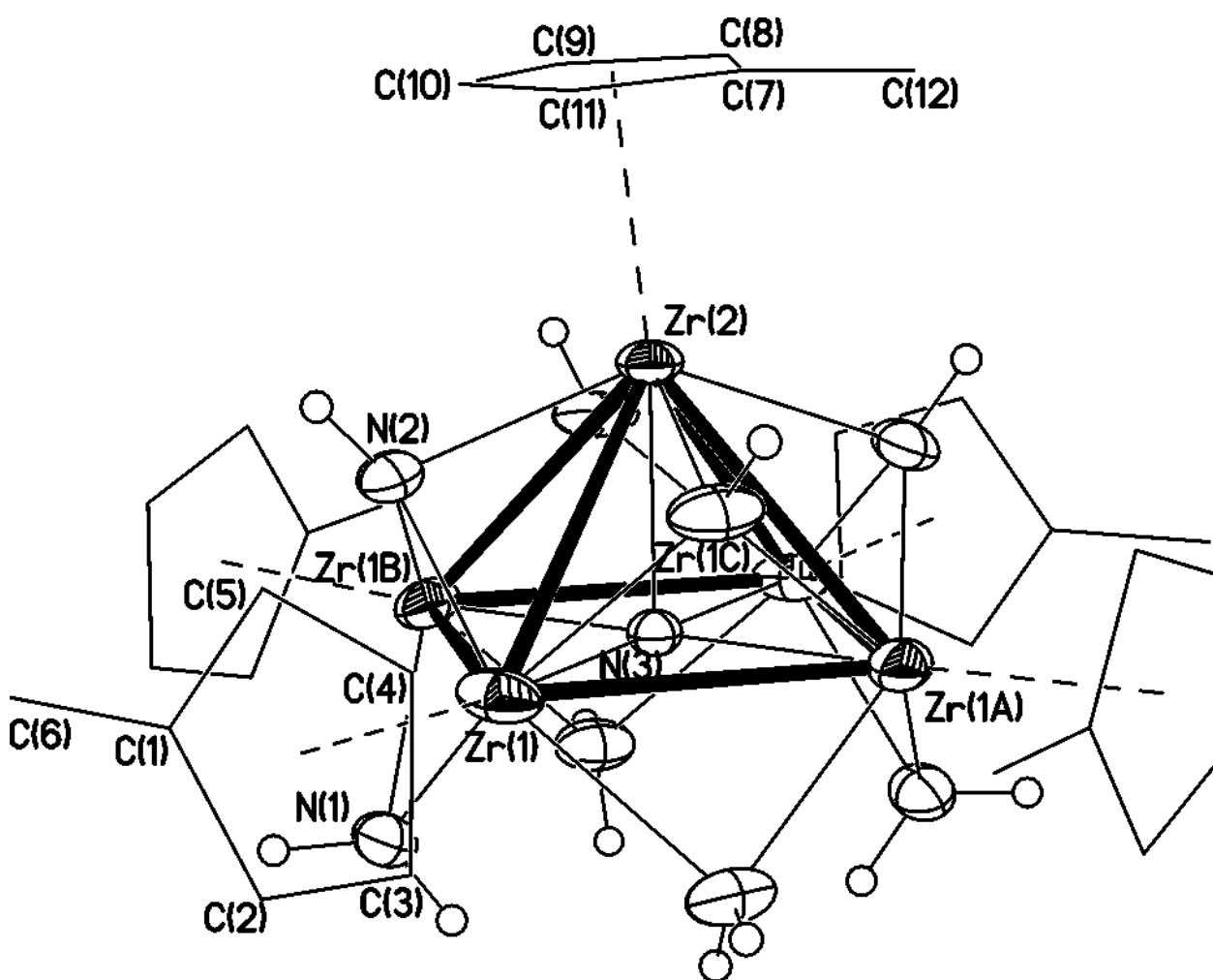
Figure 4. Molecular structure of [{(MeC$_5$H$_4$)Zr}$_5$(μ_5-N)(μ_3-NH)$_4$(μ-NH$_2$)$_4$] (3) (50% probability ellipsoids. H atoms bonded to C are omitted for clearity)
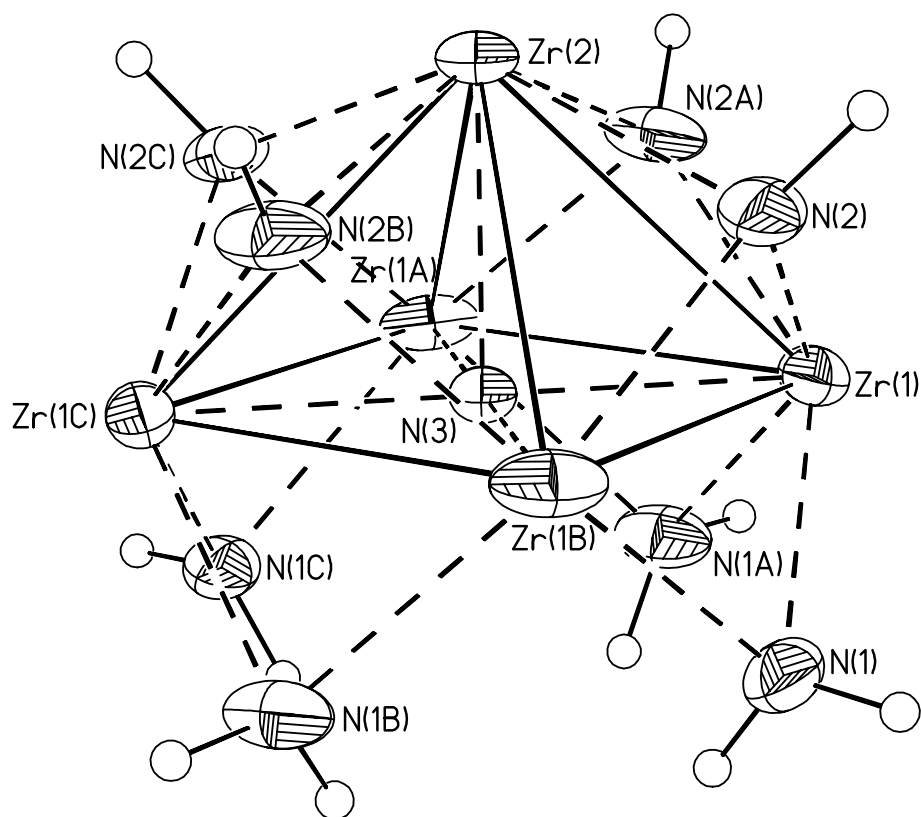
Figure 5. Central core of [{(MeC$_5$H$_4$)Zr}$_5$(μ_5-N)(μ_3-NH)$_4$(μ-NH$_2$)$_4$] (3) (50 % probability ellipsoids)

The crystal structure of **3** is constrained by a crystallographically-imposed C_4 axis passing through Zr(2) and N(3). The core of **3** consists of five Zr atoms forming a square pyramid . The four triangular faces of this pyramid are capped by NH groups, the four edges of the base are bridged by NH$_2$ groups, and in the center of the basal plane of the Zr$_5$ cluster a μ_5-N atom is located (Figure 5). The coordination sphere of the Zr atoms is completed by one MeC$_5$H$_4$ group per Zr. The average Zr(2)–N(3) (2.210 Å), Zr(1)–N(3) (2.232 Å), Zr(2)–N(2) (2.253 Å), Zr(1)–N(2) (2.186 Å) and Zr(1)–N(1) (2.296 Å) bond lengths are very similar to those found in [{(*t*-Bu$_3$CO)Zr}$_5$(μ_5-N)(μ_3-NH)$_4$(μ-NH$_2$)$_4$] (Zr$_a$–(μ_5-N) (2.35 Å), Zr$_b$–(μ_5-N) (2.23 Å), Zr$_a$–(μ_3-NH)

(2.27 Å), Zr$_b$–(μ_3-NH) (2.19 Å) and Zr$_b$–(μ-NH$_2$) (2.31 Å), Zr(2) = Zr$_a$, Zr(1) = Zr$_b$),[46] respectively.

Table 2. Selected Bond Lengths (Å) and Angles (°) for 3

Zr(1)–N(1)	2.278(6)	Zr(1)–N(2)	2.195(6)
Zr(1)–N(3)	2.2321(6)	Zr(2)–N(2)	2.253(6)
Zr(2)–N(3)	2.21(1)	Zr(1)–Zr(1B)	3.1566(8)
Zr(1)–Zr(2)	3.143(1)		
N(2A)–Zr(1)–N(2)	86.0(3)	N(2)–Zr(1)–N(3)	69.9(2)
N(2)–Zr(1)–N(1)	82.4(2)	N(3)–Zr(1)–N(1)	74.2(2)
N(2)–Zr(1)–N(1A)	143.4(2)	N(1)–Zr(1)–N(1A)	87.8(3)
Zr(2)–Zr(1)–Zr(1B)	59.86(1)	N(2A)–Zr(2)–N(2B)	138.6(3)
N(3)–Zr(2)–N(2)	69.3(1)	N(2A)–Zr(2)–N(2)	82.81(9)
Zr(1)–N(1)–Zr(1B)	86.8(2)	Zr(1B)–N(2)–Zr(1)	92.5(2)
Zr(1)–N(2)–Zr(2)	89.9(2)	Zr(2)–N(3)–Zr(1)	90.1(3)
Zr(1)–N(3)–Zr(1C)	179.8(5)		

Compound **4** is a colorless crystalline solid melting at 220 °C. **4** is very sensitive to moisture, decomposition occurs immediately in air. In the EI mass spectrum of **4** fragments at *m/z* 39 (62 %) [K$^+$] and 79 (100 %) [MeC$_5$H$_4^+$] were observed. The ^{1}H NMR spectrum of **4** shows a multiplet at δ 5.47 − 5.40 ppm for the protons of the C$_5$H$_4$ moieties and a singlet at δ 2.17 ppm corresponding to the protons of the methyl groups on the MeC$_5$H$_4$ rings.

The molecular structure of **4** is shown in Figure 6. The selected bond lengths and angles for **4** are presented in Table 3**.** Compound **4** crystallizes in the monoclinic space group *C*2/*c*. The X-ray structure analysis of this polymer reveals that **4** contains the parallelly oriented one-dimensional infinite 'supersandwich complex' units made up of a repeating sequence of potassium atoms and η^5-cyclopentadienyl rings. The methyl groups attached to the cyclopentadienyl moieties are arranged 'in gaps'.

The K–Xc distances (2.780 Å to 2.858 Å, av 2.811 Å) are comparable to those found in [(Me$_3$SiC$_5$H$_4$)K]$_n$ (2.78 Å).[112] The K–X distances (3.209 Å to 3.281 Å, av 3.245 Å) indicate an

additional weak bonding relationship between potassium atoms and the neighboring cyclopentadienyl units of the other chain, which results in a distortion of the geometry around each potassium atom and a zigzag chain structure of **4**. The Xc−K−Xc angles (126.9° to 135.7°, av 130.9°) are smaller than those found in $[(Me_3SiC_5H_4)K]_n$ (150.7°). The average K···K distances and K−K−K angles in the chains are 5.596 Å and 133.0°, respectively.
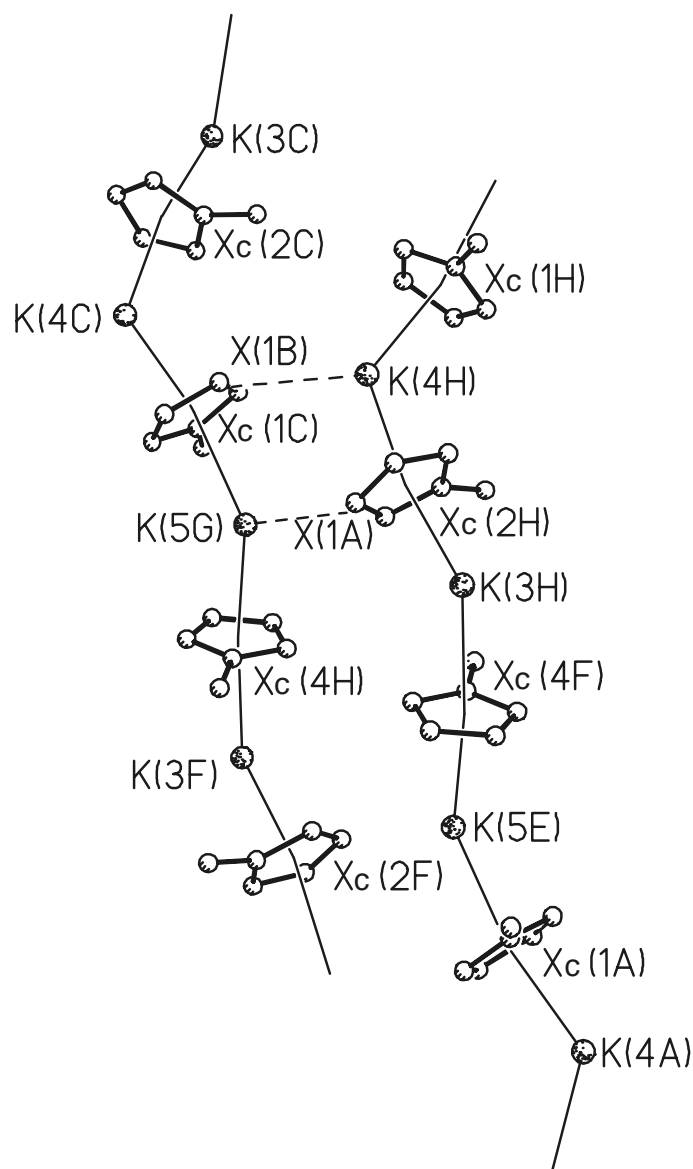
Figure 6. Molecular structure of $[(MeC_5H_4)K]_n$ (4) (H atoms bonded to C are omitted for clearity)

Table 3. Selected Bond Lengths (Å) and Angles (°) for 4[*]

K(4H)–Xc(1H)	2.786	K(4H)–Xc(2H)	2.819
K(3H)–Xc(2H)	2.780	K(3H)–Xc(4F)	2.858
K(5G)–Xc(1C)	2.842	K(5G)–Xc(4H)	2.783
K(4C)–Xc(1C)	2.786	K(4C)–Xc(2C)	2.819
K(4H)–X(1B)	3.281	K(5G)–X(1A)	3.209
K(3C)–K(4C)	5.577	K(3H)–K(4H)	5.577
K(4C)–K(5G)	5.601	K(3H)–K(5E)	5.610
Xc(2C)–K(4C)–Xc(1C)	126.9	Xc(2H)–K(4H)–Xc(1H)	126.9
Xc(2H)–K(4H)–Xc(1B)	110.1	Xc(1H)–K(4H)–Xc(1B)	120.1
Xc(4H)–K(5G)–Xc(1C)	135.7	Xc(4H)–K(5G)–X(1A)	110.5
Xc(1C)–K(5G)–X(1A)	135.7		

[*]: Xc and X represent the centers of the MeC_5H_4 rings and the centers of the adjacent carbon atoms in the MeC_5H_4 rings, respectively. The Xc and X positions are artificially calculated points. They do not correspond to the reality and only used to calculate the distances given in Table 3.

2.1.2. Synthesis and Characterization of an Imido (NH⁻) Bridged Dinuclear Zirconium Complex $[(\eta^3\text{-L})Zr(\mu\text{-NH})]_2$ (9, L = (PNtBu)$_2$(tBuN)$_2$))

Treatment of $LZrCl_2$ (see 2.7.1, compound **25**) with KH (1 : 2 molar ratio) in liquid ammonia and toluene at -78 °C yields $[(\eta^3\text{-L})Zr(\mu\text{-NH})]_2$ (**9**, Scheme 9).[113] It is assumed that the formation of **9** proceeds via two possible intermediates. The *in situ* formation of the amide (NH_2^-) from the reaction of KH with ammonia[114] leads to the diamide intermediate $[LZr(NH_2)_2]$ which after inter- or intramolecular elimination of ammonia is converted to **9**. The other proposed intermediate is the zirconium amido hydride $[LZr(NH_2)H]$ which undergoes an inter- or intramolecular hydrogen elimination to yield **9**. Recently an imido-*ansa*-zirconium dihydride was prepared from the liquid ammonia/toluene system.[106] Meanwhile, Bercaw et al.[115] reported on the ammonolysis of Cp^*MH_2 (M = Ti, Zr) that did not lead to an imido compound, instead the amido complex $Cp^*M(NH_2)H$ was formed due to the steric bulk of the Cp^* ligand. Obviously, the *in situ* formation of the amide and the liquid ammonia/toluene two phase system as well as the organic ligand are important for the generation of **9**. The KH has two functions in this reaction. First to react with

the zirconium chloride to form KCl and second to generate a Zr−H or Zr−NH$_2$ species as an intermediate.

$$2\ LZrCl_2 \xrightarrow[\text{liq NH}_3,\ \text{toluene, -78 °C}]{4\ KH} [(\eta^3\text{-L})Zr(\mu\text{-NH})]_2 + 4\ KCl + 4\ H_2$$

$$\mathbf{9}$$

L = (PN*t*Bu)$_2$(*t*BuN)$_2$

Scheme 9
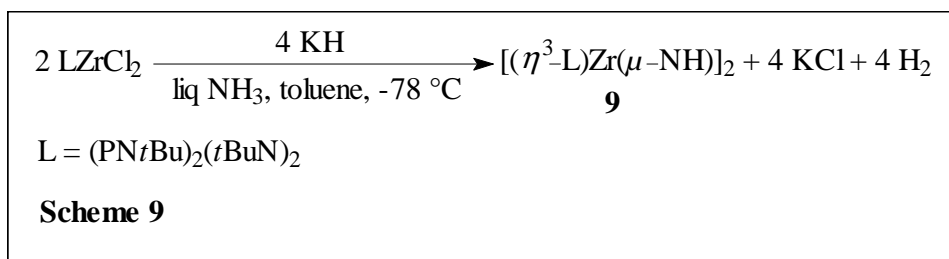
Colorless compound **9** is a crystalline solid decomposing above 220 °C. Its IR spectrum shows a broad absorption at 3378 cm^{-1}, assignable to a N-H stretching frequency. The EI mass spectrum of **9** shows peaks corresponding to [M$^+$] (*m/z* 904, 38 %) and [M$^+$ − *t*Bu − Me] (*m/z* 832, 83 %).

The molecular structure and the central inorganic core of **9** are shown in Figures 7 and 8, respectively. The selected bond lengths and angles for **9** are given in Table 4. Compound **9** crystallizes in the monoclinic space group *P*2$_1$/*c*. The central core of **9** contains an ideally planar (centrosymmetrical) four-membered Zr$_2$(μ−N)$_2$ ring. The (μ-NH)−Zr−(μ-NH) angle (78.7(3)°) is smaller, while the distances Zr−(μ-NH) (from 2.039(8) Å to 2.057(8) Å, av 2.048 Å) and Zr···Zr $_2$N)$_2$Zr(μ-N*t*Bu)]$_2$ ((μ-N*t*Bu)−Zr−(μ-N*t*Bu) 83.10(5)°, Zr−(μ-N*t*Bu) 2.060 Å, Zr···Zr 3.092(1) Å),[56] [Cp$_2$Zr(μ-NAr′)]$_2$ ((μ-NAr′)−Zr−(μ-NAr′) 80.56(7)°, Zr−(μ-NAr′) 2.096 Å, Zr···Zr 3.198(1) Å),[57a] and in [(MeC$_5$H$_4$)ZrCl(μ-NAr)]$_2$ ((μ-NAr)−Zr−(μ-NAr) 96.98°, Zr−(μ-NAr) 2.016 Å, Zr···Zr 3.087(2) Å),[58] respectively. The coordination sphere of each zirconium is completed by the η^3-bis(*tert*-butylamido)cyclodiphosph(III)azane ligand. The bond lengths of Zr(1)−N(1) (2.116(7) Å) and Zr(1)−N(4) (2.129(7) Å) are comparable to those found in [(MeSiN*t*Bu)$_2$(N*t*Bu)$_2$]ZrCl$_2$ (2.075(3) Å and 2.089(3) Å).[116] The sum of the angles at N(1) and N(4) are 359.1° and 359.2°, respectively. The approximately triangular planar coordination environment indicates that the N(1) and N(2) atoms are nearly sp^2 hybridized. Therefore, the N(1) and N(2) atoms donate their lone-pair electrons into the empty d-orbitals of zirconium as 3-electron donors, which is in agreement with the bonding situation in [(MeSiN*t*Bu)$_2$(N*t*Bu)$_2$]ZrCl$_2$. The bond lengths of P(1)−N(1) (1.686(8) Å), P(1)−N(3) (1.733(8) Å) and P(1)−N(2) (1.789(8) Å) are similar to those found in [(η^3-L)In]$_2$ (1.670(3) Å, 1.723(3) Å and 1.801(3) Å, respectively).[117]
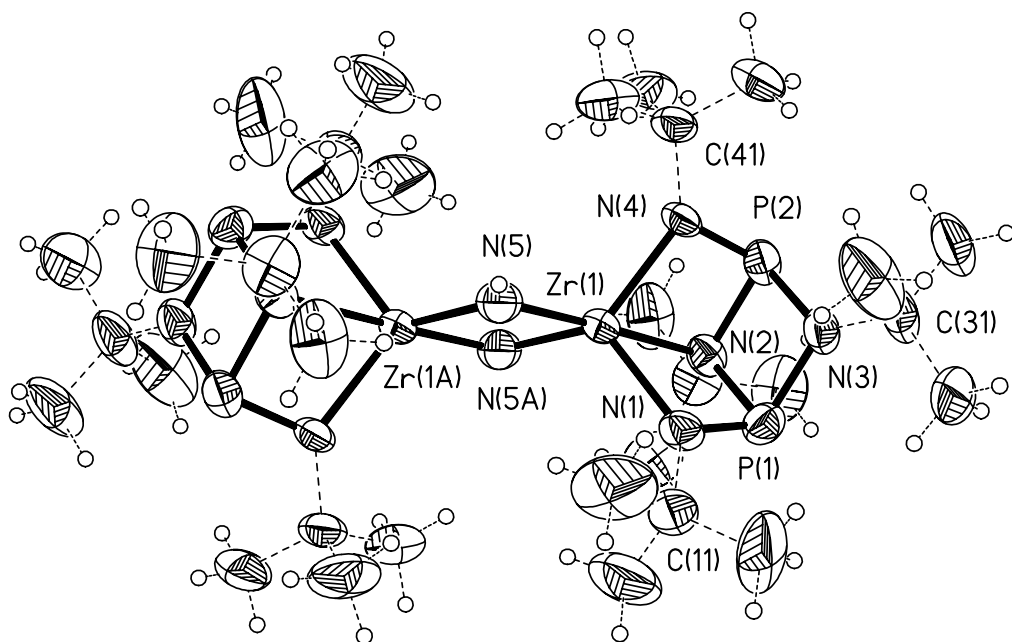
Figure 7. Molecular structure of [(η^3-L)Zr(μ-NH)]$_2$ (9) (50 % probability ellipsoids)
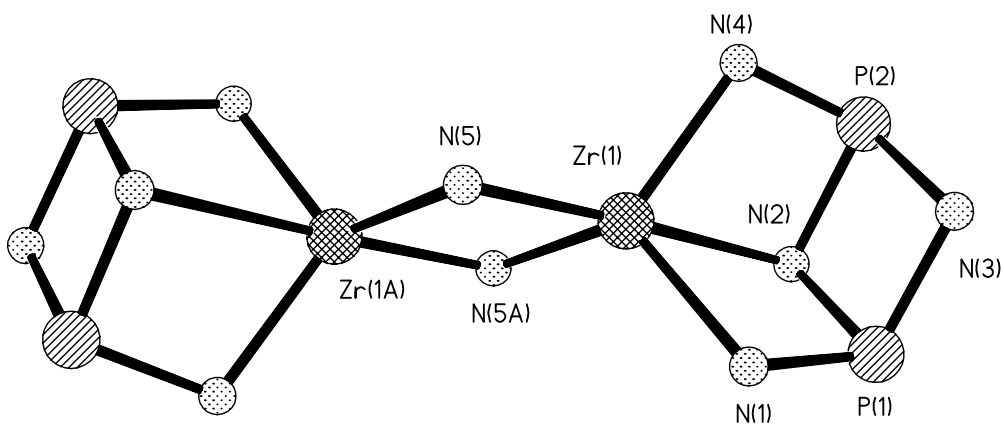
Figure 8. Central core of [(η^3-L)Zr(μ-NH)]$_2$ (9)

Table 4. Selected Bond Lengths (Å) and Bond Angles (°) for 9

Zr(1)–N(5)	2.039(8)	Zr(1)–N(5A)	2.057(8)
Zr(1)–N(1)	2.116(7)	Zr(1)–N(4)	2.129(7)
Zr(1)–N(2)	2.399(7)	Zr(1)–Zr(1A)	3.168(2)
P(1)–N(1)	1.686(8)	P(2)–N(4)	1.689(8)
P(1)–N(3)	1.733(8)	P(2)–N(3)	1.726(8)
P(1)–N(2)	1.789(8)	P(2)–N(2)	1.781(8)
N(5)–Zr(1)–N(5A)	78.7(3)	Zr(1)–N(5)–Zr(1A)	101.3(3)
N(5)–Zr(1)–N(1)	13.5(3)	N(5A)–Zr(1)–N(1)	119.4(3)
N(5)–Zr(1)–N(4)	114.5(3)	N(5A)–Zr(1)–N(4)	121.1(3)
N(5)–Zr(1)–N(2)	176.4(3)	N(5A)–Zr(1)–N(2)	97.8(3)
N(1)–Zr(1)–N(2)	67.9(3)	N(4)–Zr(1)–N(2)	67.5(3)
C(11)–N(1)–P(1)	119.7(7)	P(1)–N(1)–Zr(1)	104.4(3)
C(11)–N(1)–Zr(1)	135.0(6)	P(2)–N(4)–Zr(1)	104.1(3)
C(41)–N(4)–P(2)	118.6(6)	C(41)–N(4)–Zr(1)	136.3(6)

A smaller (μ-N)–Zr–(μ-N) angle was also found in the imido bridged complex [(Me$_4$taa)Zr(1)(μ-NAr)$_2$Zr(2)(NHAr)$_2$] (Me$_4$taaH$_2$ = tetramethyldibenzotetraaza[14]-annulene),[118] in which the (μ-N)–Zr(1)–(μ-N) angle (75.0(10)°) is smaller than the corresponding (μ-N)–Zr(2)–(μ-N) one (85.7(11)°), due to the more sterically demanding Me$_4$taa group at Zr(1). Furthermore, the imido bridge (μ-NR) has to bend more if R is a bulky group. The (μ-NAr)–Zr–(μ-NAr) angles (96.98°) in [(MeC$_5$H$_4$)ZrCl(μ-NAr)]$_2$[58] are obviously larger than those in [Cp$_2$Zr(μ-NAr′)]$_2$ (80.56(7)°).[47a] Therefore, compound **9** with a bulky ligand on zirconium and smaller imido (NH) bridges, has smaller (μ-NH)–Zr–(μ-NH) angles.

2.1.3. Synthesis and Characterization of Polyimidonitrido Octahedral Titanium Cluster [(L′Ti)$_6$(μ_3-NH)$_6$(μ_3-N)$_2$·6(C$_7$H$_8$)] (10, L′ = *p*-MeC$_6$H$_4$C(NSiMe$_3$)$_2$)

Recently Mena et al.[119] prepared (Cp*Ti)$_4$(μ_3-N)$_4$ from Cp*Ti(NMe$_2$)$_3$ and ammonia. Attempts to detect or isolate larger nitrogen-containing aggregates with the Cp* ligand on titanium so far failed. Changing the ligand on titanium and the method of preparation, from the reaction of

L'TiCl$_3$ with NaNH$_2$ in liquid ammonia/toluene no definite compound could be identified due to the insolubility of the resulting product in common organic solvents. In contrast, treatment of L'$_2$TiCl$_2$ with 2 equivs of NaNH$_2$ in liquid ammonia/toluene at -78 °C affords [(L'Ti)$_6$(μ_3-NH)$_6$(μ_3-N)$_2$·6(C$_7$H$_8$)] (**10**, Scheme 10) in low yield.[120] When the filtrate was concentrated and kept at -20 °C, during 2 weeks a yellow solid was formed. As seen from the elemental analysis, the solid was impure **10** and difficult to purify.

L'$_2$TiCl$_2$ $\xrightarrow[\text{liq NH}_3,\ \text{toluene, -78 }^{\circ}\text{C}]{2\ \text{NaNH}_2}$ [(L'Ti)$_6$(μ_3-NH)$_6$(μ_3-N)$_2$·6(C$_7$H$_8$)]

10

L' = *p*-MeC$_6$H$_4$C(NSiMe$_3$)$_2$

Scheme 10
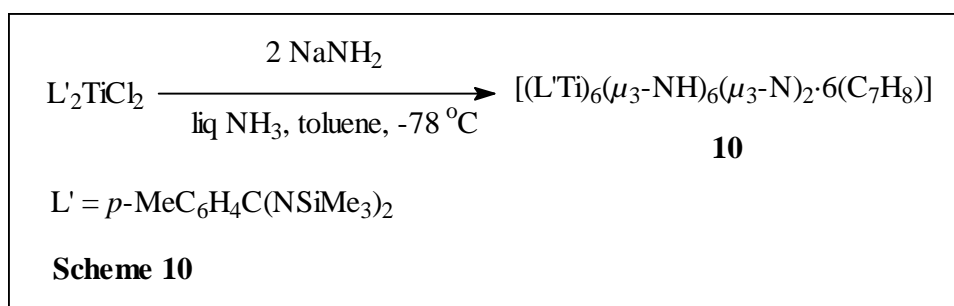
Compound **10** is a yellow and thermally stable crystalline solid. It starts to decompose at 300 °C. Under an inert atmosphere or in solution (toluene) no decomposition was observed for **10**. The IR spectrum of **10** shows a broad absorption at 3381 cm^{-1}, assignable to the N-H stretching frequency. Compound **10** can not be redissolved without decomposition to obtain reliable NMR spectra. In the ^{1}H NMR solution spectrum we observed five signals for the hydrogen atoms of the Me$_3$Si group. The largest fragment in the EI mass spectrum of **10** was observed at *m/z* 2536 [M$^+$ − NSiMe$_3$] with very low intensity due to the poor volatility of **10.**

Single crystals of **10** suitable for X-ray structure analysis were obtained from toluene by storing the reaction mixture at room temperature for three weeks. The molecular structure and the central inorganic core of **10** are shown in Figures 9 and 10. Selected bond lengths and angles for **10** are presented in Table 5. Compound **10** crystallizes in the rhombohedral space group $R\bar{3}$. The molecular structure of **10** in the crystal consists of an almost perfect octahedron with the titanium atoms positioned on the vertexes. The angles between adjacent titanium atoms are either about 60° or 90°. The titanium triangles are topped each by a nitrogen atom, and these nitrogen atoms consist of two nitrides and six imides. The six imide hydrogen atoms statistically distribute over eight facial positions, the occupancy being 0.75. The coordination sphere of each titanium is completed by the chelating ligand L.

The Ti-N bond lengths (from 1.958 Å to 2.014 Å, av 1.993 Å) are only slightly larger than those found in [(Cp*Ti)$_3$(μ-NH)$_3$(μ_3-N)] (av 1.924 Å)[104] and in (Cp*Ti)$_4$(μ_3-N)$_4$ (av 1.939 Å),[119] and are very similar to the theoretically calculated Ti-N single bond distance (1.981 Å).[121]
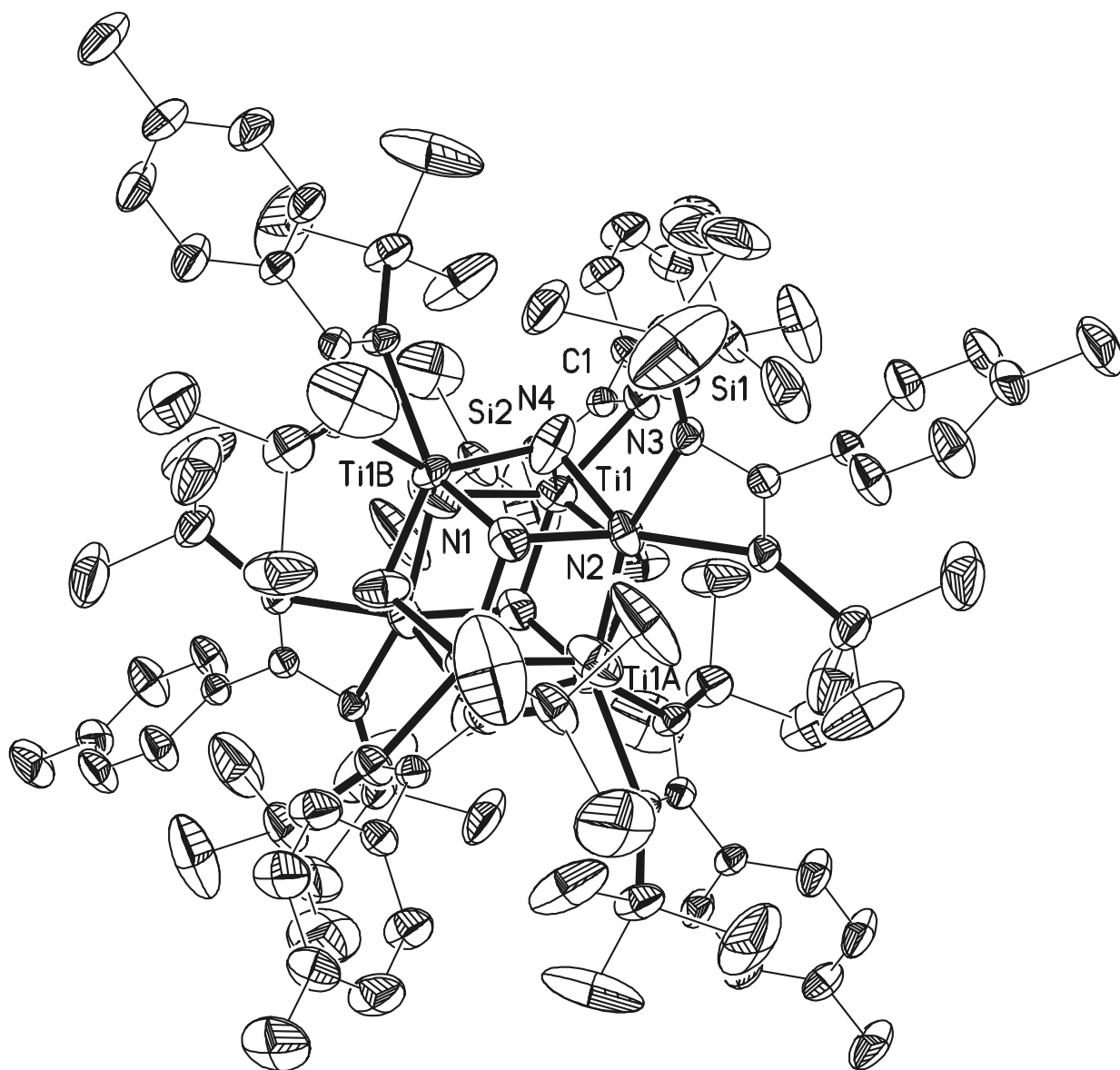
Figure 9. Molecular structure of [{*p*-MeC$_6$H$_4$C(NSiMe$_3$)$_2$Ti}$_6$(μ_3-NH)$_6$(μ_3-N)$_2$·6(C$_7$H$_8$)] (10) (50% probability ellipsoids. Toluene molecules and H atoms bonded to C and N are omitted for clearity)
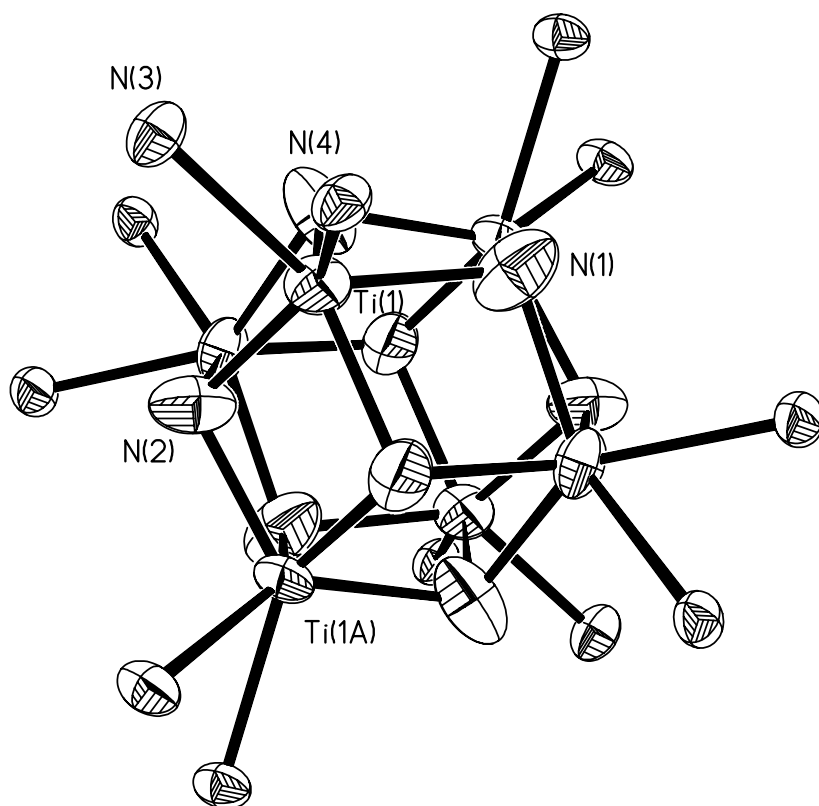
**Figure 10. Central Core of [{*p*-MeC$_6$H$_4$C(NSiMe$_3$)$_2$Ti}$_6$(μ_3-NH)$_6$(μ_3-N)$_2$·6(C$_7$H$_8$)] (10) (50 %
probability ellipsoids)**

Table 5. Selected Bond Lengths (Å) and Angles (°) for 10

Ti (1)-N(2)	1.958(5)	Ti(1)-N(1)	1.998(6)
Ti(1)-N(1A)	2.003(6)	Ti(1)-N(1B)	2.014(5)
Ti(1)-N(4)	2.193(4)	Ti(1)-N(3)	2.196(4)
N(2)-Ti(1)-N(1)	123.5(3)	N(2)-Ti(1)-N(1A)	78.6(2)
N(1)-Ti(1)-N(1A)	75.2(2)	N(2)-Ti(1)-N(1B)	78.3(2)
N(1)-Ti(1)-N(1B)	75.0(2)	N(1A)-Ti(1)-N(1B)	122.1(4)
Ti(1C)-Ti(1)-Ti(1D)	60.0	Ti(1C)-Ti(1)-Ti(1B)	90.0
Ti(1D)-Ti(1)-Ti(1B)	60.94(2)	Ti(1C)-Ti(1)-Ti(1A)	60.94(2)
Ti(1D)-Ti(1)-Ti(1A)	90.0	Ti(1B)-Ti(1)-Ti(1A)	58.12(4)

The compound **10** involving the benzamidinato-ligand shows the interesting symbiosis between symmetry effects in the cluster and in the π bonding capabilities of the ligand.[122] First of all let us note that the $[L_6Ti_6N_8]$ core of the cluster including the terminal ligands is practically very close to the T_h symmetry. There are a total of 24 Ti-N surface bonds, with $a_g+a_u+e_g+e_u+3t_g+3t_u$ representation. To accomplish the same representation, the titanium uses the bonds of $1\sigma + 2\pi + 1\delta$ local symmetry, generating the group orbitals, $(a_g+e_g+t_u) + 2\ (t_g+t_u) + (a_u+e_u+t_g)$, respectively. The above parentheses correspond (in this order) to components of scalar spherical harmonics, self-conjugate $\Pi, \overline{\Pi}$ vector harmonics and to the odd $\overline{\Delta}$ ones. The key for the stability of the whole structure based on the terminal ligands that are offering the same symmetry composition of the bonding as those appearing in the $[Ti_6N_8]$ cluster. Namely, the L_6 set gives:

$(a_g+e_g+t_u)^{(in\ phase\ \text{combination of the lone pairs})} + (t_g+t_u)^{(out\ of\ phase\ \text{combination of the lone pairs})} + (t_g+t_u)^{inner\ \psi\ \text{orbitals}} + (a_u+e_u+t_g)^{homo\ \chi\ \text{orbitals}}$.

The χ combination, which is able to interact with $\delta(d)$ orbitals, plays the essential role in the whole structure. If another terminal ligand will be imagined, like cyclopentadienyl, its bonding will consist in a $1\sigma + 2\pi$ symmetry instead of a $1\sigma + 2\pi + 1\delta$, as that of the benzamidinato ligand. In a Cp-analogue the $(a_u+e_u+t_g)$ part of the cluster core will remain as an unstabilized set of nonbonding orbitals. The pseudo-Jahn-Teller interaction between odd and even orbitals will create the possibility for a τ_u distortion, separating the complex into two halves. Indeed a $[Cp_6Ti_6N_8]$ analogous of the discussed compound does not exist, but a compound of composition $[(Cp^*Ti)(\mu\text{-}NH)]_3(\mu_3\text{-}N)$ is known.[104]

Finally, another interesting feature is that each titanium atom in **10** is hexacoordinated in a trigonal prismatic mode. The reason is related to the symmetry factors, which are imposing this coordination pattern.

2.1.4. Synthesis and Characterization of Cp$^*_2$TiNH$_2$ (11)

This compound has been previously prepared from the reaction of Cp$^*_2$TiMe with NH_3 and only structurally characterized by Brady and co-workers.[123] In comparison, treatment of Cp$^*_2$TiCl with $NaNH_2$ in liquid ammonia and toluene at -78 °C yields titanium (III) amide Cp$^*_2$TiNH$_2$ (**11**, Scheme 11) in 27 % yield.[107]

$$Cp^*{}_2TiCl + NaNH_2 \xrightarrow[-78\ °C]{\text{liq } NH_3,\ \text{toluene}} Cp^*{}_2TiNH_2 + NaCl$$

$$\mathbf{11}$$

Scheme 11
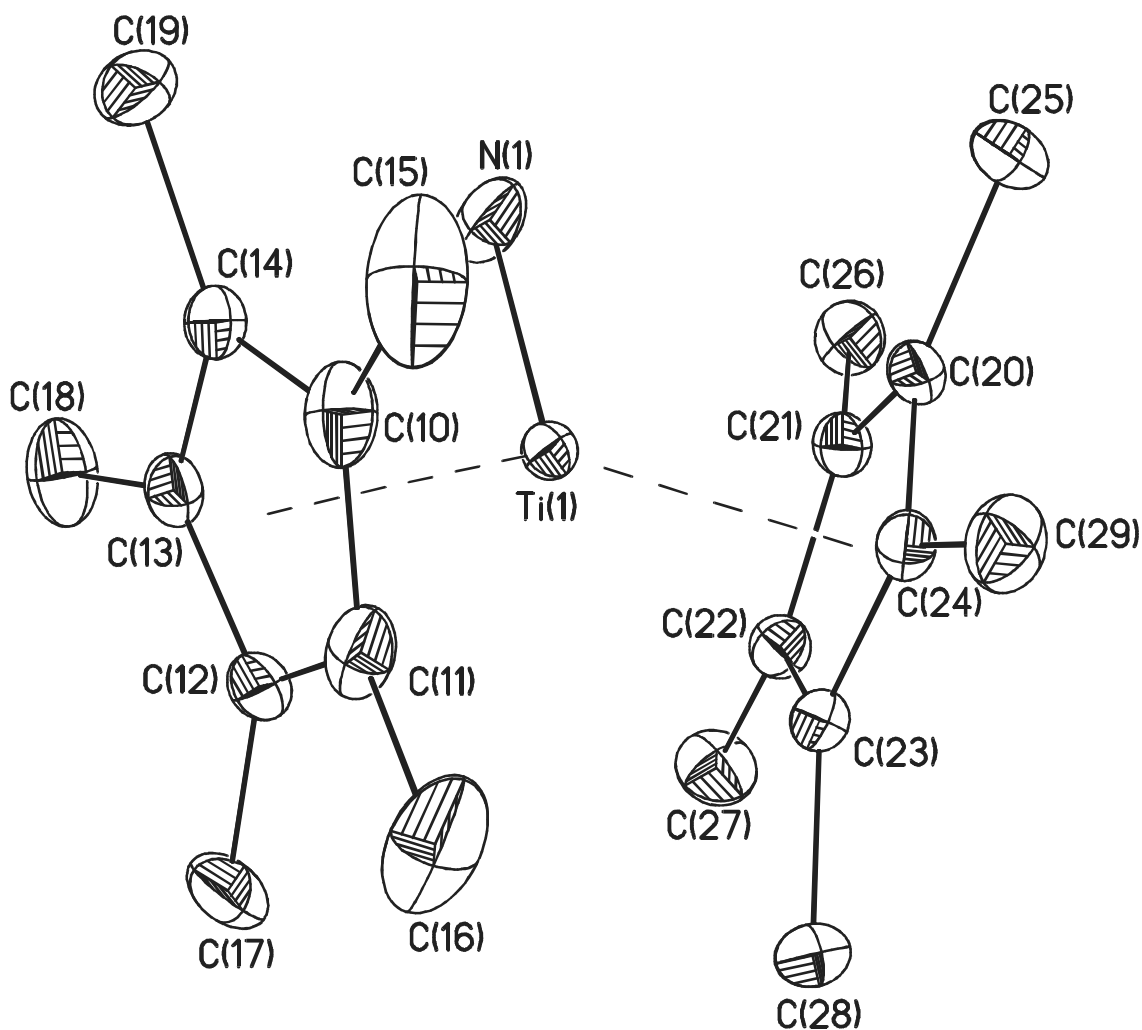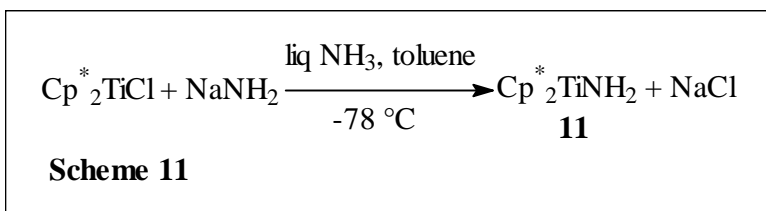
Figure 11. Molecular structure of Cp$^*{}_2$TiNH$_2$ (11) (50 % probability ellipsoids. H atoms bonded to C and N are omitted for cleariry)

Compound **11** (molecular structure is shown in Figure 11) is a black crystalline solid with a melting point of 202 °C. The IR spectrum of **11** shows a broad absorption at 3437 cm^{-1}, assignable to the NH$_2$ stretching frequency. Due to the paramagnetism of titanium(III), the ^{1}H NMR spectrum

of **11** recorded at room temperature shows broad and unresolved signals. The most intense peak in the EI mass spectrum of **11** appears at *m/z* 317 [$M^+ - NH_2 - H$], and the signal at 334 (53 %) is assigned to the molecular ion.

2.2. Synthesis of a Metal Dinitrogen Complex in a Liquid Ammonia/Toluene Two Phase System

Dinitrogen metal complexes have long been interesting as modes for biological nitrogen fixation and intermediates in synthetic applications. Dramatic progress[124] has been made since the discovery of the first dinitrogen complex [$Ru(NH_3)_5(N_2)]^{2+}$ in 1965.[125] Figure 12 gives the various possible bonding modes of N_2 to metals.

The most examples of stable dinitrogen metal complexes have been found to belong to the terminal end-on type **VIII**, in which the N−N bonds are only slightly elongated (from 1.0976 Å in free N_2 to 1.11 − 1.12 Å). Another well-known coordination mode is type **IX**, in which two metals are bonded end-on to dinitrogen with the almost linear M-N-N-M linkage. The μ-η^1:η^1-N_2 complexes can be classified into three types containing the dinitrogen $(N_2)^0$ (**IX-a**), diazenido $(N_2)^{2-}$ (**IX-b**), or hydrazido $(N_2)^{4-}$ (**IX-c**) ligand, respectively.
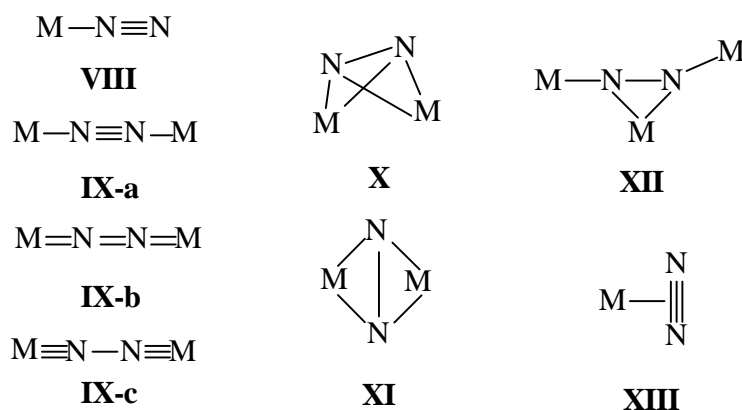
Figure 12. Binding modes of N_2 to metals

The N−N bond distances of N_2 complexes considered to have the character of type **IX-a** fall in the range 1.12 − 1.20 Å, while the N−N bonds in those represented by type **IX-c** are much longer and fall in the range of 1.25 − 1.34 Å. The dinuclear zirconium complex [($Cp^*_2Zr(\eta^1$-$N_2)]_2(\mu$-η^1:η^1-N_2) consists of two terminal N_2 units (**VIII**, N−N 1.116 (8) and 1.114(7) Å, respectively) and

one bridging μ-η^1:η^1-N$_2$ unit (**IX-a**, N–N 1.182(5) Å).[126] Other examples of type **IX** compounds are [(PhMe$_2$P)$_3$WI·(NC$_5$H$_5$)](μ-η^1:η^1-N$_2$)(ZrCp$_2$Cl) (**IX-b**, N–N 1.24(2) Å)[127] and [{iPr$_2$PCH$_2$SiMe$_2$)$_2$N}ZrCp]$_2$(μ-η^1:η^1-N$_2$) (**IX-c**, N–N 1.301(3) Å).[128]

The dinuclear titanium complex [{(Me$_3$Si)$_2$N}$_2$Ti]$_2$(μ-η^2:η^2-N$_2$)$_2$[Li(TMEDA)] (**X**) with a folded M$_2$N$_2$ ring exhibits a remarkable long N–N bond (1.38(2) Å).[129] The side-on bridged N$_2$ zirconium complex [(PhP(CH$_2$SiMe$_2$NSiMe$_2$CH$_2$)$_2$PPh)Zr]$_2$(μ-η^2:η^2-N$_2$) with a planar M$_2$N$_2$ moiety (**XI**) has a long N–N bond distance of 1.43(1) Å.[130] A type **XII** N–N bond (1.30(1) Å) has been found in the titanium compound [{C$_{10}$H$_8$)Cp$_2$Ti$_2$}{(C$_5$H$_4$)Cp$_3$Ti$_3$}(μ_3-η^1:η^1:η^2-N$_2$)].[131] The complex Cp$_2$Zr(CH$_2$SiMe$_3$)(η^2-N$_2$) was suggested to contain the η^2-N$_2$ side-on coordination to a single metal center (**XIII**) on the basis of EPR and IR data.[132] The interaction of Na$^+$ cation with the N$_2$ ligand has been demonstrated in the vanadium complex [Na(Diglyme)$_2$]$^+$[{(mes)$_2$V(mesNa)}$_2$(μ_3-η^1:η^1:η^2-N$_2$)]$^-$ (mes = 2, 4, 6-Me$_3$C$_6$H$_2$) obtained by treatment of V(mes)$_3$·(THF) with Na. The analogous reaction with K led to [K(Diglyme)$_2$]$^+$[{(mes)$_3$V}$_2$(μ-η^1:η^1-N$_2$)]$^-$, no interaction of K$^+$ cation with N$_2$ ligand was observed.[133] Dinitrogen contacts to Na$^+$ and Li$^+$ is observed in [Ph{NaO(Et)$_2$}$_2$(Ph$_2$Ni)$_2$N$_2$NaLi$_6$(OEt)$_4$·O(Et)$_2$]$_2$,[134] in which the N$_2$ ligands are bound side-on to nickel atoms. The two (Ph$_2$Ni)$_2$N$_2$ units are linked by two Na atoms and two Li$_6$(OEt)$_4$·O(Et)$_2$ groups. End-on and side-on coordination of N$_2$ to Li$^+$ was found in [(THF)$_2$Li(OEPG)Sm]$_2$(N$_2$Li$_4$) (OEPG = octaethylporphyrinogen).[135]

2.2.1. Synthesis and Characterization of the Imido Titanium(II)/Titanium(III) Potassium Dinitrogen Complex [(Cp*Ti)$_4$(μ_3-NH)$_4$(μ_4-η^1:η^1:η^2:η^2-N$_2$)$_2$K$_2$] (12)

Treatment of Cp$^*_2$TiCl with two equivs of K in liquid ammonia and toluene at -78 °C yields the imido Ti(II)/Ti(III) potassium dinitrogen complex [(Cp*Ti)$_4$(μ_3-NH)$_4$(μ_4-η^1:η^1:η^2:η^2-N$_2$)$_2$K$_2$] (**12**, Scheme 12). The loss of Cp* ligand during the preparation of **12** is similar to those found for the preparations of **4** and **10**, while the reduction of L′$_2$TiCl$_2$ by means of a solution of Na or K in liquid ammonia/toluene leads to the formation of L′$_3$Ti (**21**, see 2.5). Obviously, the Cp* ligand and the Ti(III) center are essential for the formation of **12**.

$$4 \, Cp^*_2TiCl + 8 \, K \xrightarrow[- 78 \, °C]{\text{liq } NH_3, \text{ toluene}} [(Cp^*Ti)_4(\mu_3\text{-}NH)_4(\mu_4\text{-}\eta^1{:}\eta^1{:}\eta^2{:}\eta^2\text{-}N_2)K_2]$$

12
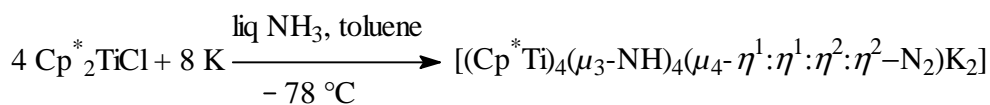
Scheme 12

Compound **12** is a black crystalline solid. No obvious decomposition was observed until 300 °C. Due to its high sensitivity, the decomposition of solid **12** was observed in a glove-box in one week (the black solid became white on the surface). The IR spectrum of **12** shows weak and broad absorptions at 3353 and 2046 cm^{-1}, assignable to the N-H and N≡N stretching frequency, respectively. The ^{1}H NMR spectrum of **12** shows broad and unresolved signals due to the paramagnetism of titanium(II) and titanium(III). The fragments [M$^+$ − 2K − 3 NH], [M$^+$ − 2 K − 2 NH − N$_2$ − H] and [Cp^{*+} − Me − H] in the EI mass spectrum of **12** were observed at *m/z* 803 (9 %), 789 (16 %) and 119 (100 %), respectively. The elemental analysis of **12** shows that the contents of C, H and N are lower than expected for **12** due to its easy decomposition.

The structure of **12** has been determined by X-ray analysis. The molecular structure and the central inorganic core of **12** are shown in Figures 13, and 14, respectively. Selected bond lengths and angles for **12** are given in Table 6. Compound **12** crystallizes in the tetragonal space group *I*4$_1$/*a*. The molecular structure of **12** consists of two distorted four-membered (Cp*Ti)$_2$(NH)$_2$ rings which are bridged by a slightly distorted octahedral K$_2$(N$_2$)$_2$ moiety placed on a symmetric center of **12** with four Ti−(μ-η^1:η^1-N$_2$) and four K−NH bonds. The coordination sphere of each titanium is completed by a Cp* ligand. Two of the end-on dinitrogen ligands further interact with two K$^+$ in a side-on manner, two potassium atoms are centrosymmetrically oriented towards the two sides of the plane formed by the two parallel N$_2$ molecules. The K−N−K angles in the K$_2$(N$_2$)$_2$ moiety are 100.8(3)° and 104.7(3)°, the angles between the two planes in the folded K$_2$N$_2$ ring are 107° (Figure 13). The side-on geometry of the coordinated N$_2$ molecules in the K$_2$(N$_2$)$_2$ unit is similar to that found in Ti(I)/Ti(II) amido complex [{(Me$_3$Si)$_2$N}$_2$Ti]$_2$(μ-η^2:η^2-N$_2$)$_2$[Li(TMEDA)].[129]

The Ti-N bond lengths (from 1.993(10) Å to 2.135((10) Å, av 2.068 Å) to the imido ligands in **12** are larger than those found in [(L'Ti)$_6$(μ_3-NH)$_6$(μ_3-N)$_2$·6(C$_7$H$_8$)] (1.993 Å),[120] [(Cp*Ti)$_3$(μ-NH)$_3$(μ_3-N)] (1.924 Å),[104] (Cp*Ti)$_4$(μ_3-N)$_4$ (1.939 Å),[119] and the theoretically calculated Ti-N

single bond distance (1.981 Å),[121] respectively, due to the low valence of titanium and end-on coordination of N_2 to titanium.

The Ti–N bond lengths (1.777(10) to 1.801(10) Å, av 1.789 Å) and the Ti–N–N angles (172.8(8) to 178.7(9) Å, av 175.8 Å) to the μ_4-N_2 ligands are similar, while the N–N bond distances (1.308(13) Å) are longer than those found in titanium(III) complex $(L''_2TiPy)_2(\mu$-η^1:η^1-$N_2)$ (L″ = $C_6H_5C(NSiMe_3)_2$, Ti–N 1.799 Å, N–N 1.264(5) Å, Ti–N–N 173.7°),[136] titanium(III) complex $(L''Ti)_2(\mu$-η^1:η^1-$N_2)$ (Ti–N 1.765 Å, N–N 1.275(6) Å, Ti–N–N 177.4°),[137] and in titanium(II) complex $[\{(Me_2Si)_2N\}TiCl(TMEDA)]_2(\mu$-$\eta^1$:$\eta^1$-$N_2)$ (Ti–N 1.762(5) Å, N–N 1.289(9) Å, Ti–N–N 168.5°),[129] respectively.
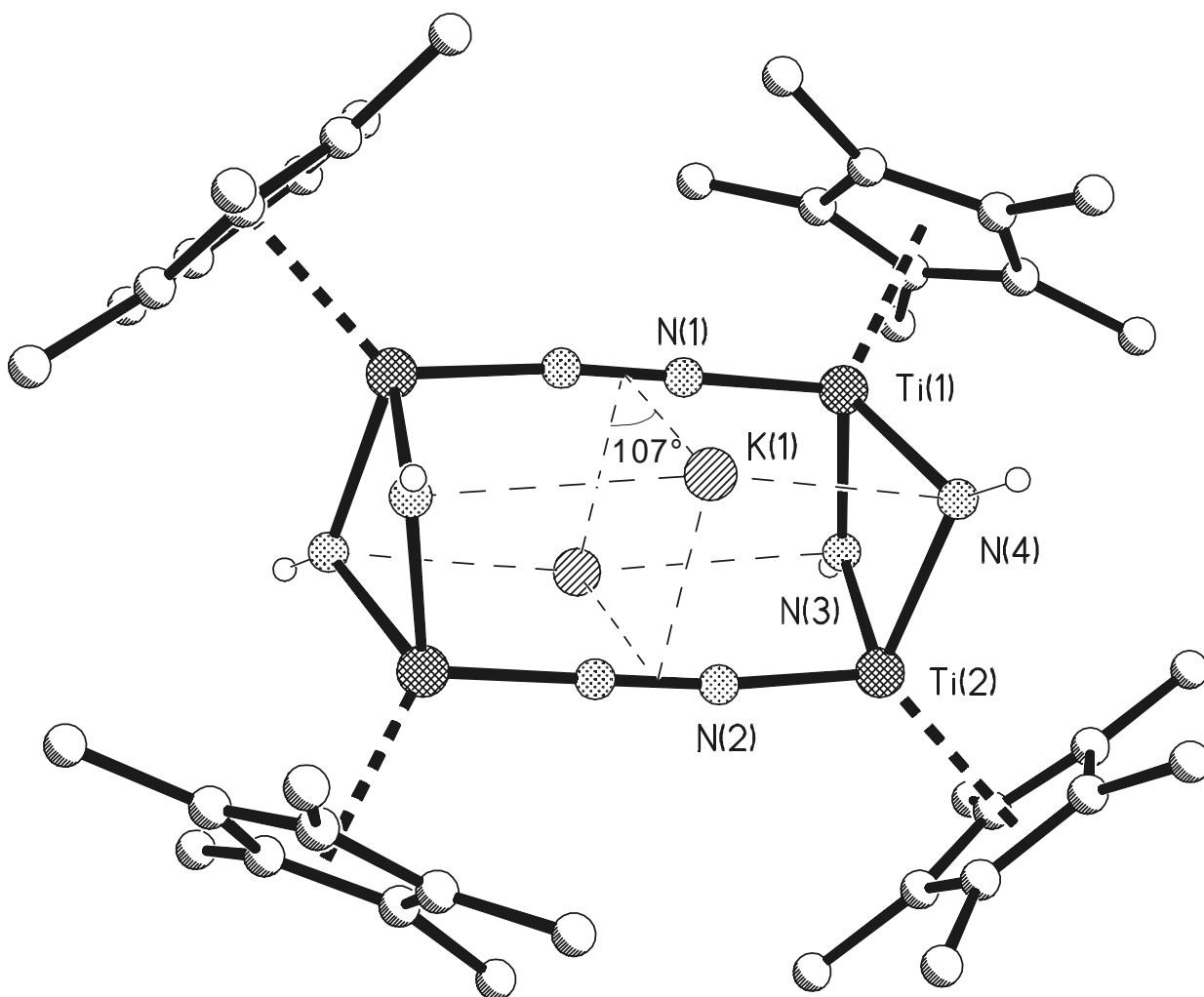
Figure 13. Molecular structure of $[(Cp^*Ti)_4(\mu_3$-$NH)_4(\mu_4$-η^1:η^1:η^2:η^2-$N_2)_2K_2]$ (12) (H atoms bonded to C are omitted for clearity)
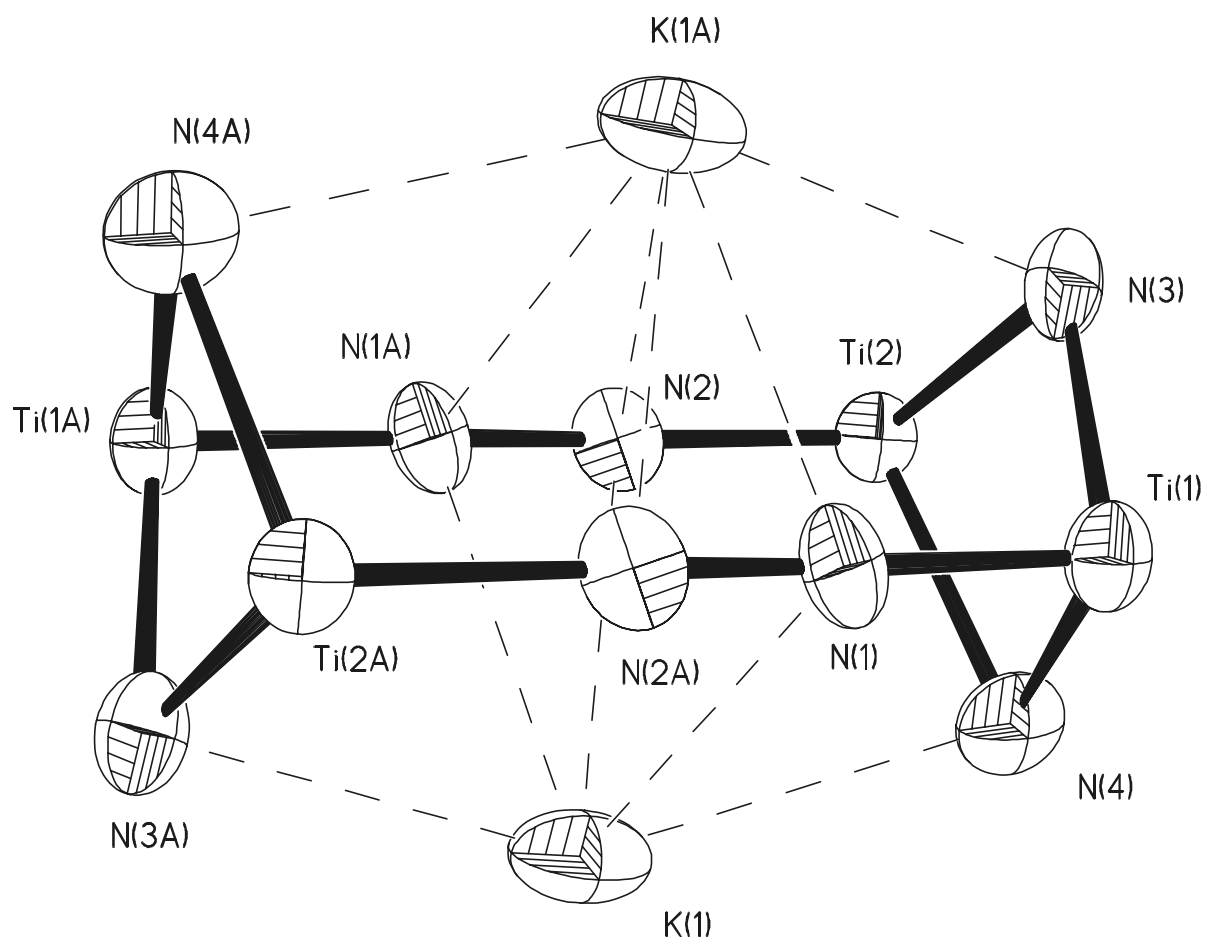
Figure 14. Central core of [(Cp*Ti)$_4$(μ_3-NH)$_4$(μ_4-η^1:η^1:η^2:η^2-N$_2$)$_2$K$_2$] (12) (50 % probability ellipsoids)

The N−N bond lengths are significantly longer than that found in titanium(II) complex (Cp*$_2$Ti)(μ-η^1:η^1-N$_2$) (1.160 Å)[138] and similar to those found in titanium(I)/titanium(II) complex [{(Me$_3$Si)$_2$N}$_2$Ti]$_2$(μ-η^2:η^2-N$_2$)$_2$[Li(TMEDA)] (1.379(2) Å).[129] The longer N−N bonds compared to those found in type **IX-a** complexes (N−N 1.12 − 1.20 Å) indicate that the N$_2$ molecules in **12** are highly reduced by end-on coordinated titanium atoms and side-on coordinated potassium atoms.

The K−N bond distances (2.839(10) to 2.993(11) Å, av 2.916 Å) to the imido ligands are longer than the K−N bond distances (2.709(9) to 2.816(11) Å, av 2.753 Å) to the side-on N$_2$ ligands and those found in [KN(SiMe$_3$)$_2$]$_2$ (2.770(3) Å and 2.803(3) Å, av 2.787 Å)[139] due to the electron donating bonds between the side-on N$_2$ ligands and the potassium atoms. The shorter

K–C distances (e.g. K(1)–C(2B) 2.92(3) Å, K(1)–C(3'B) 2.854(4) Å, K(1)-C(3B) 3.09(2) Å, K(1)-C(2'B) 3.12(6) Å) indicate additional weak bonding interactions between potassium atoms and the neighboring methyl units on the cyclopentadienyl rings in **12**.

Table 6. Selected Bond Lengths (Å) and Angles (°) for 12

Ti(1)-N(1)	1.777(10)	Ti(1)-N(3)	1.993(10)
Ti(1)-N(4)	2.135(10)	Ti(2)-N(2)	1.801(10)
Ti(2)-N(3)	2.016(9)	Ti(2)-N(4)	2.126(10)
N(2)-N(1A)	1.308(13)	N(1)-N(2A)	1.308(13)
K(1)-N(1)	2.709(9)	K(1)-N(1A)	2.725(10)
K(1)-N(2A)	2.764(9)	K(1)-N(2)	2.816(10)
N(3)-K(1A)	2.839(10	K(1)-N(4)	2.993(11)
K(1)-C(2B)	2.92(3)	K(1)-C(3'B)	2.85(4)
K(1)-C(3B)	3.09(2)	K(1)-C(2'B)	3.12(6)
N(1)-Ti(1)-N(3)	104.8(4)	N(1)-Ti(1)-N(4)	104.9(4)
N(2)-Ti(2)-N(3)	101.4(4)	N(2)-Ti(2)-N(4)	100.1(4)
N(3)-Ti(1)-N(4)	84.2(4)	N(3)-Ti(2)-N(4)	83.9(4)
Ti(1)-N(3)-Ti(2)	95.8(4)	Ti(2)-N(4)-Ti(1)	88.6(4)
N(3)-Ti(2)-Ti(1)	41.8(3)	N(4)-Ti(2)-Ti(1)	45.8(3)
N(2)-Ti(2)-Ti(1)	90.6(3)	N(2)-Ti(2)-K(1A)	49.9(3)
N(2)-Ti(2)-K(1)	46.8(3)	N(3)-Ti(2)-K(1A)	52.9(3)
N(4)-Ti(2)-K(1)	53.5(3)	N(1)-K(1)-N(1A)	75.3(3)
N(1)-K(1)-N(2A)	27.6(3)	N(1A)-K(1)-N(2A)	70.8(3)
N(1)-K(1)-N(2)	70.3(3)	N(1A)-K(1)-N(2)	27.3(3)
N(2A)-K(1)-N(2)	79.2(3)	N(2A)-N(1)-K(1)	78.5(6)
N(1A)-N(2)-K(1A)	73.8(6)	N(2A)-N(1)-K(1A)	80.2(6)
K(1)-N(1)-K(1A)	104.7(3)	K(1A)-N(2)-K(1)	100.8(3)
N(1A)-N(2)-K(1)	72.5(6)	N(1A)-N(2)-Ti(2)	172.8(8)
N(2A)-N(1)-Ti(1)	178.7(9)	Ti(2)-N(3)-K(1A)	92.6(3)
Ti(1)-N(3)-K(1A)	90.1(4)	Ti(1)-N(4)-K(1)	85.8(3)
Ti(2)-N(4)-K(1)	91.7(4)		

2.3. Syntheses of Polyoxo Metal Organic Clusters in a Liquid Ammonia/Toluene Two Phase System

Zirconium oxides have long been used as catalysts for the hydrogenation of carbon monoxide[140] and ethylene,[141] highly selective isomerization of 1-butene and the formation of 1-butene from 2-butanol or 2-butanamine,[142] and selective oxidation of hydroxyl containing organic compounds.[143] In general, complete hydrolysis of zirconium chlorides leading to zirconium oxides without residual chloride and hydroxide is difficult to achieve and only possible at very high temperatures. ZrO_2 is prepared by heating [$ZrOCl_2 \cdot 8H_2O$] at 1000 °C [144] or calcining zirconium hydroxide in O_2 at 500 °C.[140g,142a] Base-assisted hydrolysis of organozirconium chlorides results in the formation of organozirconium oxide complexes containing chloride or hydroxide ligands, such as [$(Cp_2ZrCl)_2(\mu\text{-}O)$],[71b] [$\{(Cp^*ZrCl)(\mu\text{-}OH)\}_3(\mu_3\text{-}OH)(\mu_3\text{-}O)\cdot2THF$],[76] and [$\{(Cp^*ZrCl)(\mu\text{-}OH)\}_3(\mu_3\text{-}O)(\mu\text{-}Cl)$].[77] To the best of our knowledge so far no larger aggregate of an organozirconium oxide has been isolated or detected.

As discussed in section 2.1, some interesting progress has been achieved from the reaction of early transition metal compounds in the liquid ammonia/toluene two phase system. Recently we reported on the reaction of [L'_2TiCl_2] [$L' = p\text{-}MeC_6H_4C(NSiMe_3)_2$] with $NaNH_2$ in liquid ammonia/toluene to yield [$(L'Ti)_6(\mu_3\text{-}N)_2(\mu_3\text{-}NH)_6\cdot6(C_7H_8)$],[120] and the formation of [$\{(MeC_5H_4)Zr\}_5(\mu_5\text{-}N)(\mu_3\text{-}NH)_4(\mu\text{-}NH_2)_4$] from the reaction of [$(MeC_5H_4)_2ZrCl_2$] with K in liquid ammonia/toluene.[106] The imido bridged dinuclear zirconium complex [$(\eta^3\text{-}L)Zr(\mu\text{-}NH)$]$_2$ (L = (tBuNP)$_2$(tBuN)$_2$)) was obtained by treating $LZrCl_2$ with KH in liquid ammonia/toluene.[113] These results prompted us to attempt the complete hydrolysis of metal chlorides, which otherwise is difficult to achieve under base-assisted conditions at low temperatures.

2.3.1. Synthesis and Characterization of the Polyoxozirconium Cluster [$\{(EtMe_4C_5)Zr\}_6(\mu_6\text{-}O)(\mu_3\text{-}O)_8\cdot(C_7H_8)$] (13)

The reaction of [$(EtMe_4C_5)ZrCl_3$] with H_2O (1 : 1.5 molar ratio) in toluene at room temperature with successive treatment by KH (1 : 3 molar ratio) in liquid ammonia/toluene at -78 °C proceeds via complete removal of chloride and the formation of the organozirconium oxide [$\{(EtMe_4C_5)Zr\}_6(\mu_6\text{-}O)(\mu_3\text{-}O)_8\cdot(C_7H_8)$] (13, Scheme 13).[145] A proposed mechanism for the formation of 13 is given in Scheme 14. The first step of the reaction involves the formation of the water adduct 14 (eq 11) and subsequent hydrogen chloride elimination under formation of

ammonium chloride. In the presence of KH, NH_4Cl is converted to KCl and hydrogen (eq 12). On the other hand KH reacts with ammonia under formation of KNH_2 and hydrogen (eq 13).[114] In the reaction of [(EtMe$_4$C$_5$)ZrCl$_3$] with H_2O only in liquid ammonia/toluene, **13** was not formed. Excess ammonia does not result in a complete hydrolysis of [(EtMe$_4$C$_5$)ZrCl$_3$]. Partial hydrolysis and ammonolysis have been also observed in the base-assisted hydrolysis of Cp*ZrCl$_3$[76,77] and the ammonolysis of ZrX$_4$ (X = Cl, Br) in liquid NH$_3$.[146] Moreover, we have shown that KNH_2 reacts with a compound containing a Zr−Cl bond to yield the intermediate **15** (eq 14).[106] Due to the Lewis acidity of the Zr(IV) center the OH group functions as an acid and this favors the formation of a further Zr−O bond (eq 15) rather than a Zr−N bond. Similar results have been obtained in the hydrolysis of [(Cp*$_2$HfH(NH$_2$)][115] and [(Cp*Ti)$_4$(μ_3-N)$_4$],[119] which led to [(Cp*$_2$HfH(OH)] and [(Cp*Ti)$_4$(μ-O)$_6$], respectively. Consequently, the addition of KH results in the complete hydrolysis of [(EtMe$_4$C$_5$)ZrCl$_3$]. Certainly, equations 11 − 14 are over simplified and other side reactions might occur. Obviously the KH has two functions in this reaction, it completely converts the chloride to KCl and the resulting ZrOH and ZrNH$_2$ to ZrOZr species via intermolecular ammonia and water elimination. It is well documented that Zr−Cl, Zr−OH and Zr−NH$_2$ compounds can be isolated when no KH is present in the reactions.[76,77,106] The two phase system ammonia/toluene increases the solubility of the organic and inorganic components, so that the reaction preferentially occurs at the interface. Therefore we assume that the presence of KH and the *in situ* formation of ZrNH$_2$ as well as the liquid ammonia/toluene two phase system are essential for the formation of **13**.

$$6 \text{ [(EtMe}_4\text{C}_5\text{)ZrCl}_3] + 9 \text{ H}_2\text{O} \xrightarrow[\substack{\text{2. 18 KH, liq NH}_3, \\ \text{toluene, -78 °C}}]{\substack{\text{1. toluene, RT, 2 h}}} [\{(\text{EtMe}_4\text{C}_5)\text{Zr}\}_6(\mu_6\text{-O})(\mu_3\text{-O})_8 \cdot (\text{C}_7\text{H}_8)] + 18 \text{ KCl} + 18 \text{ H}_2$$

13
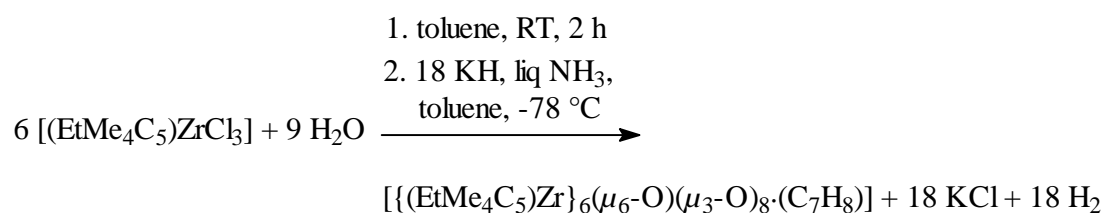
Scheme 13

Scheme 14
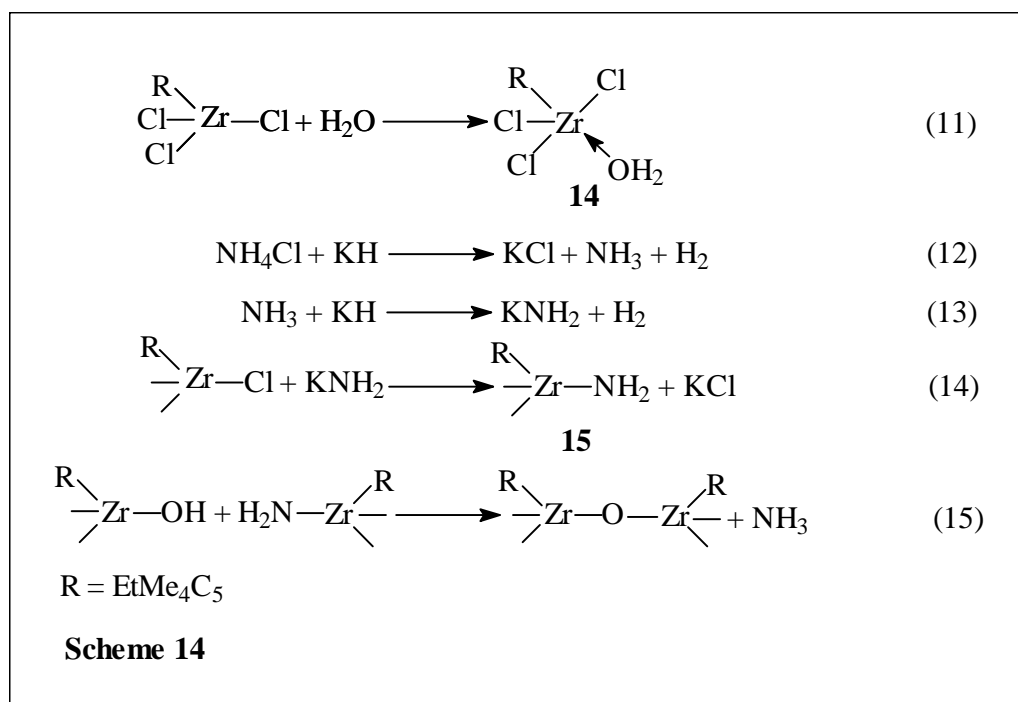
Compound **13** is a colorless crystalline solid with unusual thermal stability. Its melting point exceeds 410 °C. It is very stable to H_2O and O_2, no reaction was observed on exposing the toluene solution of **13** and H_2O or air. The most intense peak in the EI mass spectrum of **13** appears at *m/z* 1437 $[M^+ - C_7H_8 - EtMe_4C_5]$, and the signal at 1586 (4 %) is assigned to the $[M^+ - C_7H_8]$ fragment. The ^1H NMR spectral data are consistent with the structure of **13**. The integrated spectrum displays a triplet at δ 1.08 ppm ($^3J = 7.5$ Hz) and a quartet at δ 2.74 ppm ($^3J = 7.5$ Hz) with the intensity ratio of 3 : 2, corresponding the Me and CH_2 protons of the Et group on the cyclopentadienyl rings. The protons of the Me groups on the cyclopentadienyl ring resonate as two singlets at δ 2.23 and 2.17 ppm.

Single crystals of **13** suitable for X-ray structure analysis were obtained from toluene by keeping the reaction mixtures at 0 °C for one week. The molecular structure and the central inorganic core of **13** are shown in Figures 15 and 16, respectively. Compound **13** crystallizes in the triclinic space group $P\bar{1}$. The molecular structure of **13** in the crystal consists of an octahedron with $(EtMe_4C_5)Zr$ fragments arranged around an interstitial oxygen atom. Eight of the faces of the octahedron are topped each by oxygen resulting in twelve four-membered Zr_2O_2 rings. The average O–Zr–O and Zr–O–Zr angles in the Zr_2O_2 rings are 81.34° and 94.65°, respectively. The coordination sphere of each zirconium is completed by the ligand $EtMe_4C_5$. The Zr–(μ_3-O) bond

lengths (2.136(2) Å to 2.169(2) Å, av 2.156 Å) are similar to those found in [{(Cp*ZrCl)(μ-OH)}$_3$(μ_3-OH)(μ_3-O)·2THF] (Zr–(μ_3-O) (2.134 Å))[76] and in [{CpZr(μ-OH)}$_3$(μ_3-O)(μ-C$_6$H$_5$COO)$_3$]$^+$ (Zr–(μ_3-O) (2.071(11) Å)),[147] whereas the Zr–(μ_6-O) bond distances (2.231(2) Å to 2.247(2) Å, av 2.241 Å) are distinctively larger. Moreover the Zr–(μ_3-O) and Zr–(μ_6-O) bond lengths are longer than the Zr–(μ-O) bond distances found in [(Cp$_2$ZrCl)$_2$(μ-O)] (1.945(3) Å),[71b] [(Cp$_2$ZrMe)$_2$(μ-O)] (1.948(1) Å),[71c] and [{Cp$_2$Zr(μ-O)}$_3$] (1.959(3) Å),[82] respectively.
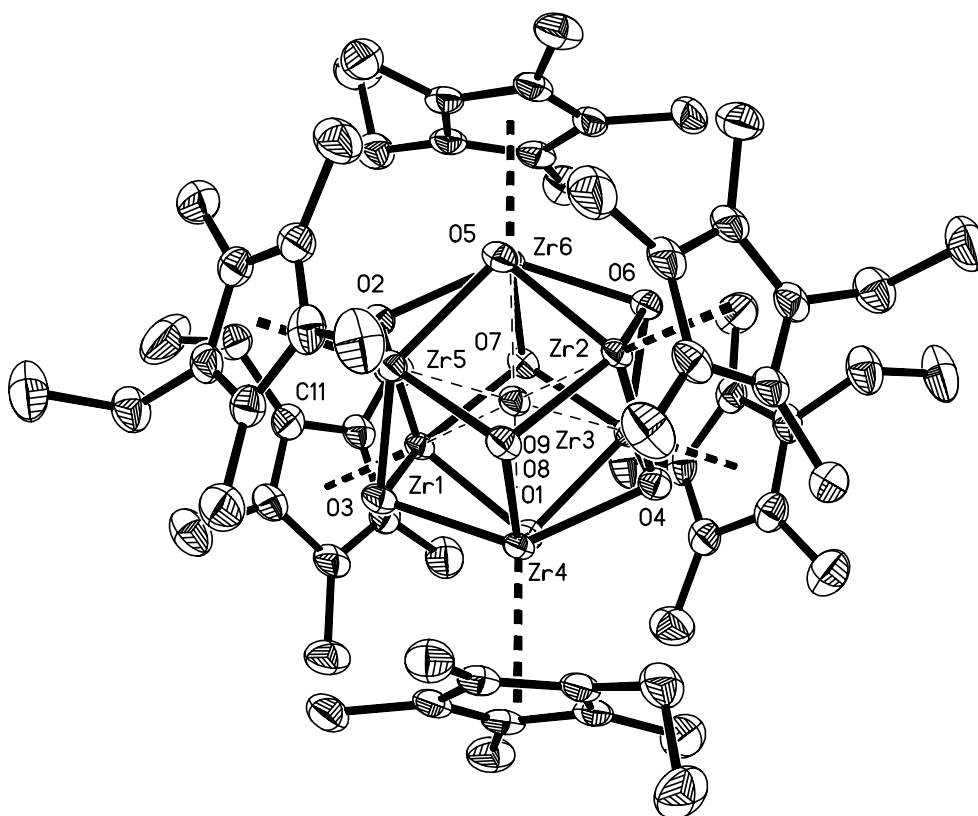
Figure 15. Molecular structure of [{(EtMe$_4$C$_5$)Zr}$_6$(μ_6-O)(μ_3-O)$_8$·(C$_7$H$_8$)] (13) (50% probability ellipsoids. Toluene molecule and H atoms bonded to C are omitted for clearity)
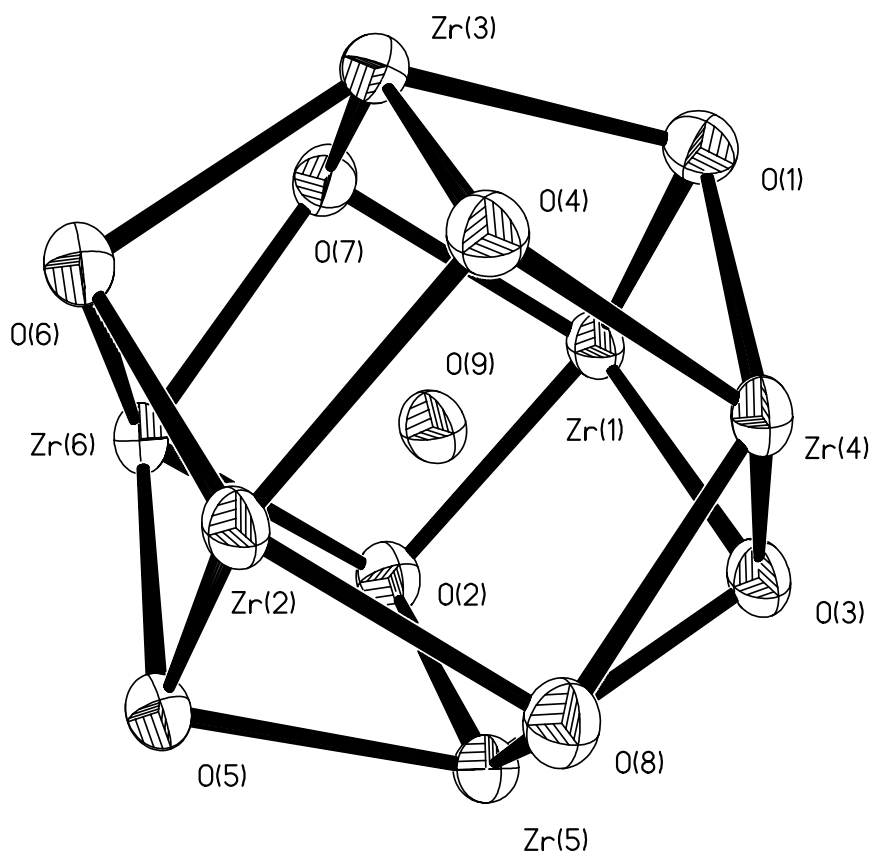
Figure 16. Central core of [{(EtMe$_4$C$_5$)Zr}$_6$(μ_6-O)(μ_3-O)$_8$·(C$_7$H$_8$)] (13) (50 % probability ellipsoids)

The Zr···Zr distances (3.1542(9) Å to 3.1709(11) Å, av 3.1635 Å) are comparable to those found in [{(MeC$_5$H$_4$)Zr}$_5$(μ_5-N)(μ_3-NH)$_4$(μ-NH$_2$)$_4$] (Zr$_a$···Zr$_b$ (3.1433(10) Å, Zr$_b$···Zr$_b$ (3.1566(8) Å), Zr$_a$ and Zr$_b$ represent the one apical and the four basal zirconium atoms of the square pyramidal cluster, respectively).[109] Furthermore the Zr···Zr distances are also similar to those exhibited by the zirconium halide clusters [KZr$_6$Cl$_{15}$C] (3.225 Å),[148] [CsZr$_6$I$_{14}$C] (3.283 Å),[149] [Zr$_6$Cl$_{12}$·K$_2$ZrCl$_6$] (3.201 Å),[150] and [Zr$_6$Cl$_{14}$B] (3.257 Å).[151]

Table 7. Selected Bond Lengths (Å) and Angles (°) for 13

Zr(1)–O(1)	2.136(2)	Zr(1)–O(3)	2.142(2)
Zr(1)–O(7)	2.165(2)	Zr(1)–O(2)	2.169(2)
Zr(2)–O(5)	2.150(2)	Zr(2)–O(6)	2.152(2)
Zr(2)–O(8)	2.155(2)	Zr(2)–O(4)	2.156(2)
Zr(3)–O(7)	2.149(2)	Zr(3)–O(6)	2.147(2)
Zr(3)–O(4)	2.158(2)	Zr(3)–O(1)	2.165(2)
Zr(1)–O(9)	2.241(2)	Zr(2)–O(9)	2.245(2)
Zr(3)–O(9)	2.237(2)	Zr(4)–O(9)	2.231(2)
Zr(5)–O(9)	2.246(2)	Zr(6)–O(9)	2.247(2)
Zr(1)–Zr(4)	3.1542(9)	Zr(1)–Zr(5)	3.1657(11)
Zr(2)–Zr(4)	3.1606(8)	Zr(2)–Zr(3)	3.1709(11)
Zr(3)–Zr(6)	3.1676(8)	Zr(5)–Zr(6)	3.1619(8)
O(1)–Zr(1)–O(3)	82.19(9)	O(1)–Zr(1)–O(7)	81.42(9)
O(3)–Zr(1)–O(2)	81.37(9)	O(7)–Zr(1)–O(2)	80.53(9)
Zr(1)–O(1)–Zr(4)	94.48(9)	Zr(1)–O(1)–Zr(3)	94.87(9)
Zr(4)–O(1)–Zr(3)	94.32(9)	Zr(6)–O(2)–Zr(1)	95.23(9)
Zr(5)–O(2)–Zr(1)	94.33(9)	Zr(6)–O(2)–Zr(5)	94.94(9)
Zr(1)–O(3)–Zr(5)	94.89(9)	Zr(1)–O(3)–Zr(4)	94.20(10)
Zr(4)–Zr(1)–Zr(5)	60.25(2)	Zr(4)–Zr(2)–Zr(3)	60.123(18)
Zr(1)–Zr(3)–Zr(6)	60.362(19)	Zr(6)–Zr(5)–Zr(1)	60.440(19)
Zr(1)–Zr(4)–Zr(2)	90.53(2)	Zr(5)–Zr(6)–Zr(3)	90.19(2)
Zr(1)–O(9)–Zr(4)	89.70(8)	Zr(1)–O(9)–Zr(6)	90.42(8)
Zr(1)–O(9)–Zr(2)	179.52(11)	Zr(1)–O(9)–Zr(3)	90.04(8)
Zr(1)–O(9)–Zr(5)	89.74(8)		

It is interesting to compare the coordination environment of Zr in **13** with that in monoclinic ZrO_2 (Figure 17).[152] **13** can be regarded as a derivative of ZrO_2. One $EtMe_4C_5$ ligand is sterically equivalent to three O_I positions, while the interstitial O coordinates to zirconium from the center of the plane formed by the four O_{II} atoms by enlarging the O_{II}–Zr–O_{II} angles (av 74.1° in ZrO_2). The

Zr–(μ_3-O) bond lengths in **13** are between the Zr–O_I (2.07 Å) and Zr–O_{II} (2.21 Å) bond lengths, while the Zr–(μ_6-O) bond lengths are comparable to those of Zr–O_{II}.
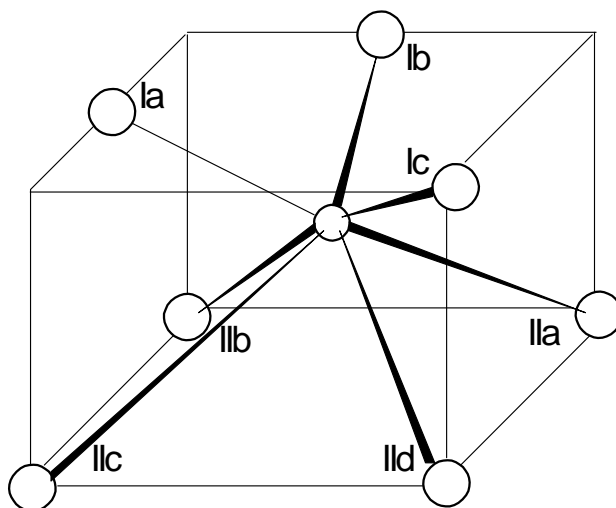
Figure 17. Monoclinic ZrO$_2$. Small circle = zirconium atom, large circles = oxygen atoms

2.3.2. Synthesis and Characterization of the Polyoxozirconium Cluster [{(EtMe$_4$C$_5$)Zr}$_6$(μ_6-O)(μ_3-O)$_8$·(C$_9$H$_{12}$)] (16)

In order to investigate the influence of the coordinating solvents in the crystalline state, cluster **16** was synthesized by recrystallizing **13** from excess mesitylene (Scheme 15).[145]

[{(EtMe$_4$C$_5$)Zr}$_6$(μ_6-O)(μ_3-O)$_8$·(C$_7$H$_8$)] $\xrightarrow[\text{– toluene}]{\text{mesitylene}}$ [{(EtMe$_4$C$_5$)Zr}$_6$(μ_6-O)(μ_3-O)$_8$·(C$_9$H$_{12}$)]

13   **16**

Scheme 15
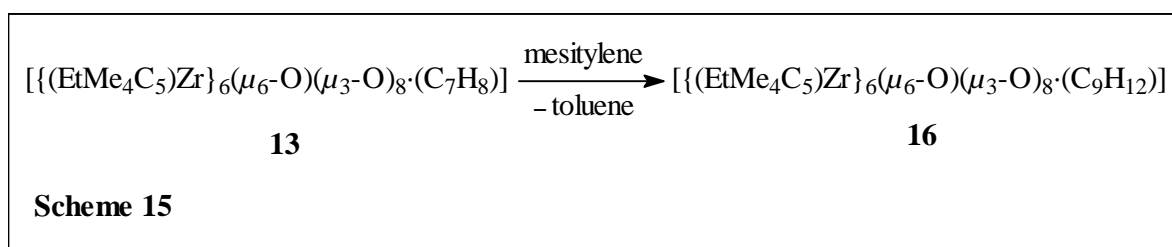
Compound **16** has the same thermal and hydrolytic stability as **13** and similar fragments in the EI mass spectrum.

Single crystals of **16** suitable for X-ray structural analysis were obtained from mesitylene by keeping the reaction mixture at 0 °C for one week. The molecular structure of **16** is shown in Figure 18. Compound **16** crystallizes in the monoclinic space group *C*2/*c*.
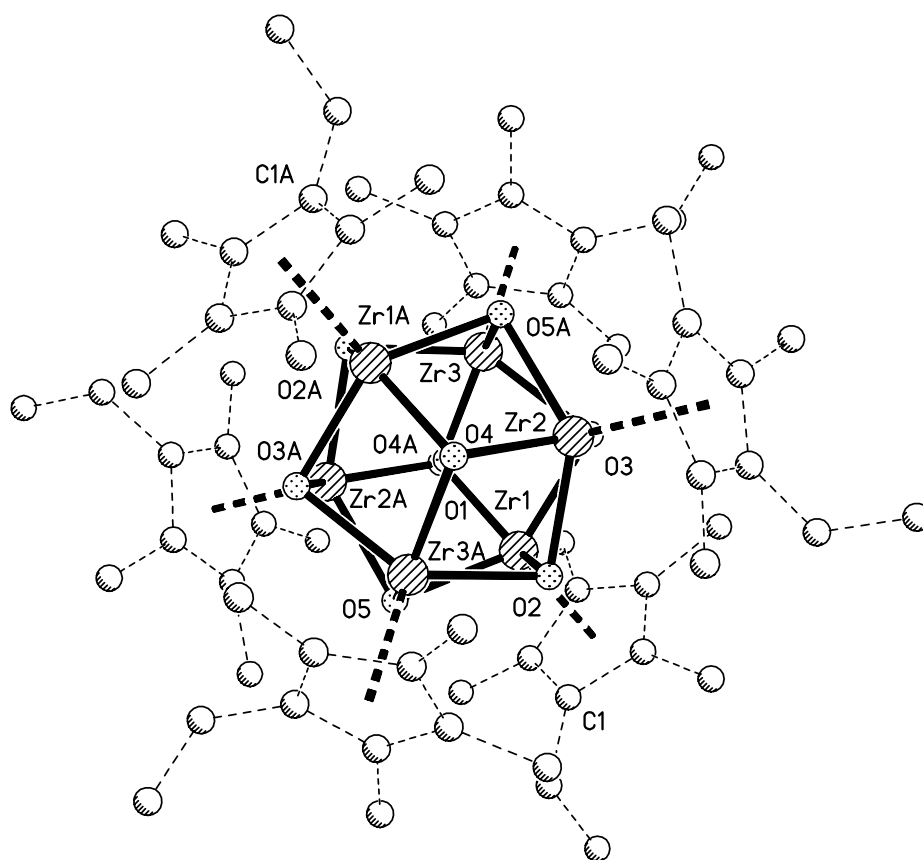
Figure 18. Molecular structure of [{(EtMe$_4$C$_5$)Zr}$_6$(μ_6-O)(μ_3-O)$_8$·(C$_9$H$_{12}$)] (16) (Mesitylene molecule and H atoms bonded to C are omitted for clearity)

The molecular structure of **16** in the crystal is more symmetrical than that of **13** due to the more symmetrically coordinated mesitylene in **16**, the central core is nearly the same as that of **16**. The bond lengths of Zr–(μ_3-O) (2.145(2) Å to 2.175(2) Å, av 2.163 Å) and Zr–(μ_6-O) (2.2407(4) Å to

2.2481(4) Å, av 2.2432 Å), the distances of Zr···Zr (3.1664(7) Å to 3.1728(7) Å, av 3.1687 Å), and the average O–Zr–O (81.35°) and Zr–O–Zr (94.61°) angles in the four-membered Zr_2O_2 rings in **16** are almost the same as those found in **13**, respectively.

Table 8. Selected Bond Lengths (Å) and Angles (°) for 16

Zr(1)–O(5)	2.145(2)	Zr(1)–O(4)	2.152(2)
Zr(1)–O(2)	2.168(2)	Zr(1)–O(3)	2.169(2)
Zr(2)–O(2)	2.147(2)	Zr(2)–O(3)	2.148(2)
Zr(2)–O(4A)	2.164(2)	Zr(2)–O(5A)	2.175(2)
Zr(3)–O(5A)	2.151(2)	Zr(3)–O(3)	2.156(2)
Zr(3)–O(4)	2.160(2)	Zr(3)–O(2A)	2.163(2)
Zr(1)–O(1)	2.2409(4)	Zr(2)–O(1)	2.2481(4)
Zr(3)–O(1)	2.2408(4)	O(1)–Zr(3A)	2.2407(4)
O(1)–Zr(1A)	2.2409(4)	O(1)–Zr(2A)	2.2481(4)
Zr(1)–Zr(3A)	3.1663(7)	Zr(1)–Zr(2)	3.1694(5)
Zr(2)–Zr(3)	3.1728(7)	Zr(3)–Zr(1A)	3.1664(7)
O(5)–Zr(1)–O(4)	81.66(8)	O(5)–Zr(1)–O(2)	81.48(8)
O(4)–Zr(1)–O(3)	81.40(8)	O(2)–Zr(1)–O(3)	80.99(8)
Zr(1)–O(4)–Zr(3)	94.69(8)	Zr(1)–O(4)–Zr(2A)	94.86(8)
Zr(2)–O(2)–Zr(1)	94.54(8)	Zr(3A)–O(2)–Zr(1)	93.95(8)
Zr(2)–O(3)–Zr(1)	94.47(8)	Zr(3)–O(3)–Zr(1)	94.34(8)
Zr(1)–O(5)–Zr(3A)	94.96(8)	Zr(1)–O(5)–Zr(2A)	94.76(8)
Zr(1)–Zr(2)–Zr(3)	60.012(12)	Zr(1A)–Zr(3)–Zr(1)	90.003(14)
Zr(3A)–Zr(1)–Zr(2)	60.160(12)	Zr(1A)–O(1)–Zr(1)	180.0
Zr(3A)–O(1)–Zr(1A)	90.098(14)	Zr(3)–O(1)–Zr(1A)	89.904(15)
Zr(3A)–O(1)–Zr(1)	89.903(14)	Zr(3)–O(1)–Zr(1)	90.095(15)

2.3.3. Synthesis and Characterization of the Polyoxozirconium Hydroxide [(Cp*Zr)$_6$(μ_6-O)(μ_3-O)$_4$(μ_3-OH)$_8$·2(C$_7$H$_8$)] (17)

Clusters **13** and **16** are a good model for ZrO$_2$ in solution, but they are too stable to be used for further reactions. In recent years, polyoxometalate-supported transition metal catalysts which can be fully investigated at the atomic level both structurally and mechanistically represent a new development of oxide-supported catalysts.[153] Organic polyoxozirconium-supported metal complexes are very rare. In accordance with this, a reactive organozirconium hydroxide cluster was considered to be prepared.

Treatment of Cp*ZrCl$_3$ with KOH containing 10-15% H$_2$O (1 : 1.5 molar ratio) in liquid ammonia and toluene at -78 °C which results in the complete removal of chloride and the formation of an organic polyoxozirconium hydroxide [(Cp*Zr)$_6$(μ_4-O)(μ-O)$_4$(μ-OH)$_8$]·2(C$_7$H$_8$) (**17**, Scheme 16).[154] The liquid ammonia affords the complete removal of the chloride and the formation of **17**. It is assumed that the formation of **17** proceeds via zirconium water adduct and hydroxide intermediates[145] which after inter- or intramolecular elimination of hydrochloride as NH$_4$Cl is converted to **17**. We were unable to isolate **17** from the reaction of Cp*ZrCl$_3$ with H$_2$O in liquid ammonia and toluene. Obviously, the KOH, H$_2$O, and the liquid ammonia system completely convert the chloride to KCl and the resulting ZrOH and Zr(OH$_2$) to ZrOZr and Zr(μ-OH)Zr species. Furthermore, the two phase system (ammonia/toluene) increases the solubility of the organic and inorganic components, so that the reaction preferentially proceeds at the interface.

$$6 \text{ Cp}^*\text{ZrCl}_3 + 9 \text{ KOH} + 4 \text{ H}_2\text{O} \xrightarrow{\text{liq NH}_3, \text{ toluene, - 78 °C}}$$

Scheme 16

$$[(\text{Cp}^*\text{Zr})_6(\mu_4\text{-O})(\mu\text{-O})_4(\mu\text{-OH})_8]\cdot 2(\text{C}_7\text{H}_8) + 9 \text{ KCl} + 9 \text{ NH}_4\text{Cl}$$

17
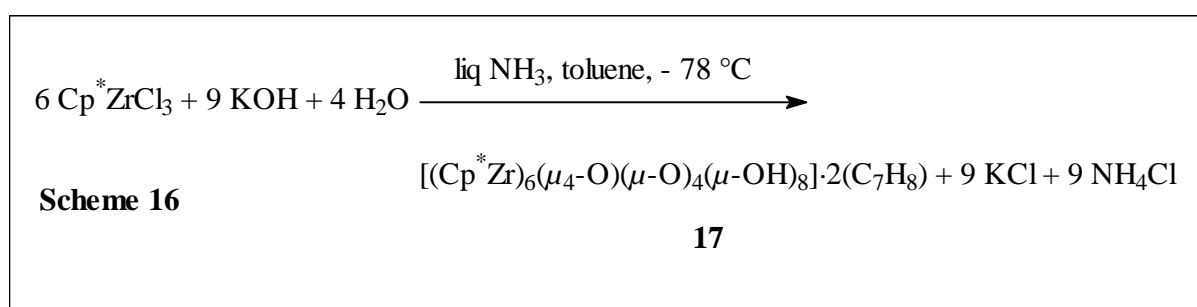
Compound **17** is a colorless crystalline solid with unusual thermal stability. The melting point of **17** exceeds 410 °C. The IR spectrum of **17** shows a broad absorption at 3689 cm^{-1}, assignable to the O-H stretching frequency. In the EI mass spectrum of **17**, the most intense peak appears at *m/z* 119 [Cp^{*+} − CH$_4$] and the signals at 1512 (18 %) and 1437 (56 %) are assigned to the [M$^+$ − C$_7$H$_8$ −

Cp^* – H_2O – H] and [M^+ – 2 C_7H_8 – Cp^* – 4 H_2O] fragments, respectively. The ^{1}H NMR of **17** exhibits a singlet (δ 2.05 ppm) for the Cp^* protons. No resonance corresponding to the protons of the OH group on zirconium is observed indicating a fast H/D exchange on the ^{1}H NMR time scale. The elemental analysis of **17** shows that the content of C and H is consistent with the formula [(Cp^*Zr)$_6$(μ_4-O)(μ-O)$_4$(μ-OH)$_8$]·2(C_7H_8).

Single crystals of **17** suitable for X-ray structural analysis were obtained from toluene by keeping the reaction mixture at room temperature for one month. The molecular structure and the central inorganic core of **17** are shown in Figures 19 and 20. Selected bond lengths and angles for **17** are shown in Table 9. Each molecule of **17** contains two molecules of toluene. Compound **17** crystallizes in the monoclinic space group *C*2/*m*.
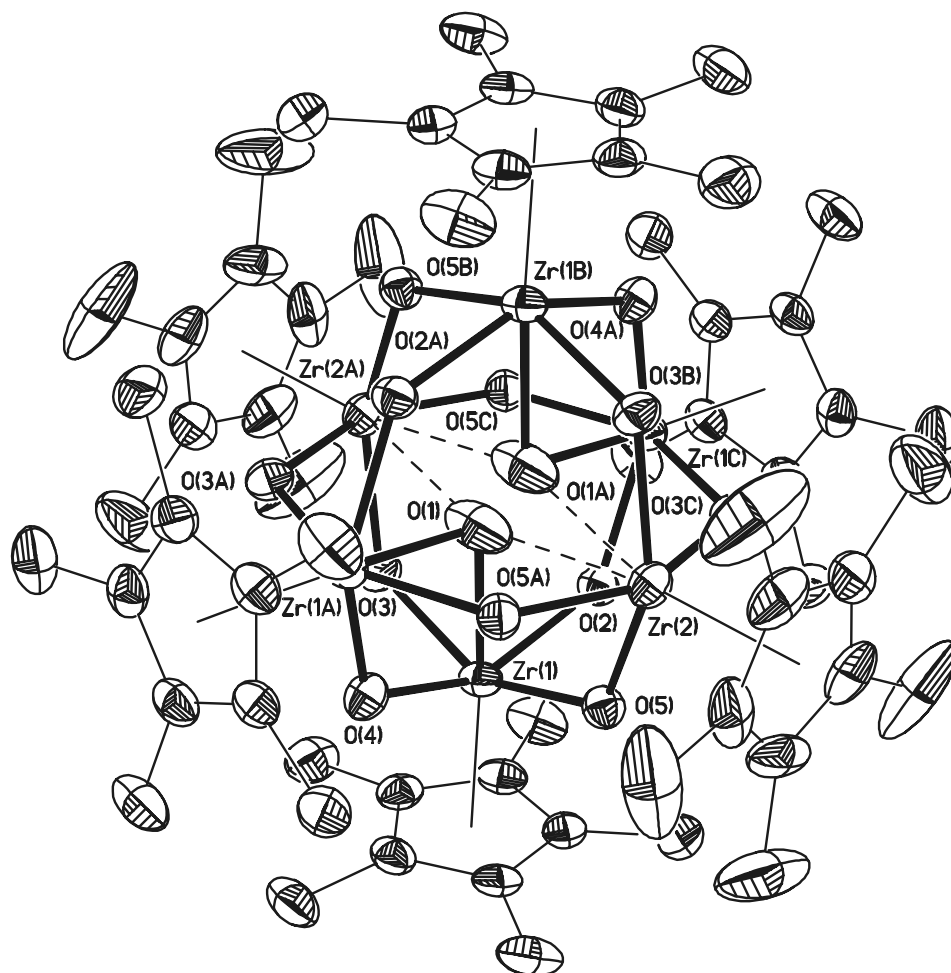
Figure 19. Molecular structure of [{(Cp^*Zr)$_6$(μ-O$_4$)(μ_3-O)$_4$(μ_3-OH)$_8$}·2(C_7H_8)] (17) (50% probability ellipsoids. Toluene molecules and H atoms bonded to C are omitted for clearity)
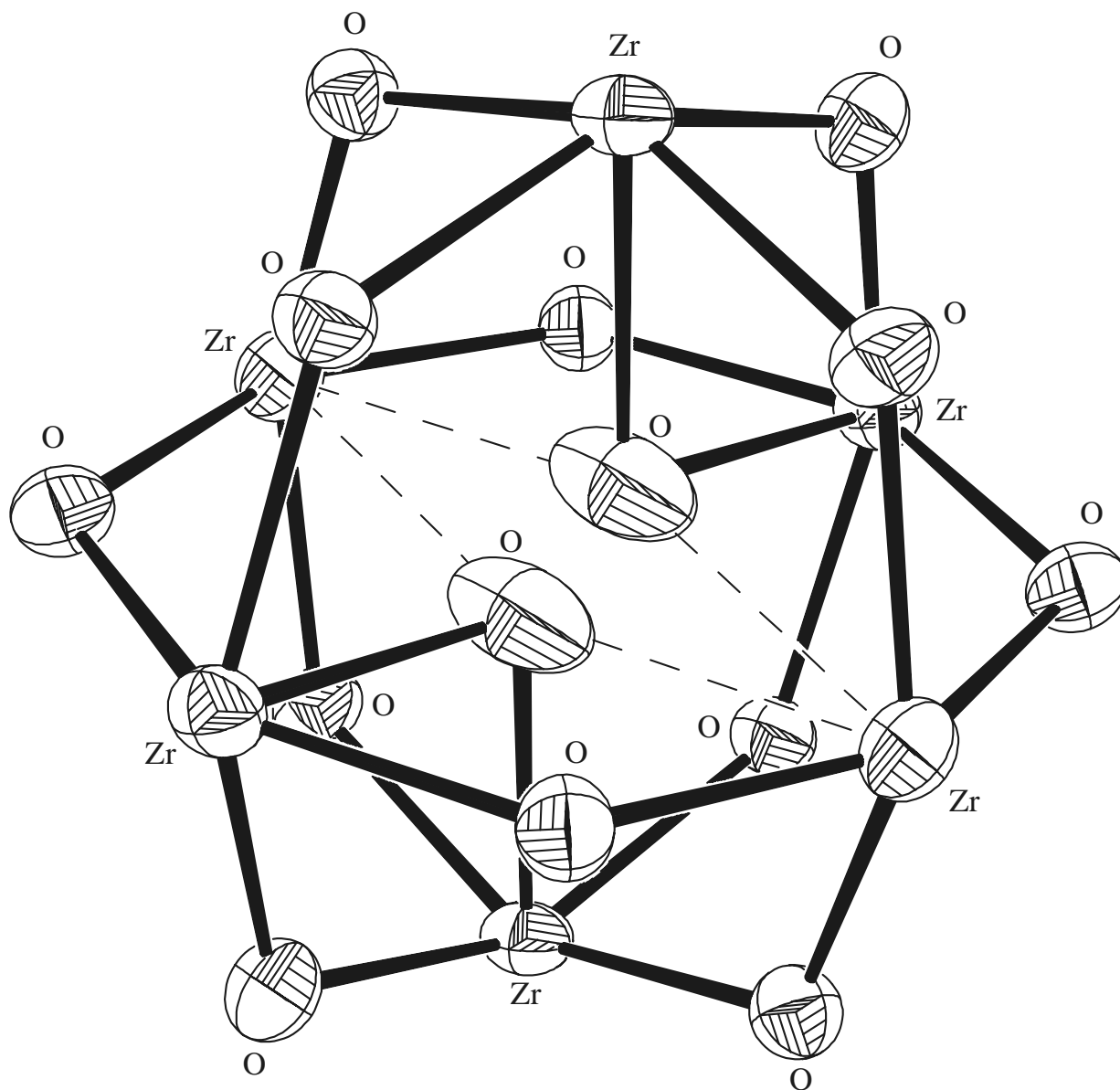
Figure 20. Central core of [{(Cp*Zr)$_6$(μ-O$_4$)(μ_3-O)$_4$(μ_3-OH)$_8$}·2(C$_7$H$_8$)] (17) (50 % probability ellipsoids)

The molecular structure of **17** in the crystal consists of an octahedron with Cp*Zr fragments arranged around an interstitial oxygen atom which occupies two positions, 0.933(13) Å away from each other. The angles between adjacent zirconium atoms are either 60° or 89°. Twelve of the edges of the octahedron are bridged each by oxygen resulting in eight six-membered Zr$_3$O$_3$ rings

with chair conformation. The average O–Zr–O and Zr–O–Zr angles in the Zr_3O_3 rings are 86.11° (82.76(6) to 88.94(10)°) and 120.56° (118.70(14) to 122.78(12)°). The eight hydroxide hydrogen atoms are statistically distributed over twelve edge positions, the occupancy being 0.67. The coordination sphere of each zirconium is completed by the Cp^* ligand.

The Zr–(μ-O) or Zr–(μ-OH) bond lengths (2.072(2) to 2.171(2) Å, av 2.106 Å) are similar to those in [{(Cp^*ZrCl)(μ-OH)}$_3$(μ_3-OH)(μ_3-O)]·2THF (Zr–(μ-OH) 2.160(2) Å).[76] Moreover the Zr–(μ-O) and Zr–(μ-OH) bond lengths are longer than those in [(Cp_2ZrCl)$_2$(μ-O)] (Zr–(μ-O) 1.945(3) Å)[71b] and [{Cp_2Zr(μ-O)}$_3$] (Zr–(μ-O) 1.959(3) Å),[82] and are comparable with the Zr–(μ_3-O) bond distances in [{(EtMe$_4$C$_5$)Zr}$_6$(μ_6-O)(μ_3-O)$_8$]·(C$_7$H$_8$) (2.136(2) to 2.169(2) Å, av 2.156 Å).[145]

Table 9. Selected Bond Lengths (Å) and Angles (°) for 17

Zr(1)–O(2)	2.171(2)	Zr(1)–O(3)	2.107(2)
Zr(1)–O(4)	2.072(2)	Zr(1)–O(5)	2.075(2)
Zr(2)–O(5)	2.081(2)	Zr(2)–O(5A)	2.081(2)
Zr(2)–O(3B)	2.130(2)	Zr(2)–O(3C)	2.130(2)
Zr(1C)–O(2)	2.171(2)	Zr(2A)–O(3)	2.130(2)
Zr(1)–O(1)	2.292(4)	Zr(1A)–O(1)	2.292(4)
Zr(2A)–O(1)	2.554(10)	Zr(2)–O(1)	2.610(10)
Zr(2)–O(1A)	2.554(10)	Zr(1A)–O(4)	2.072(2)
O(1)···Zr(1B)	2.966	Zr(1)···Zr(2)	3.608(1)
Zr(1)···Zr(1A)	3.564(1)	O(1)···O(1A)	0.933(13)
O(2)–Zr(1)–O(3)	82.76(6)	O(2)–Zr(1)–O(5)	83.39(6)
O(3)–Zr(1)–O(4)	88.35(9)	O(4)–Zr(1)–O(5)	88.94(10)
O(5)–Zr(2)–O(5A)	88.38(11)	O(5)–Zr(2)–O(3C)	85.93(8)
O(5A)–Zr(2)–O(3B)	85.93(8)	O(3B)–Zr(2)–O(3C)	85.20(11)
Zr(1)–O(3)–Zr(2A)	120.25(9)	Zr(1)–O(5)–Zr(2)	120.52(9)
Zr(1)–O(4)–Zr(1A)	118.70(14)	Zr(1)–O(2)–Zr(1C)	122.78(12)
Zr(1A)–Zr(1)–Zr(2)	60.401(12)		

The Zr···Zr distances (3.564(1) to 3.608(1) Å, av 3.586 Å) are significantly longer than those in $[\{(EtMe_4C_5)Zr\}_6(\mu_6\text{-}O)(\mu_3\text{-}O)_8]\cdot(C_7H_8)$ (3.1542(9) to 3.1709(11) Å, av 3.1635 Å) and those exhibited by the amidoimidonitrido zirconium complex[106] and the zirconium halide clusters.[148-151] The Zr(1)–O(1) (2.292(4) Å) and Zr(1A)–O(1) (2.292(4) Å) bond lengths are similar to those in $[\{(EtMe_4C_5)Zr\}_6(\mu_6\text{-}O)(\mu_3\text{-}O)_8]\cdot(C_7H_8)$ (Zr–$(\mu_6\text{-}O)$ 2.231(2) to 2.247(2) Å, av 2.241 Å). The longer distances of Zr(2)–O(1) (2.610(10) Å) and Zr(2A)–O(1) (2.554(10) Å) suggest that there are weak bonding interactions between O(1) and Zr(2) as well as Zr(2A) (the relative longer distances of Zr to bridging carboxylate oxygen atoms (2.665(10) and 2.714(10) Å) due to the steric crowding are found in $[Zr_{10}O_6(OH)_4(OOCC_6H_4OH)_8(OOCC_6H_4O)_8]\cdot6PrOH$[85]), whereas the long Zr(1B)–O(1) (2.966 Å) and Zr(1C)–O(1) (2.966 Å) contacts indicate the very weak interactions between O(1) and Zr(1B) as well as Zr(1C). It is assumed that the interstitial atoms generally exert a stabilizing influence on a metal cluster by acting as an "atomic glue". While the small size of the oxygen makes it difficult to fit into the big size of the octahedral skeleton of **17** (the average distance of the octahedron center to zirconium atoms is 2.586 Å, which is distinct longer than that of $[\{(EtMe_4C_5)Zr\}_6(\mu_6\text{-}O)(\mu_3\text{-}O)_8]\cdot(C_7H_8)$ (Zr–$(\mu_6\text{-}O)$ (2.241 Å)), only two distinct and two weaker bonds are formed.

Ab-initio calculations[155] were carried out in order to analyse the bonding scheme of the frozen off-center structure in comparison to that of the ideal μ_6-O core center. Thus, taking the experimental structure, the RHF and DFT calculations (by B3LY) are yielding the following bond orders (for DFT, noted in parentheses): 0.362 (0.393) for the shorter two contacts, 0.342(0.373) and 0.327(0.368) for the intermediate ones, and 0.193(0.256) for the two longest Zr-O separations. For the structure with the oxygen in the center of inversion the bond orders are dichotomized in two 0.324(0.352) values and four 0.294(0.346) others. The sum of bond orders of 1.821 (2.089) in the symmetrized and of 1.778 (2.039) in the distorted frame are comparable. At the RHF level, the μ_6-O core is a little more stable (13 kcal) than that of the off-center case, while the DFT calculation reveals practically almost equal energies (the distorted one becomes more stable by 0.75 kcal).

The vibrational analysis of the symmetric structure (optimized under RHF) shows many low frequency modes including the deformation of the Zr_6O moiety. The cumulated results allow to conclude that the inner μ_6-O atom possesses a floppy nature and the total bonding effects are comparable in both the centered and off-center positions. This result explains qualitatively the experimentally observed disorder. The comparison of RHF and DFT results suggests that the fine

effects of electron correlation (included in the last method) are contributing to the distortion tendency. It is worth mentioning that these results are obtained under the imposed approximation and simulation of the disorder of protons as a symmetrical averaged field. A special treatment was applied in order to simulate in the ab-initio scheme the averaged effect of fully dynamical peripheral protons. Namely, instead of considering various combinatorial possibilities in distributing 8 μ_2-hydroxo and 4 μ_2-oxo bridges on the edges of the Zr_6 octahedron, we considered 12 X groups resembling the OH ones, but with the hydrogen center having a nuclear charge $Z^* = 2/3$. In this manner, one conventionally simulates the smearing out of 8 protons on the 12 equivalent edges, while the electron count is the same as in the $(CpZr)_6O(\mu\text{-O})_4(\mu\text{-OH})_8$ species. The account of statistical or dynamical disorder of protons is prohibitive for a direct account in the calculation. However, it is presumable that slow proton dynamics are also a factor favoring the frozen cluster distortions. With respect to octahedral reference, the off-center deformation within the octahedral pattern has the shape of the pseudo Jahn-Teller distortion.[156]

The particular structural effects in **17** are similar to those which are determined in the solid phase of various perowskites (Ti, Zr or Hf)[157] and also to those phenomena of negative thermal expansion in certain mixed oxides of zirconium.[158]
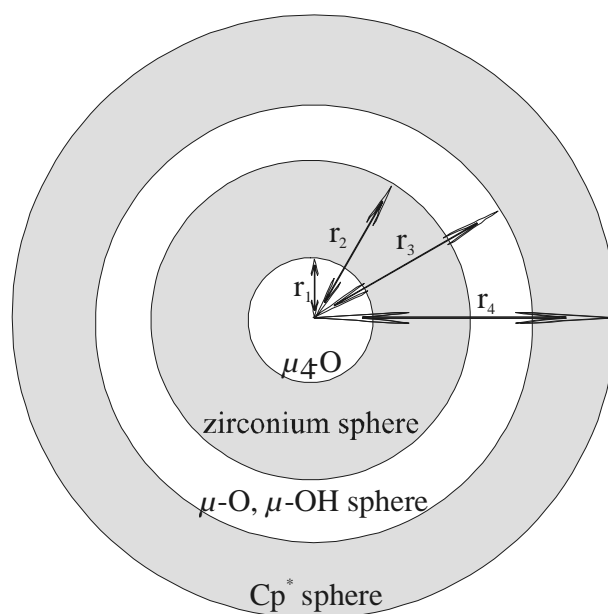
Figure 21. The coordination sphere of cluster 17. $r_1 = 0.467$ Å, $r_2 = 2.586$ Å, $r_3 = 2.871$ Å, $r_4 = 4.875$ Å (the average distance of the symmetric center to that of the Cp^* ring).

The coordination sphere of cluster **17** is shown in Figure 21. The interstitial oxygen atom (0.467 Å away from the symmetric center of the cluster) is surrounded by zirconium atoms. A zirconium oxide core is surrounded by organic ligands, thus rendering it soluble in a variety of organic solvents. The OH groups are acidic due to the Zr(IV) centers, therefore further reactions might take place preferentially at the metal oxide surface. Many metal compounds and other functional groups can be anchored on the surface of the cluster to form the new homo- or heterometallic clusters, which is very useful for the metal oxide supporting catalysts. Due to the acidic property compound **17** may be a good catalysts for many reactions in homogeneous system. Moreover, the average distance of the symmetric center to the μ-O or μ-OH ($r_3 = 2.871$ Å, Figure 3) shows that the size of the oxide core is in the nanometer range. Therefore compound **17** may be a good precursor for the preparation of nanometer size zirconium oxide.

2.3.4. Synthesis and Characterization of the Vanadium(IV)/Vanadium(V) Sodium Oxide (Cp*V)$_6$(μ-O)$_8$(μ_3-O)$_2$Na (19)

Oxidation of [Cp*V(μ-Cl)$_2$]$_3$ with O$_2$ in THF has been shown to generate Cp*VCl$_2$(O) in 65 % yield.[159] From the reaction of [Cp*V(μ-Cl)$_2$]$_3$ with NaNH$_2$ in THF at 40 °C for 24 h, we were unable to isolate chlorine free amido, imodo, or imido vanadium compounds. Further reaction of the resulting THF solution with a small amount of O$_2$ (the solution was exposed to air for a short time) generated polyoxovanadium(IV) chloride [Cp*VCl(μ-O)]$_4$·OC$_4$H$_8$ (**18**, Scheme 17. Its molecular structure is shown in Figure 22) which was obtained previously as a minor byproduct in the oxidation of [Cp*V(μ-Cl)$_2$]$_3$ by O$_2$[160] or from the reaction of Cp*VCl$_2$(O) with mercury in high yield.[159]

1. NaNH$_2$, THF, 40 °C, 24 h

2. O$_2$

4 [Cp*V(μ-Cl)$_2$]$_3$ ⟶ 3 [(Cp*VCl(μ-O)]$_4$·OC$_4$H$_8$

Scheme 17   **18**
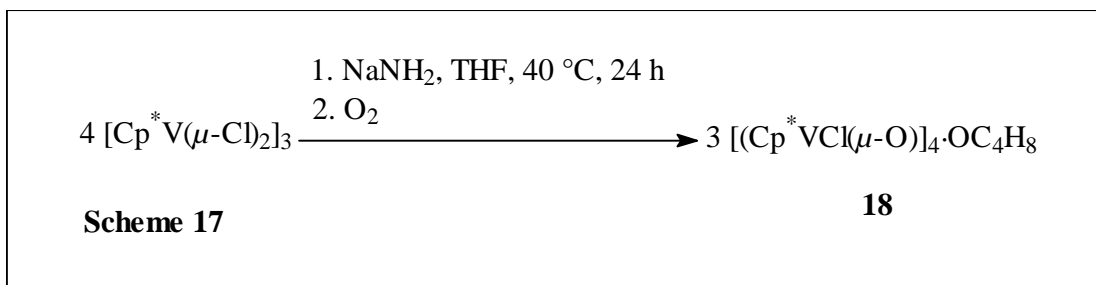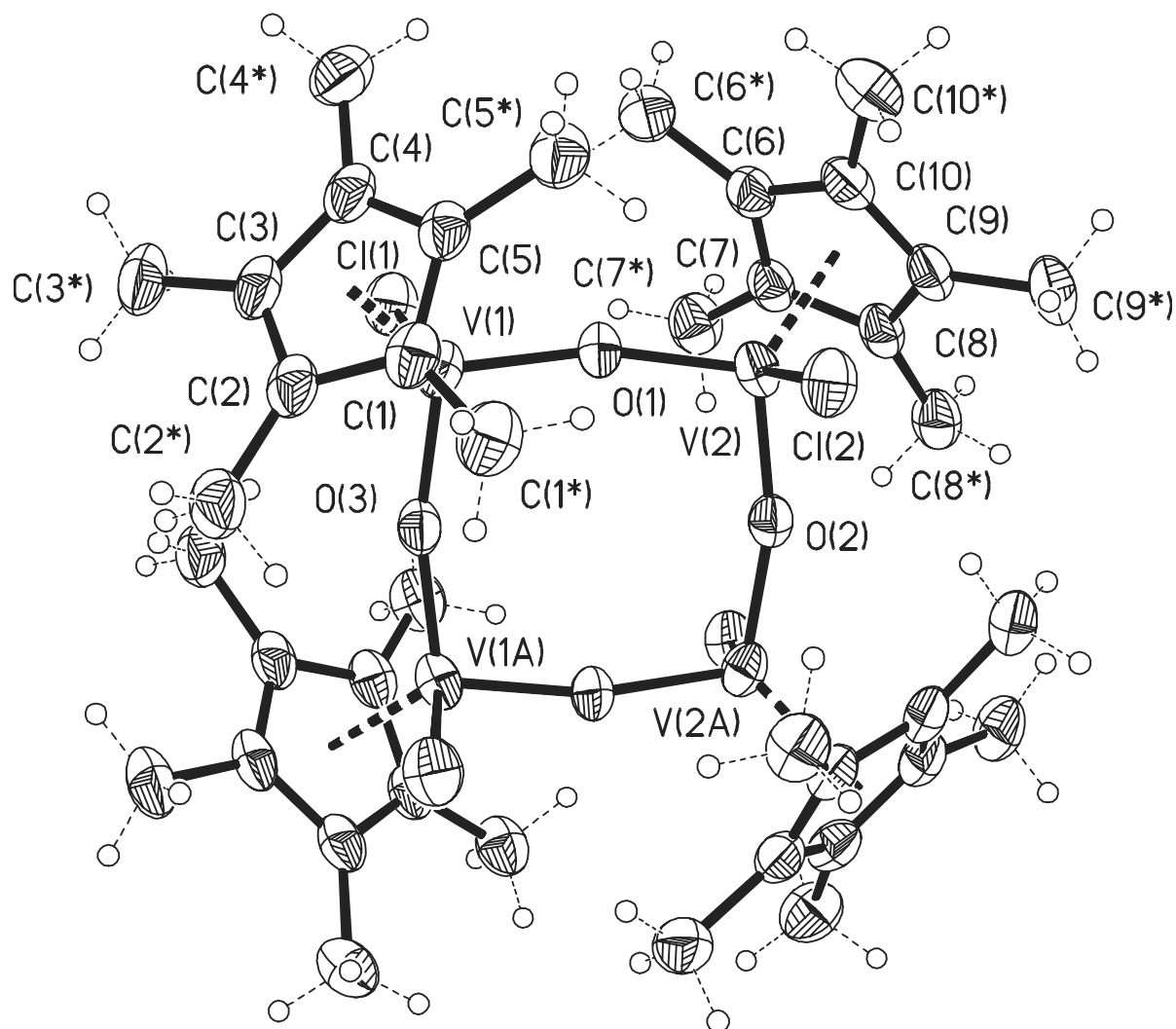
Figure 22. Molecular structure of 18 (50 % probability ellipsoids. THF molecule is omitted for clearity)

Alternatively, the reaction of $[Cp^*V(\mu\text{-}Cl)_2]_3$ with O_2 in toluene at room temperature with treatment of $NaNH_2$ in liquid ammonia and toluene at -78 °C results in the complete removal of chloride and the formation of the organovanadium sodium oxide $(Cp^*V)_6(\mu\text{-}O)_8(\mu_3\text{-}O)_2Na$ (**19**, Scheme 18). Obviously, oxidation of $[Cp^*V(\mu\text{-}Cl)_2]_3$ with O_2 in toluene under the above condition does not lead to $Cp^*VCl_2(O)$ or leads to $Cp^*VCl_2(O)$ in low yield. The formation of **19** is proposed to proceed via vanadium(IV) and/or vanadium(V) oxide intermediates or via the oxidation of $[Cp^*V(\mu\text{-}Cl)_2]_3$ with O_2 in liquid ammonia and toluene in the presence of $NaNH_2$, and the extra oxygen atoms in **19** come from coordinated or free O_2 in the solution.

1. O_2, toluene, RT, 2 h
2. 24 $NaNH_2$, liq NH_3,
toluene, -78 °C

2 $[Cp^*V(\mu\text{-}Cl)_2]_3$ $\xrightarrow{\hspace{3cm}}$ $(Cp^*V)_6(\mu\text{-}O)_8(\mu_3\text{-}O)_2Na$

19

Scheme 18
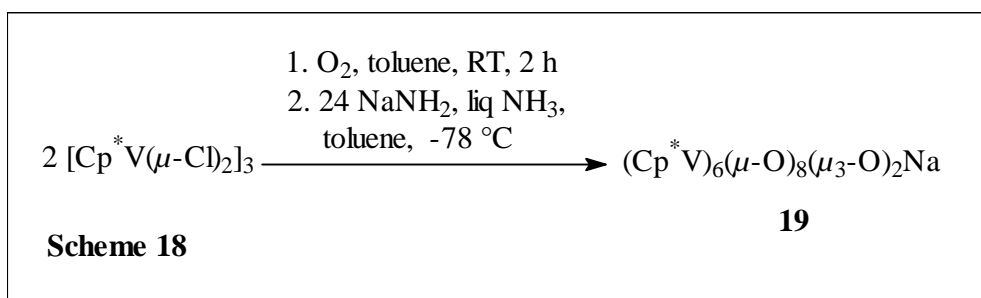
Compound **19** is a green crystalline solid. No large fragment in the EI mass spectrum of **19** was observed due to the poor volatility of **19**. Only a few green crystals of **19** suitable for X-ray determination were obtained. The solid products obtained by concentration of the solution proved not to be pure enough for further characterization of **19**.

The molecular structure and the central core of **19** are shown in Figures 23 and 24. Compound **19** crystallizes in the triclinic space group $P\bar{1}$. Selected bond lengths and angles for **19** are shown in Table 10. The X-ray analysis reveals that **19** is a sandwich like molecule. The central core of **19** consists of four six-membered $(VO)_3$ rings, two four-memebered $(VO)_2$ rings and four six-membered $Na(VO)_2O$ rings.

The V–O bond lengths in the two four-membered $(VO)_2$ rings (1.827(6) Å to 1.853 Å, av 1.836 Å) are similar to the V(IV)–(μ-O) single bond distances found in $[Cp^*VCl(\mu\text{-}O)]_4$ (1.800(2) Å)[160] and $(Cp^*V)_4(\mu\text{-}O)_6$ (1.799(9) Å to 1.818(7) Å, av 1.809 Å).[159] The V(5)–O(8) bond (1.616(7) Å) is longer than those found in $Cp^*VCl_2(O)$ (V(V)=O 1.576(8) Å), and in $(Q_2VO)_2O$ (QH = 8-quinolinol, V(V)=O 1.587(6) Å),[161] similar to those detected in $K_5V_3O_{10}$ (V(V)=O 1.615 Å),[162] and shorter than those found in $(Q_2VO_2)^-$ (1.628(2) Å),[163] whereas the V(3)–O(4) bond (1.634(7) Å) is longer.

Longer V(3)–O(1) (1.933(6) Å) and V(3)–O(2) (1.937(6) Å) bonds compared to V(5)–O(6) (1.822(6) Å) and V(5)–O(7) (1.805(6) Å) bonds, and shorter V(2)–O(2) (1.725(6) Å) and V(1)–O(1) (1.733(6) Å) bonds are found in **19**. The bond distances of V(1)–V(2) (2.423(2) Å) and V(4)–V(6) (2.420(2) Å) indicate the presence of V(1)–V(2) and V(4)–V(6) single bonds in **19** (these bond lengths are comparable to the V–V single bond length (2.462(2) Å) found in $Cp_2V_2(CO)_2$[164]). The Na(1)–O(4) bond length is similar, and the Na(1)–O(8) (2.345(8) Å), Na(1)–O(5) (2.358(7) Å) and Na(1)–O(10) (2.532(7) Å) bond distances are longer than those found in $(Me_3CONa)_9$ (2.26 Å) and in $(Me_3CONa)_6$ (2.24 Å).[165]
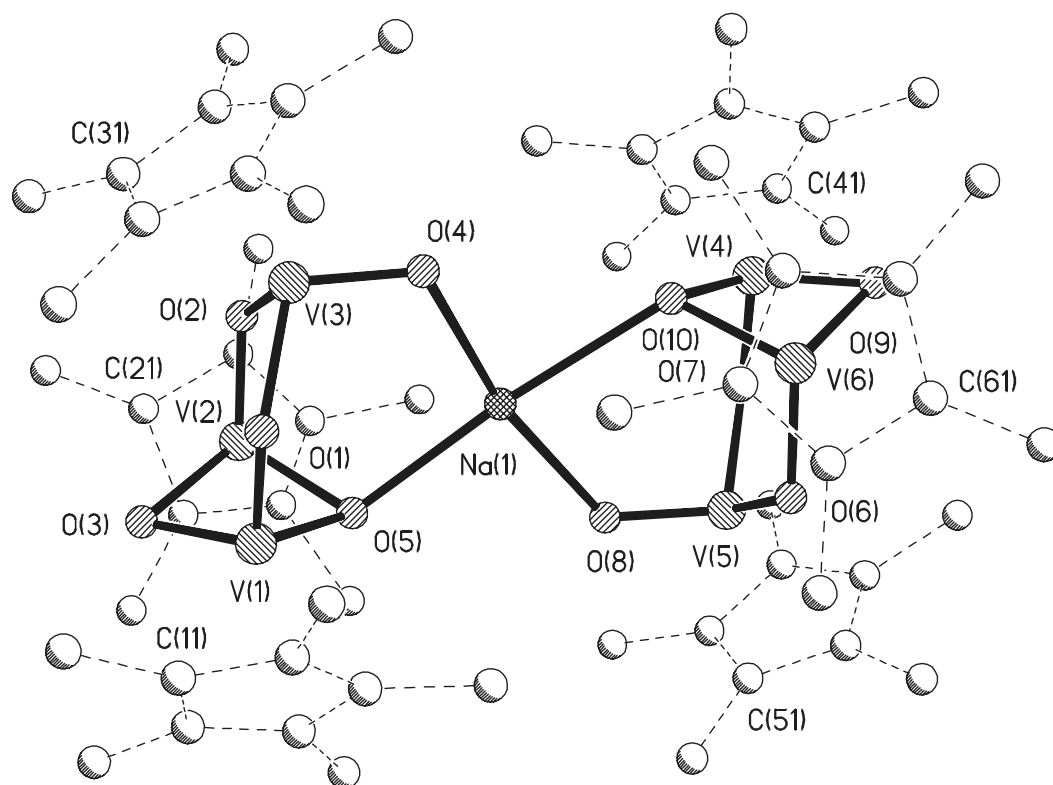
Figure 23. **Molecular structure of (Cp*V)₆(*μ*-O)₈(*μ*₃-O)₂Na (19) (H atoms bonded to C are omitted for clearity)**
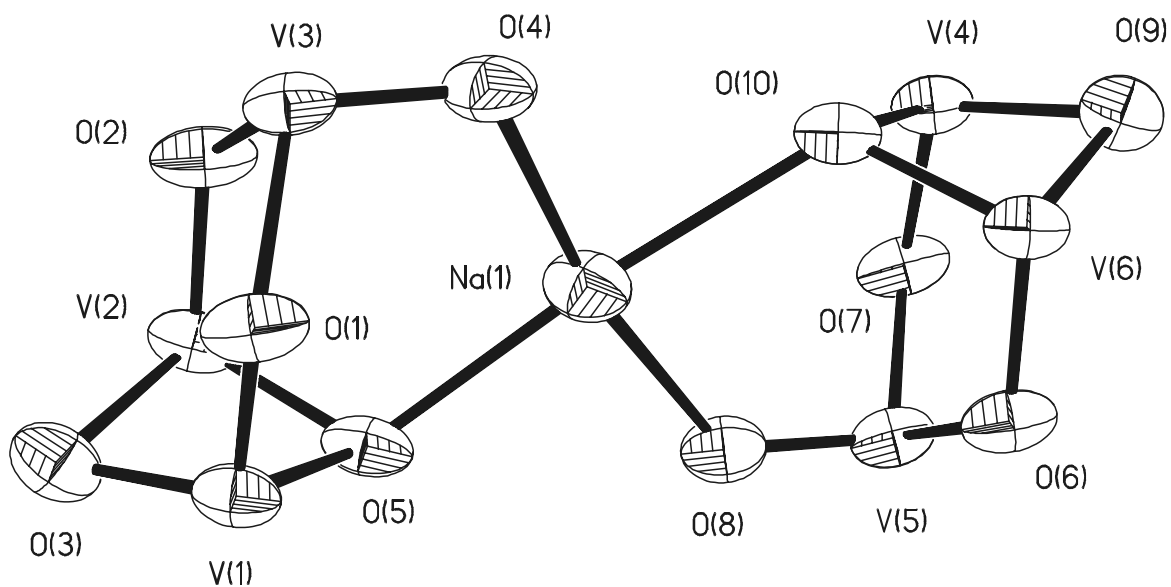
Figure 24. **Central core of (Cp*V)₆(*μ*-O)₈(*μ*₃-O)₂Na (19) (50 % probability ellipsoids)**

Table 10. Selected Bond Lengths (Å) and Angles (°) for 19

Na(1)-O(4)	2.287(7)	Na(1)-O(8)	2.345(7)
Na(1)-O(5)	2.358(7)	Na(1)-O(10)	2.532(7)
V(1)-O(1)	1.733(6)	V(1)-O(3)	1.826(7)
V(1)-O(5)	1.853(6)	V(2)-O(2)	1.725(6)
V(2)-O(3)	1.839(6)	V(2)-O(5)	1.851(7)
V(3)-O(4)	1.634(7)	V(3)-O(1)	1.933(6)
V(3)-O(2)	1.937(6)	V(4)-O(7)	1.814(6)
V(4)-O(9)	1.820(7)	V(4)-O(10)	1.840(6)
V(5)-O(8)	1.616(7)	V(5)-O(7)	1.805(6)
V(5)-O(6)	1.822(6)	V(5)-V(6)	3.081(2)
V(6)-O(6)	1.796(6)	V(6)-O(9)	1.827(6)
V(6)-O(10)	1.832(6)	V(1)-V(2)	2.423(2)
V(4)-V(6)	2.420(2)	V(4)-V(5)	3.081(2)
O(4)-Na(1)-O(8)	168.5(3)	O(4)-Na(1)-O(5)	98.7(3)
O(8)-Na(1)-O(5)	92.1(2)	O(4)-Na(1)-O(10)	85.4(2)
O(8)-Na(1)-O(10)	83.6(2)	O(5)-Na(1)-O(10)	175.3(3)
O(1)-V(1)-O(3)	107.6(3)	O(1)-V(1)-O(5)	106.4(3)
O(3)-V(1)-O(5)	92.7(3)	O(2)-V(2)-O(3)	108.4(3)
O(2)-V(2)-O(5)	106.4(3)	O(3)-V(2)-O(5)	92.4(3)
O(4)-V(3)-O(1)	105.5(3)	O(4)-V(3)-O(2)	105.8(3)
O(1)-V(3)-O(2)	95.8(3)	O(7)-V(4)-O(9)	108.0(3)
O(7)-V(4)-O(10)	106.4(3)	O(9)-V(4)-O(10)	91.8(3)
O(8)-V(5)-O(7)	104.7(3)	O(8)-V(5)-O(6)	105.3(3)
O(7)-V(5)-O(6)	104.6(3)	O(6)-V(6)-O(9)	108.4(3)
O(6)-V(6)-O(10)	106.5(3)	O(9)-V(6)-O(10)	91.8(3)
V(1)-O(1)-V(3)	122.3(3)	V(2)-O(2)-V(3)	122.1(3)
V(1)-O(3)-V(2)	82.8(3)	V(2)-O(5)-V(1)	81.7(3)
V(3)-O(4)-Na(1)	114.7(3)	V(2)-O(5)-Na(1)	113.6(3)
V(1)-O(5)-Na(1)	118.9(3)	V(5)-O(8)-Na(1)	127.1(4)
V(6)-O(10)-Na(1)	119.4(3)	V(4)-O(10)-Na(1)	122.9(3)

If the V(5) atom is considered to be V(V) and the other vanadium atoms to be V(IV), and the compound **19** is regarded to consist of a V(IV) anion $[(Cp^*V)_3O_5]^-$ and a V(IV)/V(V) unit $[(Cp^*V)_3O_5]$ linked together by a Na^+ cation, the differences between the shorter V(5)–O(8) bond and longer V(3)–O(4) bond and between the shorter Na(1)–O(4) bond and the longer Na(1)–O(8), Na(1)–O(5) as well as Na(1)–O(10) bonds can be explained. Furthermore, in the anionic unit, the high electron density on V(3) enlarges the V(3)–O(2) and V(3)–O(2) bonds, which is also reflected in the shorter V(2)–O(2) and V(1)–O(1) bonds (due to the stronger O→V electron donating bonds) and smaller O(1)–V(3)–O(2) angle (95.8(3)°) than that of O(7)–V(5)–O(6) (104.6(3)°).

2.4. Synthesis of a Zirconium Dihydride in a Liquid Ammonia/Toluene Two Phase System

Organozirconium hydride complexes provide valuable catalysts[166] and reagents for the selective synthesis of various organic derivatives[167] and for CO reduction.[168] In general the hydrides are obtained by treating zirconium precursors with various hydride sources ($LiAlH_4$, $LiBH_4$, $LiBH_3Me$, $LiBHEt_3$, $NaBHEt_3$, H_2SiR_2, $LiAlH(OCMe_3)_3$, $NaAlH_2(OCH_2CH_2OMe)_2$).[169] A series of zirconocene dihydride complexes have been prepared by hydrogenation of the corresponding dimethyl complexes.[170] Pez et al.[171] obtained $[(Cp)_2Zr(C_{10}H_7)(\mu\text{-H})Zr(Cp)_2]$ from $(Cp)_2ZrCl_2$ and potassium naphthalenide. In general, alkali metal ammonia solutions have not been used for the preparation of transition metal hydrides due to the easy formation of H_2.

2.4.1. Synthesis and Characterization of the Imido-*ansa*-Zirconocene Dihydride $[\{HN(SiMe_2C_5H_4)_2ZrH(\mu\text{-H})\}_2 \cdot C_7H_8]$ (20)

Treatment of $(ClMe_2SiC_5H_4)_2ZrCl_2$ with K (Na) in liquid ammonia/toluene at -78 °C results in the formation of the *ansa*-zirconocene dihydride $[\{HN(SiMe_2C_5H_4)_2ZrH(\mu\text{-H})\}_2 \cdot C_7H_8]$ (**20**, Scheme 19).[106] Due to the faster cleavage reaction of the Si−Cl bond in comparison to the Zr−Cl bond in $(ClMe_2SiC_5H_4)_2ZrCl_2$ (this step is comparable to the hydrolysis of *rac*-[1-(BrMe_2Si)THI]_2ZrBr_2 (THI = 4,5,6,7-tetrahydroindenyl)[172] which gave the *ansa*-metallocene *rac*-[μ-O-(1-Me_2SiTHI)_2]ZrBr_2) and the kinetically more stable *ansa*-metallocenes compared to the unbridged congeners,[173] therefore, the *ansa*-zirconocene formation should be the first step of the reaction. We assume that the Si−NH−Si exerts a stabilizing effect for the formation of the zirconium hydride.

$$2 \ (ClMe_2SiC_5H_4)_2ZrCl_2 \xrightarrow[\substack{\text{liq NH}_3,\ \text{toluene},\ -78\ ^\circ C \\ -\ 8\ KCl}]{8\ K} [\{HN(SiMe_2C_5H_4)_2ZrH(\mu\text{-}H)\}_2{\cdot}C_7H_8]$$

Scheme 19   **20**
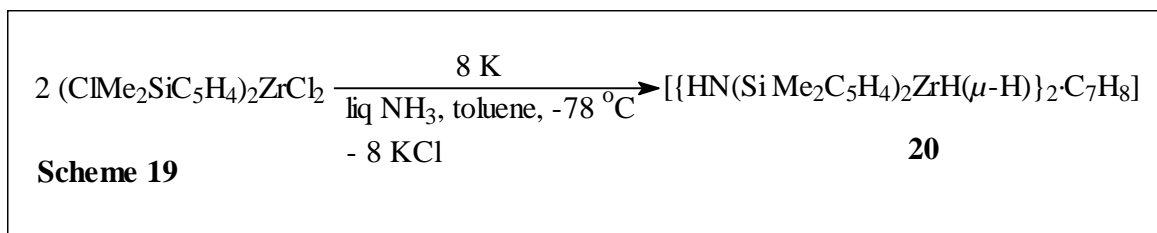
Compound **20** is a pale yellow crystalline solid which decomposes above 200 °C. It is sensitive to moisture and oxygen, but in solution (toluene or THF) no decomposition is observed over a period of one year under inert gas atmosphere. However, the reactivity of **20** toward ammonia is highly reduced in comparison to $Cp^*_2ZrH_2$.[115] In the EI mass spectrum the peaks due to the fragments $[M^+ - H]$ (*m/z* 795, 1 %) and $[M^+ - C_7H_8 - HN(SiMe_2C_5H_4)_2 - C_5H_4 - 2\ Me - H]$ (*m/z* 348, 100 %) are observed, which is additional evidence for the dimeric nature of **20**. The ^1H NMR spectrum of **20** in THF-d_8 was found to contain the expected signals in the correct ratio of integration a multiplet in the region $\delta\ 6.41 - 5.33$ ppm for the protons of the C_5H_4 groups, a triplet at $\delta\ 3.03$ ppm for the terminal hydrides as a result of coupling with the bridging hydrides (^2J(H, H) = 7.5 Hz), the signals at $\delta\ 1.33$, 0.28 and 0.23 ppm for the protons of the NH, and SiMeMe′ moieties, respectively, and a triplet at $\delta\ -3.94$ ppm (^2J (H, H) = 7.5 Hz) for the bridging hydrides.

The molecular structure and the electron density map of **20** are shown in Figures 25 and 26, selected bond lengths and angles for **20** are presented in Table 11.

The molecular structure of **20** is constrained by a crystallographic mirror plane passing through the two Zr and two N atoms. The core of **20** consists of a four-membered $Zr_2(\mu\text{-}H)_2$ ring, with each Zr atom bound to a terminal H atom.

The Zr···Zr distance (3.462(1) Å) is very similar to those found in $[\{(RC_5H_4)_2ZrH(\mu\text{-}H)\}_2]$ (3.44 Å, R = $SiMe_3$, CMe_3),[166c] $[\{(MeC_5H_4)_2ZrH(\mu\text{-}H)\}_2]$ (3.4599(2) Å)[169g] and $[\{(t\text{-}BuC_5H_4)_2ZrH(\mu\text{-}H)\}_2]$ (3.4708(7) Å).[169h] Due to the problems mentioned above, the bond lengths and angles of the four hydrogen atoms cannot be calculated precisely.

Generally, and especially in the presence of heavy atoms it is difficult to localize hydrogen atoms precisely in an electron density map derived from an X-ray diffraction experiment. Residual electron density for each of the four independent hydrides was resolved in an electron-density difference map. As shown in Figure 26, the hydride positions become visible in the *Fo-Fc* map. The chelating $HN(SiMe_2C_5H_4)_2$ group functions as two η^5-ligands (Figure 25).
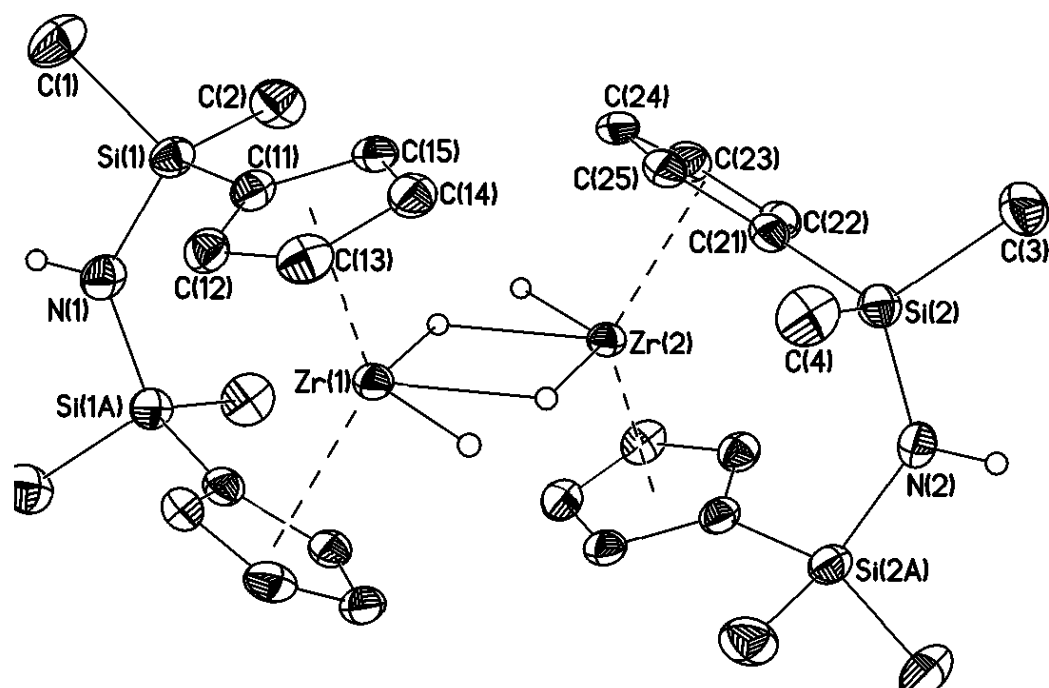
Figure 25. **Molecular structure of [{HN(SiMe$_2$C$_5$H$_4$)$_2$ZrH(μ-H)}$_2$·C$_7$H$_8$] (20) (50%**

probability ellipsoids. Toluene molecule and H atoms bonded to C are omitted for clearity)
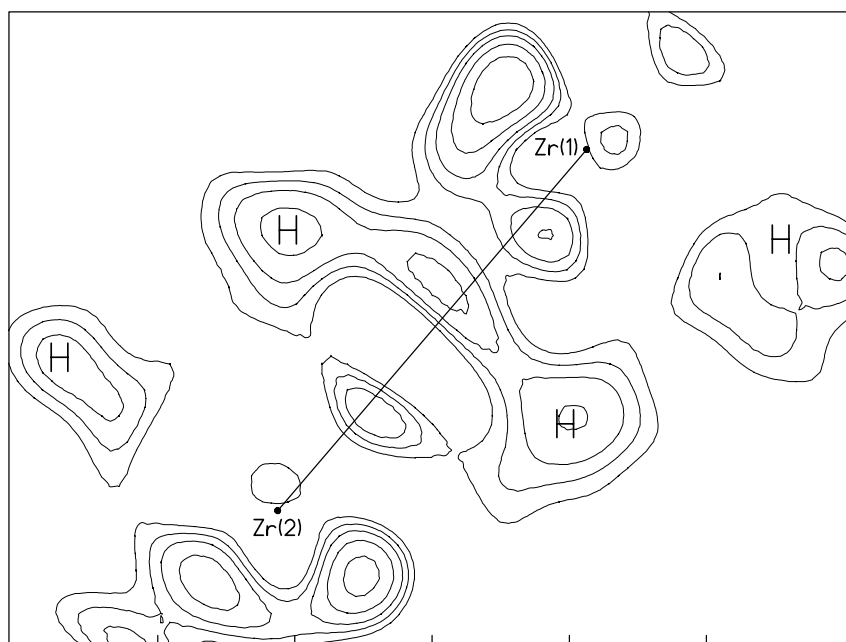
Figure 26. **Electron density map of [{HN(SiMe$_2$C$_5$H$_4$)$_2$ZrH(μ-H)}$_2$·C$_7$H$_8$] (20)**

Table 11. Selected Bond Lengths (Å) and Angles (°) for 20

Zr(1)–Zr(2)	3.462(1)	H(1B)–Zr(1)	1.903
H(1B)–Zr(2)	2.207	H(1T)–Zr(1)	1.822
H(2B)–Zr(1)	2.148	H(2B)–Zr(2)	2.014
H(2T)–Zr(2)	1.771	Si(1)–N(1)	1.7312(19)
Si(2)–N(2)	1.7303(19)	Zr(1)–H(1B)–Zr(2)	113.5
Zr(1)–H(2B)–Zr(2)	112.5	Si(1A)–N(1)–Si(1)	132.9(3)
Si(2A)–N(2)–Si(2)	131.3(2)		

2.5. Synthesis and Characterization of the Titanium(III) Compound L'_3Ti (21, L' = p-$MeC_6H_4C(NSiMe_3)_2$)

Treatment of L'_2TiCl_2 with 2 equivs of $NaNH_2$ in liquid ammonia/toluene at -78 °C affords $[(L'Ti)_6(\mu_3\text{-}NH)_6(\mu_3\text{-}N)_2\cdot6(C_7H_8)]$ (**10**, see 2.1.3). In contrast, The reduction of L'_2TiCl_2 by means of a solution of Na or K in liquid ammonia and toluene leads to the formation of L'_3Ti (Scheme 20).[120] The labile character of L' is essential for the preparation of **21**.

$$L'_2TiCl_2 \xrightarrow[\text{liq NH}_3,\ \text{toluene, -78 °C}]{2\ K} L'_3Ti$$
$$\textbf{21}$$

L' = p-$MeC_6H_4C(NSiMe_3)_2$

Scheme 20
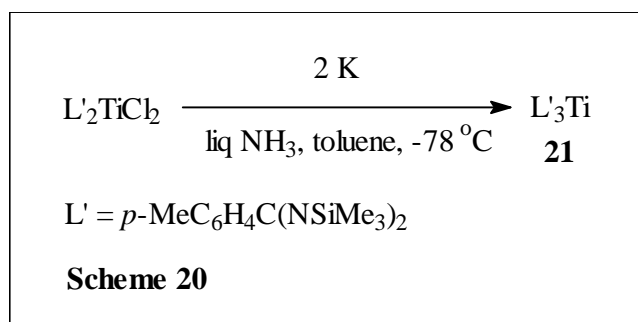
Compound **21** is a green crystalline solid and stable above the melting point (301 °C). Under an inert atmosphere or in solution (toluene) no decomposition was observed for **21.** However, **21** is sensitive to air and moisture. Compound **21** exhibits the peak of the molecular ion at m/e 879 with 62 % relative intensity in the EI mass spectrum. The ^{1}H NMR shows two multiplets in the regions δ 8.58 − 8.62 and 8.31 − 8.34 ppm for the protons of the C_6H_4 moieties, one singlet at δ 2.16 ppm for the methyl protons of the MeC_6H_4 groups, and a broad singlet at δ 0.21 ppm for the protons of the Me_3Si groups due to the paramagnetism of Ti(III).

The molecular structure of **21** is shown in Figure 27, selected bond lengths and angles for **21** are presented in Table 12. Compound **21** crystallizes in the triclinic space group $P\bar{1}$.
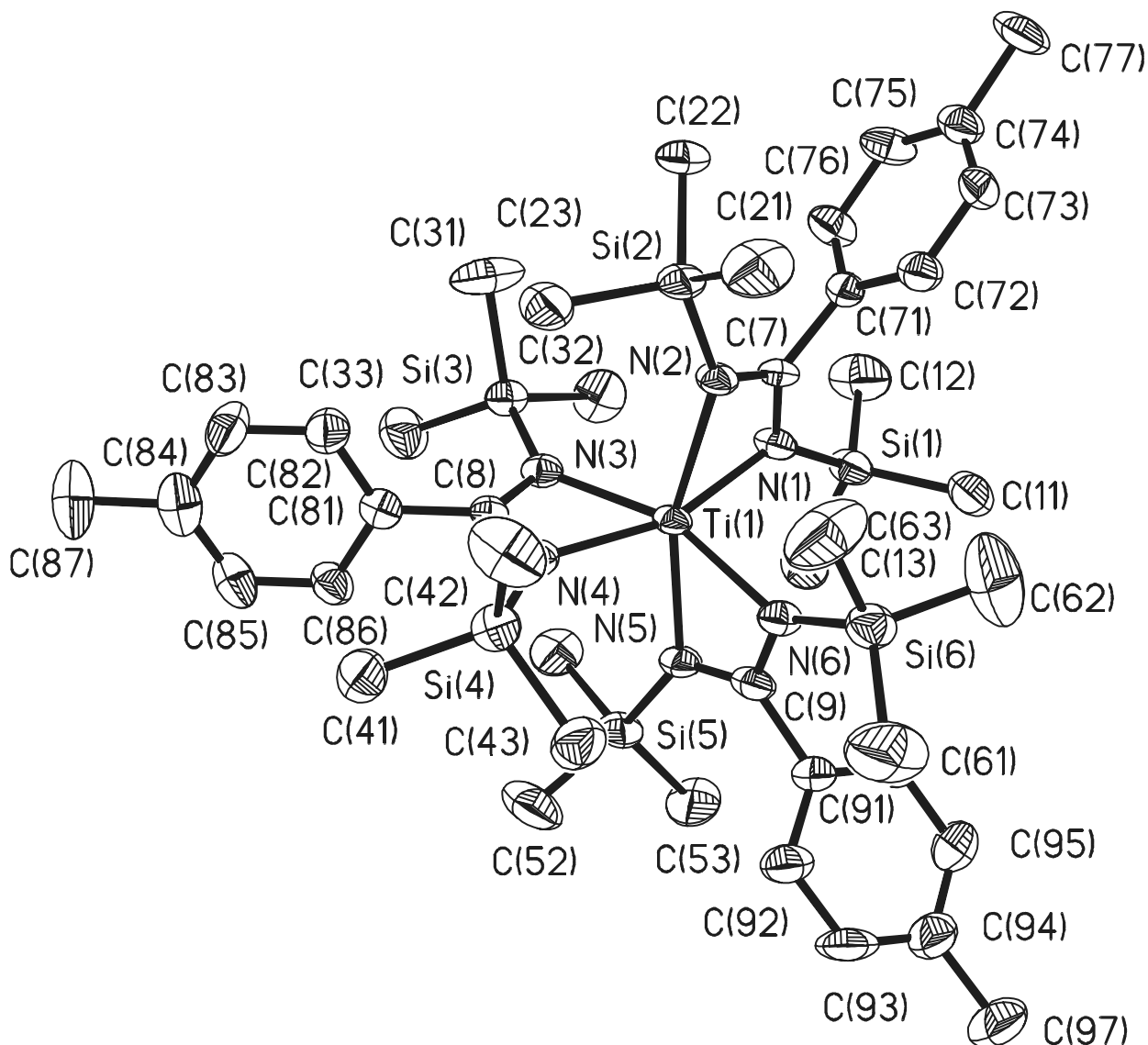
Figure 27. Molecular structure of [*p*-MeC₆H₄C(NSiMe₃)₂]₃Ti (21) (50 % probability ellipsoids. H atoms bonded to C are omitted for clearity)

The molecular structure of **21** in the crystal shows that three L ligands complete the coordination sphere of Ti, and the core of **21** resembles a paddle-wheel. Comparable arrangements are found in [(Cp₂TiF₂)₃Ti],[174] in which the Ti(III) is surrounded by three Cp₂TiF₂ ligands and in

[{PhC(NSiMe$_3$)$_2$}$_2$TiCl],[138] in which the Ti(III) is surrounded by two PhC(NSiMe$_3$)$_2$ ligands and one Cl atom. The average Ti–N bond length (2.163 Å) of **21** is comparable to that found in [{PhC(NSiMe$_3$)$_2$}$_2$TiCl] (av 2.101 Å).

Table 12. Selected Bond Lengths (Å) and Angles (°) for 21

Ti(1)–N(3)	2.133(5)	Ti(1)–N(6)	2.154(5)
Ti(1)–N(2)	2.160(4)	Ti(1)–N(1)	2.164(5)
Ti(1)–N(5)	2.177(4)	Ti(1)–N(4)	2.188(5)
N(3)–Ti(1)–N(6)	160.1(2)	N(3)–Ti(1)–N(2)	95.3(2)
N(6)–Ti(1)–N(2)	102.5(2)	N(3)–Ti(1)–N(1)	102.2(2)
N(6)–Ti(1)–N(1)	93.7(2)	N(2)–Ti(1)–N(1)	63.6(2)
N(3)–Ti(1)–N(5)	101.1(2)	N(6)–Ti(1)–N(5)	63.4(2)
N(2)–Ti(1)–N(5)	60.6(2)	N(1)–Ti(1)–N(5)	102.4(2)
N(3)–Ti(1)–N(4)	63.7(2)	N(6)–Ti(1)–N(4)	102.5(2)
N(2)–Ti(1)–N(4)	105.2(2)	N(1)–Ti(1)–N(4)	162.3(2)
N(5)–Ti(1)–N(4)	91.4(2)		

The small bite angle of benzamidinato ligand in compound **21** (~63.5°) is expected to generate an unusual coordination sphere.[122] Indeed, routine calculations help to identify some spectacular features. First of all, one may argue that this type of ligand offers a clear case for the resolution of the effects related to the so-called phase coupling problem.[175] Namely, the $\pi_\perp$ orbitals can be conceived as coupled *in-phase* (ψ) or *out-of phase* (χ) (see representation *b* in Figure 28). The real existence of the effect is still a mater of debate for usual chelates, while the present ligand seems to be an unequivocal example where the χ-phase of the coupling overrides the ψ-combination. This is due to the χ-symmetry, which is clearly revealed to be HOMO, while ψ-one is the well-separated LUMO orbital of the ionized ligand. While the relatively high oxidation state of the metal precludes any π-acceptor features of the ligand in compound **21**, the ψ-type orbital (LUMO) cannot properly enter into action. A ψ-type orbital of the N-C-N π-system is also quite low in energy and therefore less available for outer donation. Due to the simplicity of coordinating frame, it is

obvious that the coordination is predominantly based on the π-donation exerted from the HOMO orbital of the χ type. Unfortunately, spectral data are not available at the moment, but are kept in the focus of future investigations, in order to understand related consequences of optical properties.
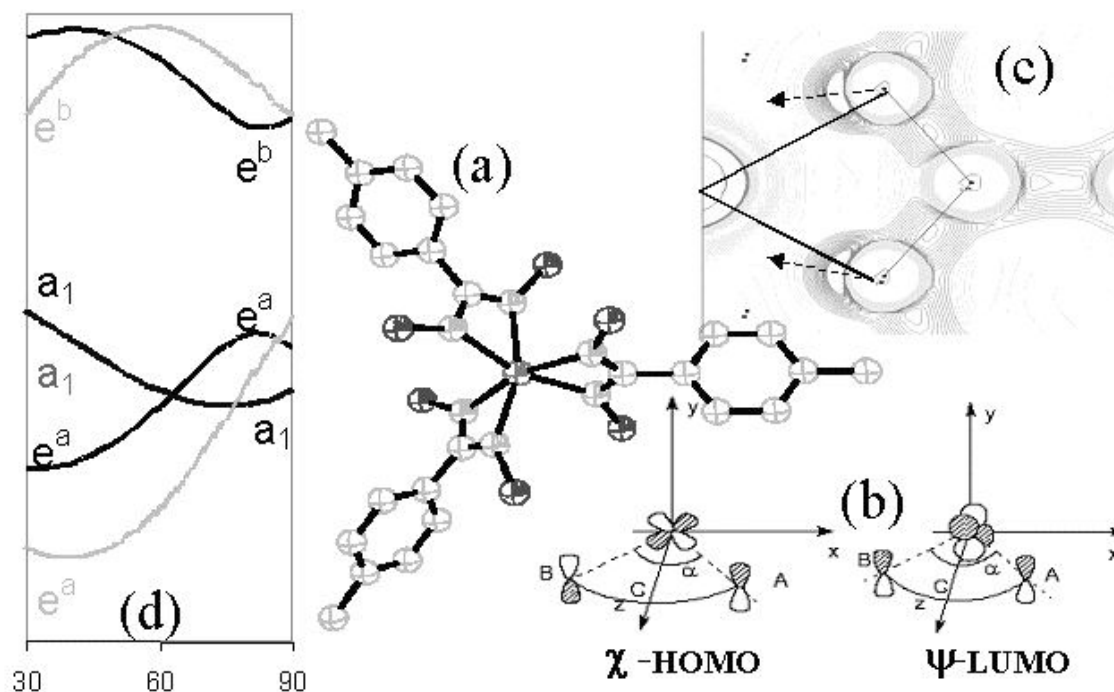
Figure 28. A brief representation of the coordination effects appearing in the trischelate (a) of compound 21, strong phase coupling (b), miss-directed lone pair (c) and Jahn-Teller effect in the e_g ground state (d)

The same ligand carries other interesting coordination features. At a first glance the Laplacian of electron density in the plane of the coordinated ligand (map c in Figure 28, a section of the chelating plane of **21**) shows that the areas assignable to the lone pairs are not geometrically directed toward the metal. The combined effect of small bite angle and χ phase coupling creates the possibility of the degenerate e-type ground state and the premise of $e \otimes \varepsilon$ Jahn-Teller activity in a trigonal arrangement. The section (d) of Figure 28 contains the qualitative representation of relative ordering of the d orbitals as function of the bite angle. The dark curves are estimated

without phase coupling effect, while the lighter ones are representing the χ-type phase coupling. One may see that even without phase coupling, bellow 65°, the degenerate e^a orbitals are becoming the lowest in energy (the crossing point changes between 60-65° as function of relative σ-π strength ratio). However, when the phase coupling is included, the e orbitals are definitely ground state for bite angles smaller than 90°. Moreover, the qualitative simulation with arbitrary values of ligand field parameter shows that **21** is the subject of an $e \otimes \varepsilon$ Jahn-Teller effect. This is also confirmed by electronic structure calculation[176] using the GVB-type average of states. The type of bonding in this ground state is predominantly π, therefore the distortion is less manifested in the variation of the bond length (ranging from 2.13 to 2.19 Å) but strong in the tilt angles of the chelates (dihedral angle with respect to the planes containing the trigonal axis). The three rings of **21** have values 32.93°, 36.65° and 34.71°.

2.6. Syntheses of Nitrogen Containing Titanium and Zirconium Compounds via the Reactions of Corresponding Metal Compounds with Diazo Derivatives and Aniline

2.6.1. Synthesis and Characterization of the Imido (NSiMe₃) Bridged Dinuclear Titanium Compound [(MeC₅H₄)TiCl(μ-NSiMe₃)]₂ (22)

The reaction of a THF solution of $(MeC_5H_4)TiCl_3$ with one equiv of $Me_3SiCLiN_2$ at -78 °C results in the formation of reddish brown crystals of the imido bridged dinuclear complex $[(MeC_5H_4)TiCl(\mu\text{-}NSiMe_3)]_2$ (**22**, Scheme 21).[177] The mechanism for the formation of **22** is not clear. One intermediate might be a terminal nitrogen atom $\mu\text{-}\eta^1$ binding a dinuclear titanium center ($\mu\text{-}\eta^1$-metal diazoalkane complexes are known[91] and the imido dinuclear titanium complex is accessible and stable in the sterically less demanding RR′Ti system[115]), which then undergoes rearrangement of the trimethylsilyl group from carbon to the terminal nitrogen atom. The elimination of a CN group leads to the imido dinuclear complex **22**. However, we were not able to identify any CN-species. Furthermore, an intermolecular migration of a Me_3Si moiety could also be possible. Me_3SiCl formed in the first step under the condition reported could then go on to react with other nitrogen-containing species to yield compound **22**. This result is in contrast to those obtained from the reaction of diazo derivatives with a wide variety of other metal compounds, which lead to the formation of metal carbene complexes concurrent with the liberation of N_2 or metal complexes with retention of N_2. No reaction was observed when $(MeC_5H_4)_2TiCl_2$

was treated with $Me_3SiCLiN_2$ under the same condition. Meanwhile, Bergman et al.[178] reported on the synthesis of an η^2-N_2-titanium diazoalkane complex $Cp^*_2Ti(\eta^2$-$N_2CHSiMe_3)$ from the reaction of $Cp^*_2Ti(C_2H_4)$ with Me_3SiCHN_2. An η^3-N,N,O-titanium compound $Cp_2Ti(\eta^3$-DEDM) (DEDM = $EtO_2CCN_2)$[179] was prepared from the reaction of $Cp_2Ti(CO)_2$ with DEDM. Furthermore, we were not able to isolate the imido bridged dinuclear complex from the reaction of Cp^*TiCl_3 with $Me_3SiCLiN_2$. Obviously, the stronger Lewis acidic and less sterically hindered Ti(IV) center is crucial for the formation of **22**.

$$(MeC_5H_4)TiCl_3 + Me_3SiCLiN_2 \xrightarrow[-78\ °C]{THF} [(MeC_5H_4)TiCl(\mu\text{-}NSiMe_3)]_2$$
$$\mathbf{22}$$
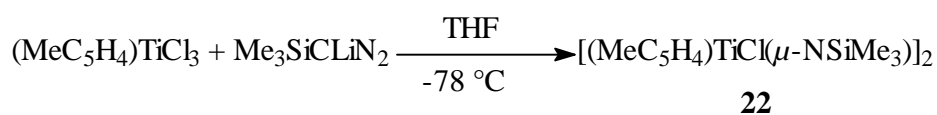
Scheme 21

Compound **22** is a reddish brown crystalline solid and stable above the melting point (242 °C). The most intense peak in the EI-MS of **22** appears at m/z 483 [M^+ − Me], and the signal at 498 (32 %) is assigned to the molecular ion. The ^{1}H NMR spectrum of **22** shows two multiplets in the region δ 6.37 − 6.40 and 5.53 − 5.55 ppm attributed to the C_5H_4 protons, two singlet resonances at δ 2.77 and 0.04 ppm assigned to the Me protons of the MeC_5H_4 rings and the Me_3Si moieties, respectively.

The molecular structure of **22** is shown in Figure 29. Compound **22** crystallizes in the tetragonal space group $P\bar{4}2_1/c$. The selected bond lengths and angles for **22** are presented in Table 13. The central core of **22** contains a planar four-memberd $Ti_2(\mu$-N$)_2$ ring with each titanium bonded to a MeC_5H_4 group and a terminal chlorine atom. The $Ti_2(\mu$-N$)_2$ plane is distorted with slightly different $Ti-(\mu$-$NSiMe_3)$ bond lengths (1.916(2) Å and 1.878(2) Å). The $Ti-(\mu$-$NSiMe_3)$ bond lengths and the Ti···Ti distance (2.7758(10) Å) as well as the $(\mu$-$NSiMe_3)-Ti-(\mu$-$NSiMe_3)$ angles (85.94(11)°) are typical for imido bridged titanium dimers.[64-67] The $SiMe_3$ groups are slightly bent out of the $Ti_2(\mu$-N$)_2$ plane toward the same side where the chlorine atoms are oriented, which minimizes the steric repulsion between the MeC_5H_4 and $SiMe_3$ groups.
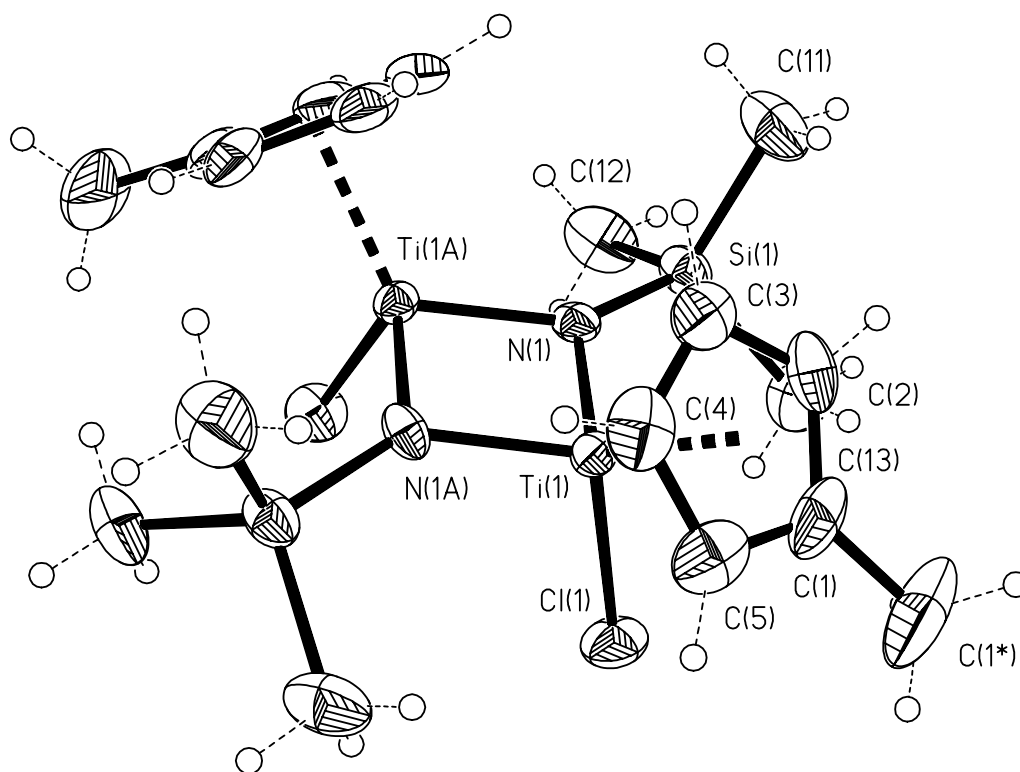
Figure 29. **Molecular structure of [(MeC$_5$H$_4$)TiCl(μ-NSiMe$_3$)]$_2$ (22) (50 % probability ellipsoids)**

Table 13. Selected Bond Lengths (Å) and Angles (°) for 22

Ti(1)–N(1A)	1.878(2)	Ti(1)–N(1)	1.916(2)
Ti(1)–Ti(1A)	2.7758(10)	Ti(1)–Cl(1)	2.2831(11)
N(1)–Si(1)	1.758(2)	N(1)–Ti(1A)	1.878(2)
N(1A)–Ti(1)–N(1)	85.94(11)	Ti(1A)–N(1)–Ti(1)	94.05(11)
N(1A)–Ti(1)–Cl(1)	105.69(8)	N(1)–Ti(1)–Cl(1)	104.11(8)
Si(1)–N(1)–Ti(1A)	135.18(15)	Si(1)–N(1)–Ti(1)	130.14(14)

2.6.2. Synthesis and Characterization of the η^2-Hydrazonato Zirconium Complex Cp$_2$ZrCl(η^2-NHNCHSiMe$_3$)·C$_7$H$_8$ (23)

The direct reaction of Cp$_2$ZrHCl with Me$_3$SiCHN$_2$ in toluene at room temperature produces the η^2-hydrazonato complex Cp$_2$ZrCl(η^2-NHNCHSiMe$_3$)·C$_7$H$_8$ (**23**, Scheme 22) in high yield.[177] The intermediate for the formation of **23** is assumed to be the diazoalkane coordinated η^1 to the electrophilic zirconium(IV) through the more basic terminal nitrogen atom.[180] Hydrozirconation of the zirconium-bonded dinitrogen leads to the insertion of the diazoalkane into the zirconium hydrogen bond and the formation of **23**.

Cp$_2$ZrHCl + Me$_3$SiCHN$_2$ $\xrightarrow{\text{toluene}}$ Cp$_2$ZrCl(η^2-NHNCHSiMe$_3$)·C$_7$H$_8$

Scheme 22   **23**
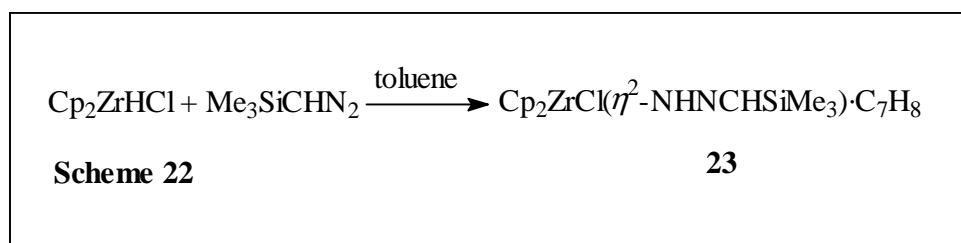
Colorless compound **23** is a crystalline solid which starts to decompose at 143 °C. The IR spectrum of **23** shows absorptions at 3381 and 3080 cm^{-1}, assignable to the N–H and NC–H stretching frequencies, respectively. In solution the ^{1}H NMR spectrum of **23** shows two resonances (δ 0.13 and 0.07) for the hydrogen atoms of the Me$_3$Si group, additional two (δ 6.01 and 5.63) for the hydrogen atoms of the Cp groups and two resonances (δ 6.84 and 6.82) for the hydrogen atom of the NH group, however only a singlet (δ 1.06) is found for the NC–H proton. This phenomenon is indicative for the electronic delocalization over the C–N–N unit which leads to an easy interconversion of the *cis* and *trans* isomers in solution.

Compound **23** crystallizes in the monoclinic space group *P*2$_1$/*c*. Selected bond lengths and angles for **23** are presented in Table 14, and its molecular structure is shown in Figure 30. The X-ray structure analysis of **23** reveals that the diazoalkane ligand is bound to zirconium in a side-on fashion through the two nitrogen atoms. The bond lengths Zr–N(1) (2.142(3) Å), Zr–N(2) (2.193(3) Å), N(1)–N(2) (1.331(4) Å), and C(11)–N(2) (1.293(4) Å) are comparable to those found in Cp$_2$Zr(η^2-NHNCPh$_2$) (Zr–N(1) 2.103(3) Å, Zr–N(2) 2.283(3) Å, N(1)–N(2) 1.338(4) Å, and C(17)–N(2) 1.307(4), respectively).[180] The difference between Zr–N(1) and Zr–N(2) (0.051 Å) is less pronounced than that in Cp$_2$ZrCl(η^2-NHNCPh$_2$) (0.180 Å).
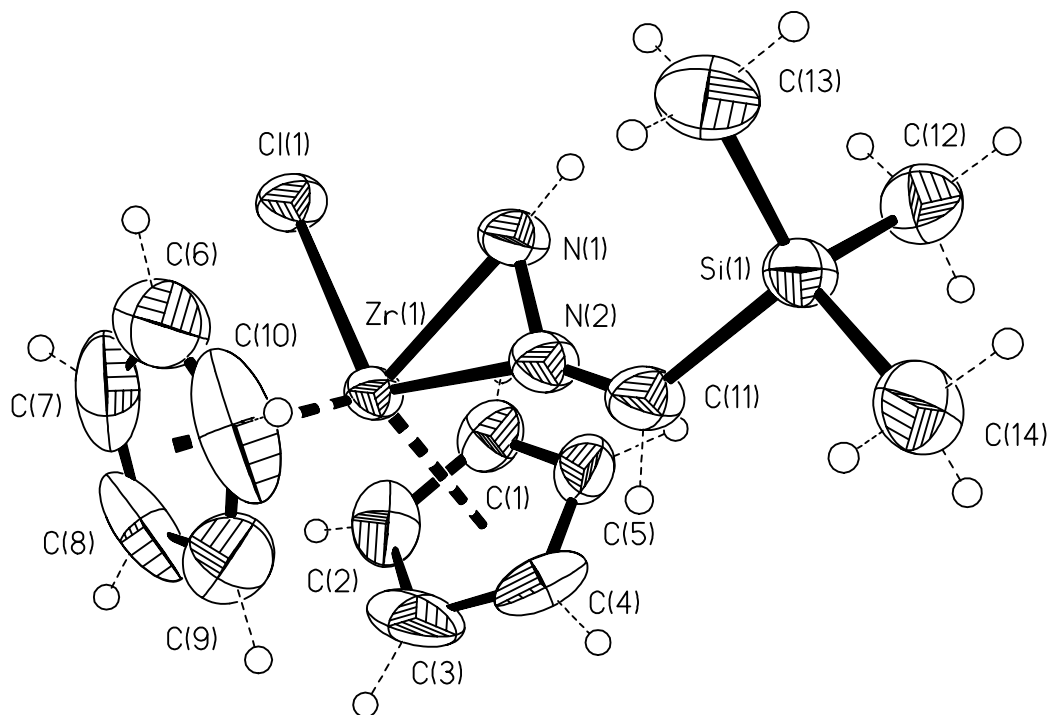
Figure 30. Molecular structure of Cp$_2$ZrCl(η^2-NHNCHSiMe$_3$)·C$_7$H$_8$ (23) (50 % probability ellipsoids. Toluene molecule is omitted for clearity)

Table 14. Selected Bond Lengths (Å) and Angles (°) for 23

Zr–N(1)	2.142(3)	Zr–N(2)	2.193(3)
N(1)–N(2)	1.331(4)	N(2)–C(11)	1.293(4)
Si–C(11)	1.866(3)	Zr–Cl	2.5299(9)
N(1)–Zr–N(2)	35.72(10)	N(2)–N(1)–Zr	74.2(2)
N(1)–N(2)–Zr	70.1(2)	N(2)–C(11)–Si	129.2(3)
N(2)–Zr–Cl	122.20(7)	N(1)–Zr–Cl	86.48(7)

The N(1)–N(2) bond distance is shorter than expected for a N–N single bond (N–N 1.434(4) Å in $Cp_2Zr(\eta^2\text{-}N_2Ph_2)$[181]), but longer than a N=N double bond (N=N 1.254 Å in MeN=NMe[182]). The C(11)–N(2) distance of 1.293(4) Å is intermediate between a C–N single (C–N 1.474(4) Å in MeN=NMe) and double (C=N 1.269(35) Å in $[Os_3(\mu\text{-}H)(CO)_{10}(\mu\text{-}NHNCPh_2)]$[183]) bond. The partial N–N and C–N double bond character indicates an electronic delocalization over the C–N–N unit in agreement with the ^1H NMR spectrum.

2.6.3. Synthesis and Characterization of the Imido (NPh) Bridged Dinuclear Zirconium Compound [Cl₂Zr(*µ*-NPh)·2THF]₂ (24)

Treatment of $ZrCl_4$ with $PhNH_2$ and potassium in toluene at 110 °C, produces the dinuclear zirconium compound $[Cl_2Zr(\mu\text{-}NPh)\cdot2THF]_2$ (**24**, Scheme 23) in 21 % yield after filtration and extraction with THF.[184] Due to the poor solubility in organic solvents, even in warm THF, the yield of crystalline **24** is relatively low.

$$2\ ZrCl_4 + 2\ PhNH_2 \xrightarrow[\text{(2) extr with THF}]{\begin{array}{c}\text{(1) 4 K, toluene}\\ \text{110 °C, 72 h}\end{array}} [Cl_2Zr(\mu\text{-}NPh)\cdot2THF]_2 + 4\ KCl + 2\ H_2$$

29

Scheme 23
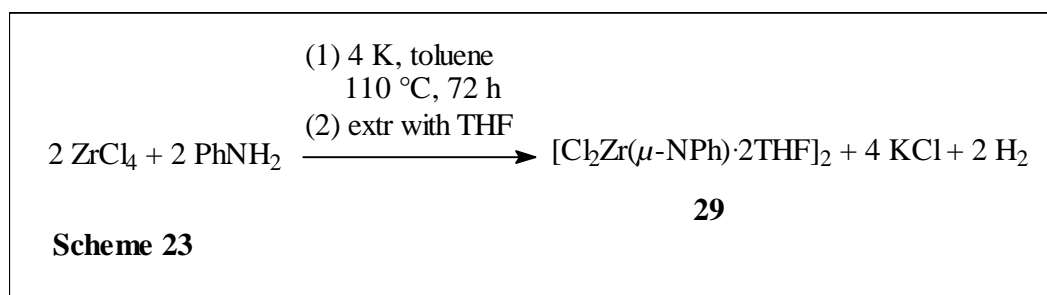
Compound **24** is a light yellow crystalline solid melting at 249 °C. The elemental analysis of **24** shows that the contents of C and H are slightly lower than the calculated ones and that of N is slightly higher than expected for **24**. Obviously, during the evaporation of the solvent *in vacuo* some coordinated THF solvent molecules were removed (calculated ca. 0.6 mole of THF). The ^1H NMR spectrum of **24** exhibits two multiplets at δ 7.15 − 6.94 and 6.56 − 6.47 ppm for the C_6H_5 protons.

The molecular structure of **24** is shown in Figure 31 and selected bond lengths and angles are presented in Table 15. Compound **24** crystallizes in the monoclinic space group *P*2/*c*. The X-ray structure analysis of the THF solvate revealed the presence of a nearly equilateral $Zr_2(\mu\text{-}N)_2$ four-membered ring in **24**. The bond lengths of Zr–(μ-NPh) (2.067(2) Å) and the distance of Zr···Zr

(3.1434(8) Å) as well as the (μ-NPh)–Zr–(μ-NPh) angles (80.05(12)°) are typical for bridged imido zirconium dimers.[47a,52b,56,58,68]

Interestingly, in **24** the chlorides and the coordinated THF molecules have two different types of orientation. Cl(1) and Cl(1A) on Zr(1) are almost lying on the equatorial plane of the $Zr_2(\mu$-NPh)$_2$ moiety, while Cl(2) and Cl(2A) at Zr(2) are arranged on both sides of the plane. The THF molecules and chlorine atoms complete the octahedral coordination sphere at the Zr atoms.
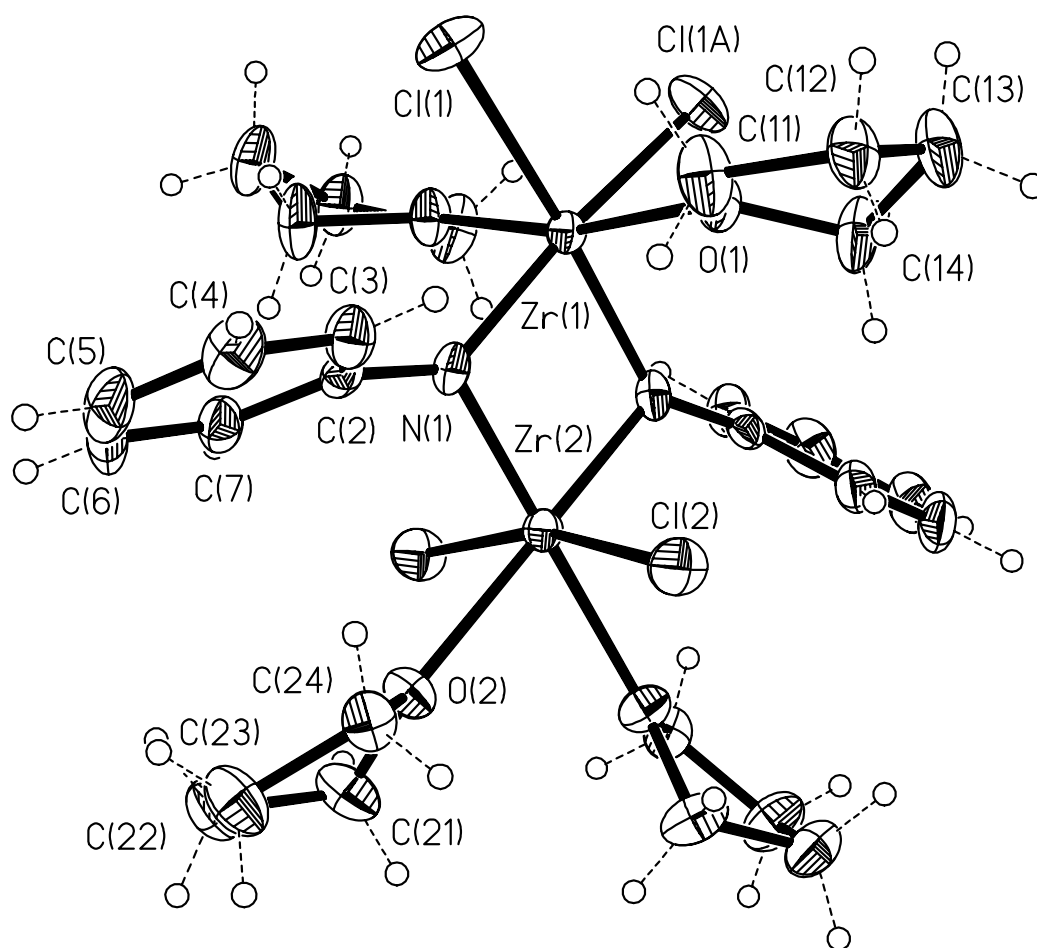
Figure 31. Molecular structure of [Cl$_2$Zr(μ-NPh)·2THF]$_2$ (24) (50 % probability ellipsoids)

Table 15. Selected Bond Lengths (Å) and Angles (°) for 24

Zr(1)–N(1)	2.069(2)	Zr(2)–N(1A)	2.050(2)
Zr(1)–Cl(1)	2.5157(8)	Zr(2)–Cl(2)	2.4915(10)
Zr(1)–Zr(2)	3.1434(8)	N(1A)–Zr(1)–N(1)	80.05(12)
N(1)–Zr(2)–N(1A)	80.98(13)	Zr(2)–N(1)–Zr(1)	99.48(10)
Cl(1A)–Zr(2)–Cl(1)	96.82(4)	N(1)–Zr(1)–Cl(1)	91.86(7)
N(1)–Zr(1)–O(1)	99.03(8)	N(1)–Zr(1)–O(1A)	90.38(8)
O(1)–Zr(1)–O(1A)	167.74(11)	C(2)–N(1)–Zr(2)	121.5(2)
C(2)–N(1)–Zr(1)	138.8(2)	N(1)–Zr(2)–O(2)	100.07(8)
O(2A)–Zr(2)–O(2)	78.97(10)	N(1)–Zr(2)–Cl(2)	93.45(7)
N(1)–Zr(2)–Cl(2A)	97.53(7)	Cl(2)–Zr(2)–Cl(2A)	165.55(4)
Cl(2)–Zr(2)–Zr(1)	97.22(2)		

The angle Cl(1)–Zr(1)–Cl(1A) (96.82(4)°) is comparable to those found in Cp$_2$ZrCl$_2$ (97.1(2)°)[185] and (*t*BuC$_5$H$_4$)$_2$ZrCl$_2$ (94.2(6)°),[186] but the angle of Cl(2)–Zr(2)–Cl(2A) (165.55(4)°) is substantially larger. The Zr(1)−Cl(1) bond length (2.5157(8) Å) is slightly longer than that of Zr(2)–Cl(2) (2.4915 Å), which indicates that the nearly perpendicular orientation of Cl(2) (Cl(2)–Zr(2)–Zr(1) 97.22(2)°) to the four-membered ring leads to a better HOMO-LUMO overlap between Cl(2) and Zr(2) than that of Cl(1) and Zr(1). The carbon atoms C(2) and C(2A) which are bonded to the bridging imido nitrogen atoms are almost in the same plane with the Zr$_2$N$_2$ ring, while the phenyl substituents are tilted toward the side where the chlorine atoms are in the *cis*-arrangement. This minimizes the steric repulsion between the PhN groups and the THF molecules on Zr(1).

2.7. Syntheses of Bis(*tert*-butylamido)cyclodiphosph(III)azane Zirconium Complexes

In recent years, the interest in developing supporting ligands with a major goal being the tailoring of chemical reactivity and other properties[187] in transition metal chemistry has been increased. As discussed in section 2.1.3, by changing the ligand on titanium and the method of preparation, the biggest imidonitrido titanium cluster [{*p*-MeC$_6$H$_4$C(NSiMe$_3$)$_2$Ti}$_6$(μ_3-NH)$_6$(μ_3-N)$_2$·6(C$_7$H$_8$)] (**13**) was obtained.[120] This result encourages investigations of similar reactions by changing the ligand on zirconium. Unfortunately, from the reactions of [{*p*-

MeC$_6$H$_4$C(NSiMe$_3$)$_2$]ZrCl$_3$ and [*p*-MeC$_6$H$_4$C(NSiMe$_3$)$_2$]$_2$ZrCl$_2$ with K (Na) or NaNH$_2$ in liquid ammonia and toluene no definite compounds were isolable due to the insolubility of the resulting products in organic solvents. Bis(*tert*-butylamido)cyclodiphosph(III)azane is an interesting ligand due to its variety of coordination modes for the metal centers (η^1- to η^4-), variable sterical properties, and good solubility of the resulting products in organic solvents.

2.7.1. Synthesis and Characterization of LZrCl$_2$ (25, L = (PN*t*Bu)$_2$(*t*BuN)$_2$))

Treatment of ZrCl$_4$ with L(Li·THF)$_2$ in toluene at 80 °C results in the formation of colorless crystals of LZrCl$_2$ (**25**; Scheme 24) in 66 % yield.[113]

$$\text{ZrCl}_4 + \text{L(Li·THF)}_2 \xrightarrow[\text{110 °C, 48 h}]{\text{toluene}} \text{LZrCl}_2 + 2\ \text{LiCl}$$
$$\textbf{25}$$

L = (PN*t*Bu)$_2$(*t*BuN)$_2$

Scheme 24
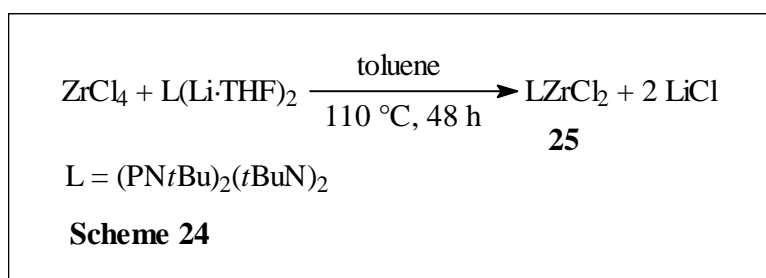
Compound **25** is a colorless crystalline solid melting at 170 °C. The most intense peak in the EI mass spectrum of **25** appears at *m/z* 493 [M$^+$ − Me], and the signal at 508 (7 %) is assigned to the molecular ion. Only two singlets at δ 1.41 and 1.27 ppm were found for the *t*Bu group protons in the ^{1}H NMR spectrum of **25**. This result indicates that L acts as a η^2-ligand coordinated to Zr. The elemental analysis of **25** is in agreement with the proposed composition.

2.7.2. Synthesis and Characterization of (η^3-L)(η^1-LH)ZrCl (26, L = (PN*t*Bu)$_2$(*t*BuN)$_2$))

Treatment of ZrCl$_4$ with 2 equiv of LH$_2$ and 3 equiv of *n*BuLi in toluene leads to the formation of the η^3/η^1-bis(*tert*-butylamido)cyclodiphosph(III)azane zirconium chloride (η^3-L)(η^1-LH)ZrCl (**26**, Scheme 25).[188]

Compound **26** is a colorless crystalline solid decomposing at 255 °C (Mp: 288 °C). The IR spectrum shows a broad absorption (3378 cm^{-1}) for **26**, assignable to the N-H stretching frequency. The most intense peak in the EI mass spectrum of **26** appears at *m/z* 471 [M$^+$ − LH], and the signal at 818 (8 %) is assigned to the molecular ion. The ^{1}H NMR spectral data are consistent with the structure of **26**. The methyl protons of the *tert*-butyl groups give rise to six singlets at δ 1.94 (9 H),

1.68 (18 H), 1.54 (9 H), 1.51 (18 H), 1.31 (9 H), 1.19 (18 H) ppm, respectively. The resonance of the NH proton appears as two broad singlets at δ 3.30 and 3.28 ppm.

$$\text{ZrCl}_4 + 2 \text{ LH}_2 + 3 \text{ } n\text{BuLi} \xrightarrow{\text{toluene, 80 °C, 48 h}} (\eta^3\text{-L})(\eta\text{-LH})\text{ZrCl} + 3 \text{ LiCl} + 3 \text{ } n\text{BuH}$$

26

L = (PNtBu)$_2$(NtBu)$_2$

Scheme 25
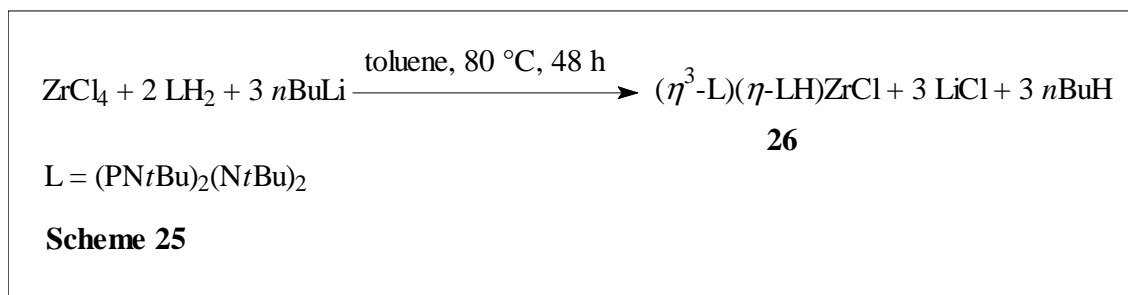
The molecular structure and the central core of **26** are shown in Figures 32 and 33, selected bond lengths and angles for **26** are presented in Table 16. Compound **26** crystallizes in the monoclinic space group $P2_1/n$. The molecular structure of **26** in the crystal shows that one η^3-L, one η^1-LH and one chlorine atom complete the coordination sphere of Zr. The chlorine atom is tilted away from the N(2)tBu moiety and the η^1-LH ligand, which minimizes the steric repulsion between the Cl atom and N(2)tBu group as well as the η^1-LH ligand.

The bond lengths Zr(1)–N(1) (2.104(2) Å) and Zr(1)–N(4) (2.103(7) Å) are comparable to those found in [(η^3-L)Zr(μ-NH)]$_2$ (2.116(7) Å and 2.129(7) Å)[113] and in [(MeSiNtBu)$_2$(NtBu)$_2$]ZrCl$_2$ (2.075(3) Å and 2.089(3) Å).[116] The sum of the angles at N(1) or N(4) is 359.2°. The approximately trigonal planar coordination indicates that the N(1) and N(4) atoms are nearly sp^2 hybridized, the N(1) and N(4) atoms donate their lone-pair electrons into the empty d-orbitals of zirconium as 3-electron donors in analogy to the bonding situation in [(η^3-L)Zr(μ-NH)]$_2$ and [(MeSiNtBu)$_2$(NtBu)$_2$]ZrCl$_2$. The bond lengths P(1)–N(1) (1.698(2) Å), P(1)–N(3) (1.730(2) Å) and P(1)–N(2) (1.785(2) Å) are similar to those found in [(η^3-L)Zr(μ-NH)]$_2$ (1.686(8) Å, 1.733(8) (Å) and 1.789(8) (Å), respectively) and [(η^3-L)In]$_2$ (1.670(3) Å, 1.723(3) Å and 1.801(3) Å, respectively).[117] The sp^2 hybridized N(6) atom (the sum of the angles at N(6) is 360.00°) results in a Zr(1)–N(6) bond length (2.210(2) Å) similar to those of Zr(1)–N(1) and Zr(1)–N(4).
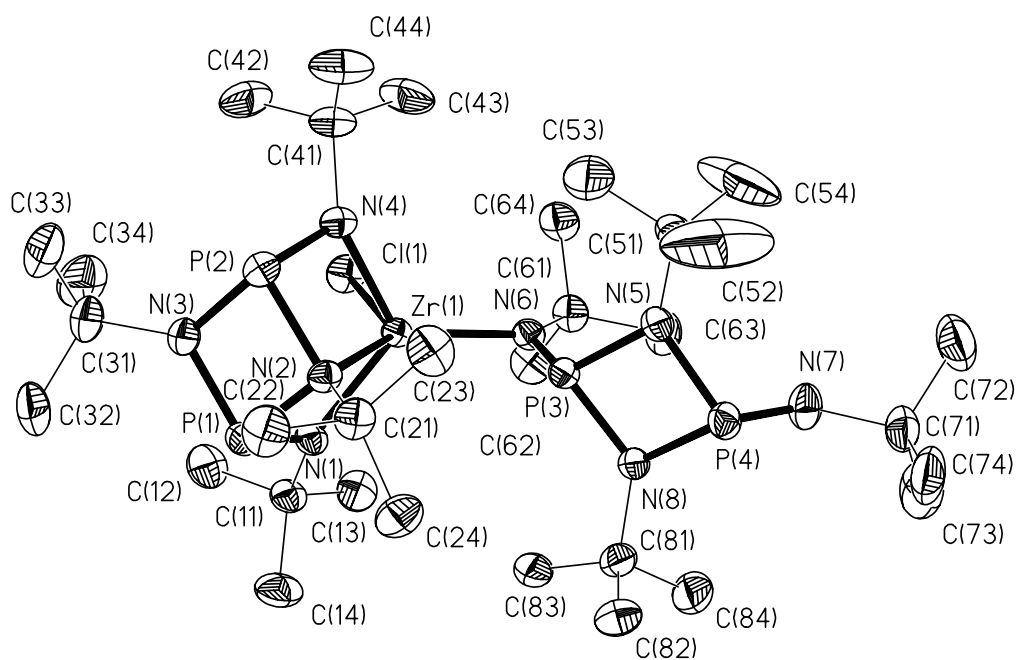
Figure 32. Molecular structure of (η^3-L)(η^1-LH)ZrCl (26) (50 % probability ellipsoids. H atoms bonded to C and N are omitted for clearity)
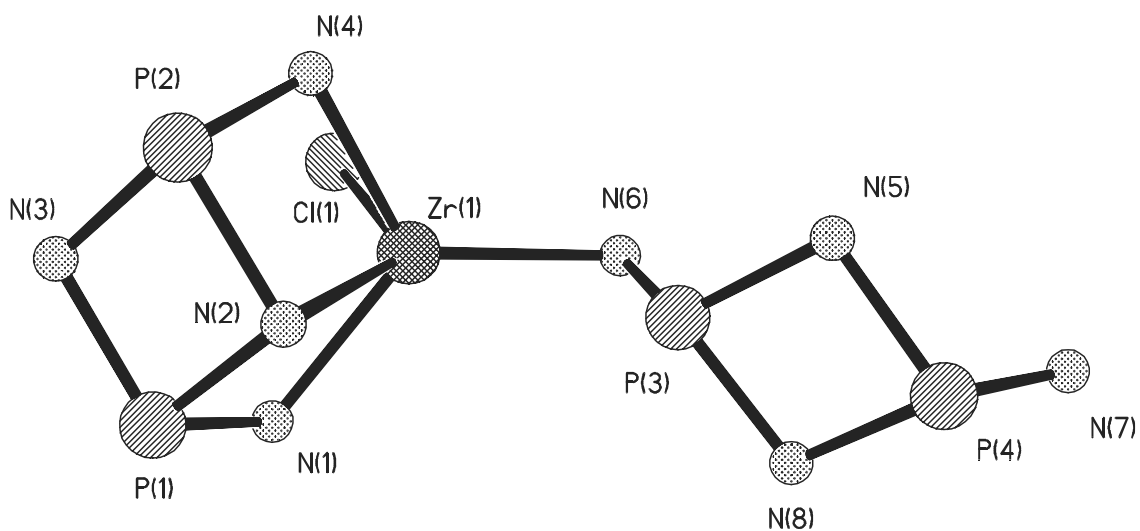
Figure 33. Central core of (η^3-L)(η^1-LH)ZrCl (26)

Table 16. Selected Bond Lengths (Å) and Angles (°) for 26

Zr(1)-N(1)	2.104(2)	Zr(1)-N(2)	2.376(2)
Zr(1)-N(4)	2.103(2)	Zr(1)-N(6)	2.210(2)
Zr(1)-Cl(1)	2.4723(8)	P(1)-N(1)	1.698(2)
P(1)-N(2)	1.785(2)	P(1)-N(3)	1.730(2)
P(1)-P(2)	2.6594(11)	P(2)-N(2)	1.785(2)
P(2)-N(3)	1.735(2)	P(2)-N(4)	1.697(2)
P(3)-P(4)	2.6181(10)	P(3)-N(5)	1.716(2)
P(3)-N(6)	1.629(2)	P(3)-N(8)	1.719(2)
P(4)-N(5)	1.729(2)	P(4)-N(7)	1.668(2)
P(4)-N(8)	1.736(2)		
N(1)-Zr(1)-N(4)	113.05(9)	N(4)-Zr(1)-N(6)	124.46(8)
N(1)-Zr(1)-N(6)	122.48(8)	N(2)-Zr(1)-N(4)	67.30(8)
N(1)-Zr(1)-N(2)	67.37(8)	N(2)-Zr(1)-N(6)	135.26(8)
N(4)-Zr(1)-Cl(1)	88.66(7)	N(1)-Zr(1)-Cl(1)	89.62(7)
N(6)-Zr(1)-Cl(1)	90.63(6)	N(2)-Zr(1)-Cl(1)	134.12(6)
N(1)-P(1)-N(3)	111.31(12)	N(1)-P(1)-N(2)	91.46(10)
N(3)-P(2)-N(4)	111.56(12)	N(2)-P(2)-N(4)	91.38(11)
N(2)-P(2)-N(3)	81.64(11)	N(2)-P(1)-N(3)	81.76(11)
P(1)-N(2)-P(2)	96.31(11)	P(1)-N(3)-P(2)	100.28(12)
N(5)-P(3)-N(6)	118.77(12)	N(6)-P(3)-N(8)	118.56(12)
N(5)-P(3)-N(8)	81.17(11)	N(5)-P(4)-N(8)	80.32(11)
P(3)-N(5)-P(4)	98.92(12)	P(3)-N(8)-P(4)	98.53(11)
N(5)-P(4)-N(7)	105.98(12	N(7)-P(4)-N(8)	106.40(12)
P(2)-N(2)-Zr(1)	91.21(9)	P(1)-N(2)-Zr(1)	91.25(9)
P(2)-N(4)-Zr(1)	103.83(11)	P(1)-N(1)-Zr(1)	103.81(11)
C(61)-N(6)-P(3)	133.78(19)	C(61)-N(6)-Zr(1)	139.20(17)
P(3)-N(6)-Zr(1)	87.02(10)		

The slightly longer P(1)–N(2) bond length compared to that of P(1)–N(3) is caused by the higher electron density on N(2) due to the back donation of electrons from Zr(1) to N(2), while

nearly the same bond lengths P(3)–N(5) (1.716(2) Å) and P(3)–N(8) (1.719(2) Å) were found in the η^1-L ligand in **26**. The formation of the N(2)→Zr(1) donor bond results in the distortion of the P(1)N(2)P(2)N(3) four-memberd ring in the η^3-L ligand (the sum of the angles in the ring is 348.99°), while the η^1-L ligand contains a nearly planar P(3)N(5)P(4)N(8) four-memberd ring (the sum of the angles in the ring is 358.94°).

2.7.3. Synthesis and Characterization of $[(\eta^1\text{-LH})\text{Zr}(N\textit{t}Bu)\{(N\textit{t}Bu)_2\text{PPN}\textit{t}Bu\}\{K\cdot(\eta^6\text{-}C_7H_8)\}]\cdot0.5C_7H_8$ (27, L = (PN\textit{t}Bu)$_2$(\textit{t}BuN)$_2$))

It has been reported that the reduction of organic amidozirconium chlorides leads to zirconium dinitrogen complexes.[111] Treatment of **26** with K/Na alloy in toluene at room temperature for 48 h, and then at 110 °C for 24 h with stirring yields **27** (Scheme 26).[188] In this reaction, cleavage of two P–N bonds of the η^3-L ligand in **26** by alkali metals results in the formation of a Zr=N double bond, a P–P single bond, and K–N bonds. The bulky ligands on zirconium are stabilizing the imido zirconium monomer **27**.

(η^3-L){η-LH}ZrCl + 2 K/Na $\xrightarrow{\begin{array}{l}\text{(1) toluene, RT, 24 h}\\ \text{(2) toluene, 110 °C, 48 h}\end{array}}$ NaCl + KCl +

26

$[(\eta^1\text{-LH})\text{Zr}(N\textit{t}Bu)\{(N\textit{t}Bu)_2\text{PPN}\textit{t}Bu\}\{K\cdot(\eta^6\text{-}C_7H_8)\}]\cdot0.5C_7H_8$

27

L = (PN\textit{t}Bu)$_2$(N\textit{t}Bu)$_2$
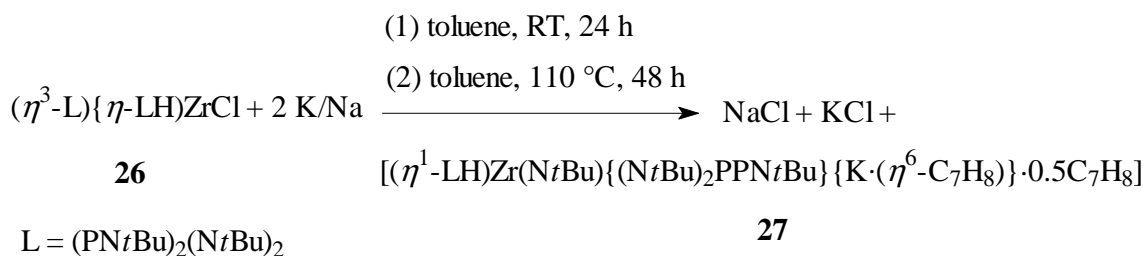
Scheme 26

Compound **27** is a colorless crystalline solid with a melting point of 273 °C. The IR spectrum shows two absorptions (3377 and 3334 cm^{-1}) for **27**, assignable to the N-H stretching frequencies. Compound **27** exhibits the fragments [M$^+$ − K − 1.5 C$_7$H$_8$ + H], [M$^+$ − K − 1.5 C$_7$H$_8$ − \textit{t}Bu + H], and [L$^+$ − \textit{t}Bu] at 784 (9 %), 727 (11 %), and 276 (100 %). While the signal at 915 [M$^+$ − 0.5 C$_7$H$_8$] was observed with very low intensity due to the easy loss of the C$_7$H$_8$ molecule (no bonding relationship with K) under EI-MS condition in compound **27**. The ^{1}H NMR spectral data of **27** is consistent with the structure of **27**. The methyl protons of the *tert*-butyl groups give rise to seven

singlets (δ 1.94 (9 H), 1.69 (18 H), 1.60 (18 H), 1.40 (18 H), 1.28, 1.27 (9 H), 1.11 (9 H) ppm). The resonance of the NH proton appears as two singlets (δ 3.38 and 3.34 ppm). The elemental analysis of **27** shows that the contents of C and H are slightly lower than the calculated ones due to its sensitivity to moisture and the partial removal of the toluene molecule from the crystalline solid *in vacuo*.

The molecular structure and the central core of **27** are shown in Figures 34 and 35, and selected bond lengths and angles for **27** are presented in Table 17. Compound **27** crystallizes in the triclinic space group $P\bar{1}$. The X-ray diffraction analysis of **27** reveals that the four coordination sites at zirconium are occupied by one η^1-L ligand, one imido moiety and two amido nitrogen atoms, respectively.
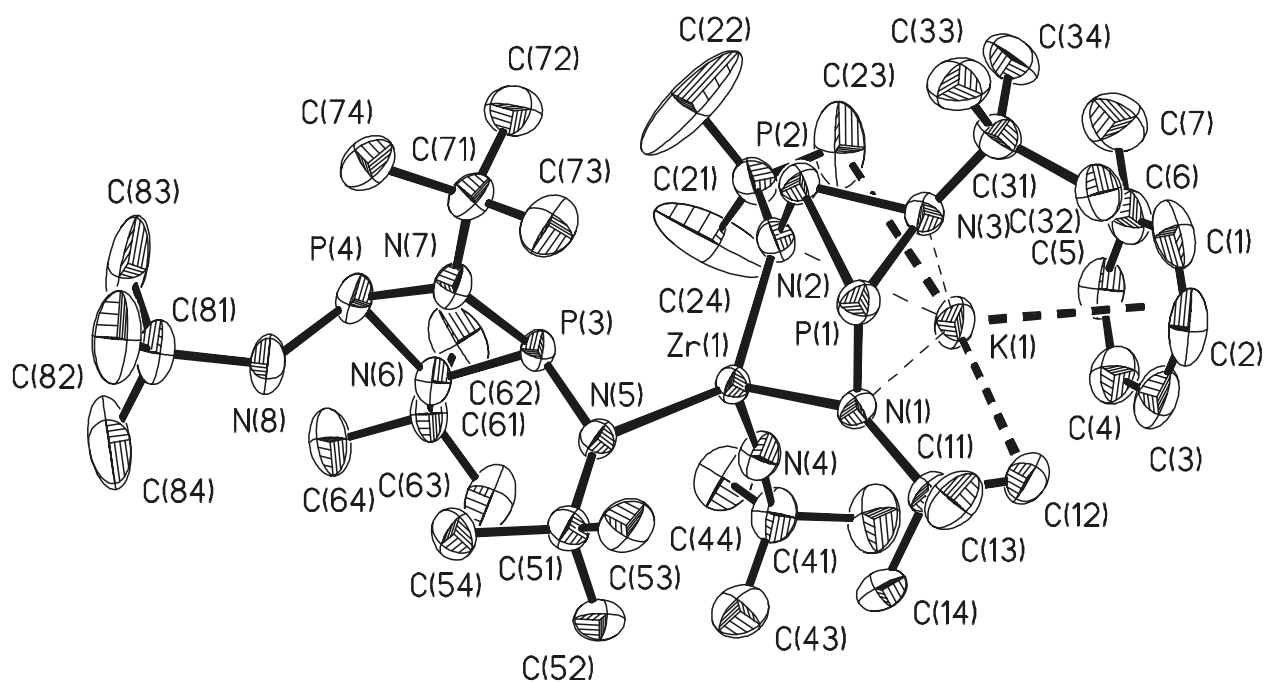
Figure 34. Molecular structure of [(η^1-LH)Zr(N*t*Bu){(N*t*Bu)$_2$PPN*t*Bu} {K·(η^6-C$_7$H$_8$)}·0.5C$_7$H$_8$] (27) (50 % probability ellipsoids. 0.5 toluene molecule and H atoms bonded to C and N are omitted for clearity)
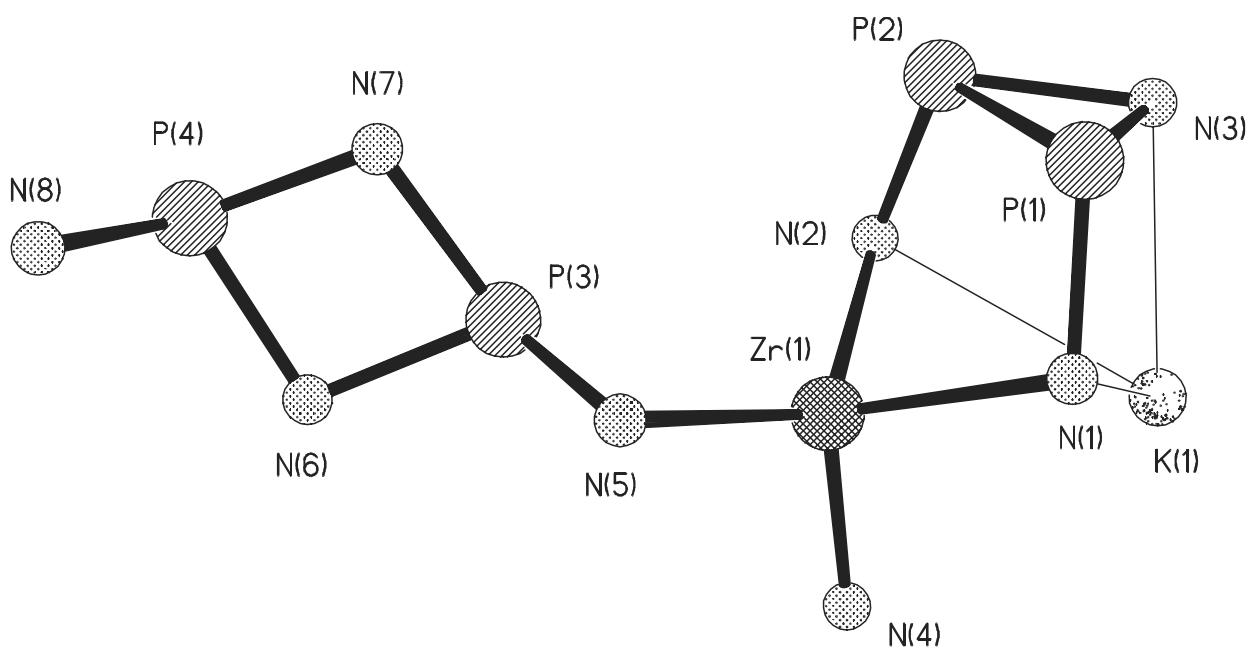
Figure 35. Central core of [(η^1-LH)Zr(N*t*Bu){(N*t*Bu)$_2$PPN*t*Bu} {K·(η^6-C$_7$H$_8$)}·0.5C$_7$H$_8$] (27)

Table 17. Selected Bond Lengths (Å) and Angles (°) for 27

Zr(1)-N(1)	2.167(3)	Zr(1)-N(2)	2.194(3)
Zr(1)-N(4)	1.864(3)	Zr(1)-N(5)	2.263(3)
P(1)-N(1)	1.689(3)	P(1)-N(3)	1.774(3)
P(1)-P(2)	2.236(2)	P(3)-P(4)	2.626(2)
P(2)-N(2)	1.687(3)	P(2)-N(3)	1.771(3)
N(1)-K(1)	3.086(3)	N(2)-K(1)	2.859(3)
N(3)-K(1)	2.892(4)	C(1)-K(1)	3.406(5)
C(2)-K(1)	3.302(5)	C(3)-K(1)	3.260(5)
C(4)-K(1)	3.311(5)	C(5)-K(1)	3.417(5)
K(1)-C(6)	3.466(5)	K(1)-C(c)*	3.07
K(1)-C(12)	3.14	K(1)-C(23)	3.30
P(3)-N(5)	1.618(3)	P(3)-N(6)	1.734(3)
P(3)-N(7)	1.745(3)	P(4)-N(6)	1.734(3)
P(4)-N(7)	1.735(3)	P(4)-N(8)	1.671(3)
N(4)-Zr(1)-N(4)	105.06(13)	N(2)-Zr(1)-N(4)	105.04(14)

Table 17. Selected Bond Lengths (Å) and Angles (°) for 27 (continued)

N(1)-Zr(1)-N(2)	94.33(12)	N(4)-Zr(1)-N(5)	112.54(13)
N(1)-Zr(1)-N(5)	105.75(11)	N(2)-Zr(1)-N(5)	130.17(11)
N(1)-P(1)-N(3)	106.08(15)	N(1)-P(1)-P(2)	106.67(11)
N(2)-P(2)-P(1)	106.46(12)	N(2)-P(2)-N(3)	105.71(15)
N(3)-P(1)-P(2)	50.84(10)	N(3)-P(2)-P(1)	50.97(10)
P(1)-N(3)-P(2)	78.19(13)	P(1)-N(1)-Zr(1)	102.48(13)
P(1)-N(1)-K(1)	96.84(12)	Zr(1)-N(1)-K(1)	80.25(10)
P(2)-N(2)-Zr(1)	102.10(14)	P(2)-N(2)-K(1)	100.11(13)
Zr(1)-N(2)-K(1)	85.28(11)	N(5)-P(3)-N(6)	116.61(15)
N(5)-P(3)-N(7)	116.10(14)	N(6)-P(3)-N(7)	80.30(14)
N(6)-P(4)-N(7)	80.58(14)	P(3)-N(6)-P(4)	98.41(15)
P(3)-N(7)-P(4)	97.95(15)	P(2)-N(3)-K(1)	96.83(13)
P(1)-N(3)-K(1)	101.85(13)	N(6)-P(4)-N(8)	106.00(16)
N(7)-P(4)-N(8)	105.02(16)	N(6)-P(4)-P(3)	40.80(10)
N(7)-P(4)-P(3)	41.16(10)	P(3)-N(5)-Zr(1)	89.47(12)
C(51)-N(5)-P(3)	133.9(2)	C(51)-N(5)-Zr(1)	136.39(19)
N(2)-K(1)-N(3)	57.30(9)	N(1)-K(1)-N(2)	64.96(9)
N(1)-K(1)-N(3)	55.05(9)	C(11)-N(1)-P(1)	117.7(2)
C(11)-N(1)-Zr(1)	139.1(2)	P(1)-N(1)-Zr(1)	102.48(13)

The bond lengths Zr(1)–N(5) (2.263(3) Å), P(3)–N(5) (1.618(3) Å), P(3)–N(6) (1.734(3) Å) and P(3)–N(7) (1.745(3) Å) as well as the P(3)–P(4) distance (2.626(2) Å) in the η^1-LH ligand are comparable with those found in the η^1-LH ligand of compound **26** (2.210(2) Å, 1.629(2) Å, 1.716(2) Å, 1.719(2) Å, 2.618(10) Å, respectively). A slightly distorted P(3)N(6)P(4)N(7) four-membered ring (the sum of the angles in the ring is 357.24°) is found in **27**.

The Zr(1)–N(4) (imido) bond length (1.864(3) Å) is comparable with those found in [P$_2$N$_2$]Zr=NtBu ([P$_2$N$_2$] = PhP(CH$_2$SiMe$_2$NSiMe$_2$CH$_2$)$_2$PPh, 1.8413(15) Å),[60] (TTP)Zr=NAr (TTP = *meso*-tetra-*p*-tolylprophyrinato dianion, Ar = 2,6-diisopropylphenyl, 1.863(2) Å),[59] [{(η^3-L)Zr=NtBu(HNtBu)}$^-${K·(η^6-C$_7$H$_8$)}$^+$] (1.893(9) Å),[189] and in Cp*Zr=NAr(NHAr)·(C$_5$H$_5$N) (1.876(4) Å).[68] The P(1)–P(2) bond length (2.236(2) Å) is comparable with a P–P bond (2.234

Å) in black phosphorus[190] and those found in polyphosphides (2.215 − 2.230 Å).[191] The K(1)–N(2) (2.859(3) Å) and K(1)–N(3) (2.892(4) Å) bond lengths are comparable with those in [KN(SiMe$_3$)$_2$]$_2$ (2.770(3) Å and 2.803(3) Å)[139] and [K(NPPh$_3$)]$_6$·4C$_7$H$_8$ (2.691(5) Å to 2.975(5) Å, av 2.805 Å),[192] and are shorter than those in the ionic complex [{(η^3-L)Zr=NtBu(HNtBu)}$^-$ {K·(η^6-C$_7$H$_8$)}$^+$] (2.910(9) Å, 3.012(13) Å and 3.069(11) Å).[189] The relatively long K(1)–N(1) (3.086(3) Å) bond length indicates only a weak interaction between N(1) and K(1). Furthermore, the approximately trigonal planar coordination geometry (the sum of the angles at N(1) and N(2) is 359.3° and 354.8°) shows that N(1) and N(2) atoms are nearly sp^2 hybridized, the N(1) and N(2) atoms donate their lone-pair electrons into the empty d-orbitals of zirconium and the s-orbital of potassium as a 3-electron donor. Due to the formation of N−K bonds, the Zr(1)−N(1) (2.167(3) Å) and the Zr(1)−N(2) (2.194(3) Å) bond lengths are longer than those found in [(η^3-L)Zr(μ-NH)]$_2$ (2.116(7) Å)[113] and (η^3-L)(η^1-LH)ZrCl (2.104(2) Å).

The distances of K(1) to the carbon atoms of the toluene ring (3.260(5) to 3.466(5) Å, av 3.359 Å) are similar to those in the K·(η^6-benzene) complexes [(η^6-C$_6$H$_6$)·KOSiMe$_2$Ph]$_4$ (3.233(14) to 3.308(6) Å, av 3.275 Å)[193] and L′K·C$_7$H$_8$ (L′ = 18-crown-6, 3.044(5) to 3.311(5) Å).[194] The distance from K(1) to the centroid of the toluene ring (3.07 Å) is comparable to those reported in [K{Sn[CH$_2$$t$Bu)$_3$}·3($\eta^6$-C$_7H_8$)] (3.13 to 3.41 Å, av 3.30 Å)[195] and Lu{CH(SiMe$_3$)$_2$}$_3$(μ-Cl)K·3(η^6-C$_7$H$_8$) (3.003 and 3.128 Å).[196] Kebarle and co-workers[197] have calculated the bonding energy of benzene to K$^+$ as ca 80 KJ mol^{-1}. Interestingly, additional weak bonding relationship between potassium and two methyl groups (K(1)–C(12) 3.14 Å, K(1)–C(23) 3.30 Å) is observed in the structure of **27** in analogy to the K···Me attraction in [iPr$_2$NK·TMEDA]$_2$ (TMEDA = N, N, N′, N′-tetramethylenediamine; K–C 3.34 to 3.47 Å)[198] and KC(SiMe$_3$)$_2$(SiMe$_2$NMe$_2$) (K–C 3.11 to 3.49 Å).[199] The interactions between K(1) and η^6-C$_7$H$_8$ as well as with the two methyl groups are important to stabilize the potassium ion in addition to the K−N contacts.

3. Summary and Outlook

3.1. Summary

New methods for the preparations of nitrogen- and oxygen-containing early transition metal compounds and imido-*ansa*-metal hydrides, which are difficult to achieve by other methods, have been developed during the present work. For the preparations the liquid ammonia/toluene two phase system was used for the first time. A series of amido, imido and/or nitrido group 4 metal compounds, an imido titanium potassium dinitrogen complex, a zirconium dihydride, and organometallic zirconium and vanadium oxides have been prepared in liquid ammonia/toluene by treatment of the corresponding metal chlorides with K (Na), $NaNH_2$, KH, or KOH, respectively. These reactions have in common that all the chlorine atoms are removed, and in some cases, the R$-$M bonds are cleaved by either alkali metals or another strong base in the liquid ammonia/toluene two phase system.

Reactions of $(MeC_5H_4)_2ZrCl_2$ with alkali metal ammonia/ toluene mixtures are similar to those with alkali metal amides in liquid ammonia/toluene or in THF, which lead to the larger nitrogen zirconium aggregate **3** with elimination of the MeC_5H_4 group as $(MeC_5H_4M)_n$ (**4**, M = K). The formation of **3** can be rationalized to proceed via amido and amidoimidozirconium intermediates.
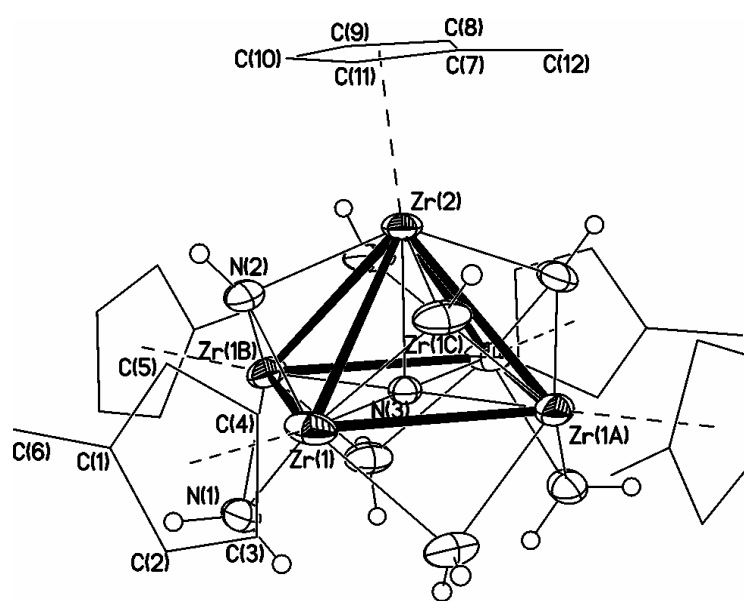
Molecular structure of 3   **Molecular structure of 4**
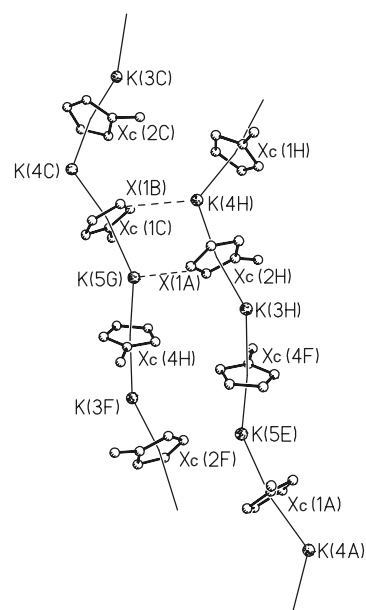
The first unsubstituted imido (NH) bridged zirconium compound **9** has been prepared in the presence of KH in liquid ammonia/toluene. The bis(*tert*-butylamido)cyclodiphosph(III)azane ligand is important for the stabilization of **9**. The nearly planar coordination geometry at the amido nitrogen atoms suggests that the two nitrogen atoms are serving as 3-electron donors for each metal.
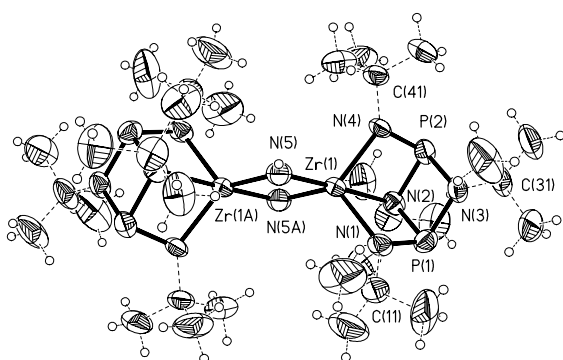
Molecular Structure of 9   **Molecular Structure of 10**
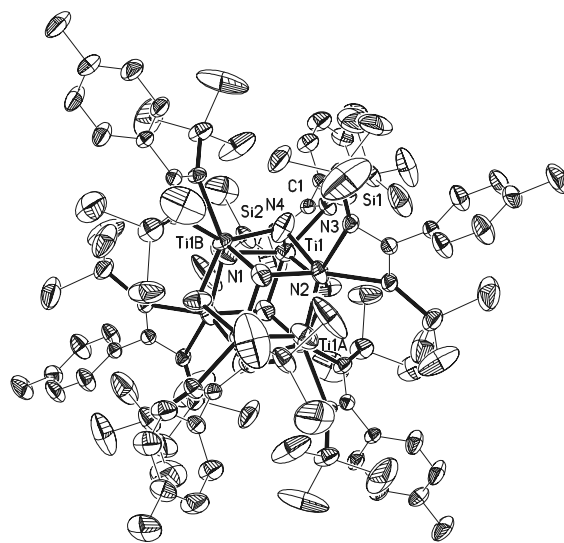
Changing the ligand on titanium and the preparation method leads to the nitrogen titanium cluster **10** when [p-MeC$_6$H$_4$C(NSiMe$_3$)$_2$]$_2$TiCl$_2$ is treated with NaNH$_2$ in liquid ammonia/toluene. Compound **10** contains the largest Ti-N cluster so far reported, and can be regarded having the dimeric core of the previously reported [(Cp*Ti)$_3$(μ-NH)$_3$(μ_3-N)].

The reaction of [p-MeC$_6$H$_4$C(NSiMe$_3$)$_2$]$_2$TiCl$_2$ with K (Na) in liquid ammonia/toluene gives a reduced titanium species **21** under migration of L. Moreover, the reactions yielding **10** and **21** have in common that L-Ti bonds are cleaved by either NaNH$_2$ or potassium (sodium) in liquid ammonia/toluene.

The reaction of Cp*$_2$TiCl with one equiv of NaNH$_2$ in liquid ammonia/toluene yields titanium(III) amide **11.**
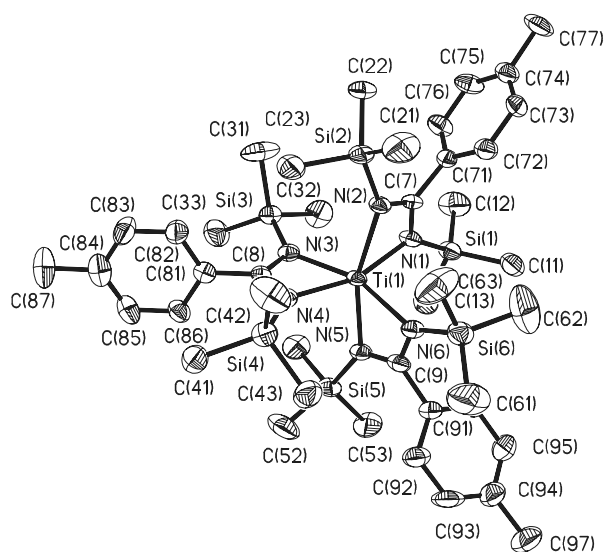
Molecular structure of 21
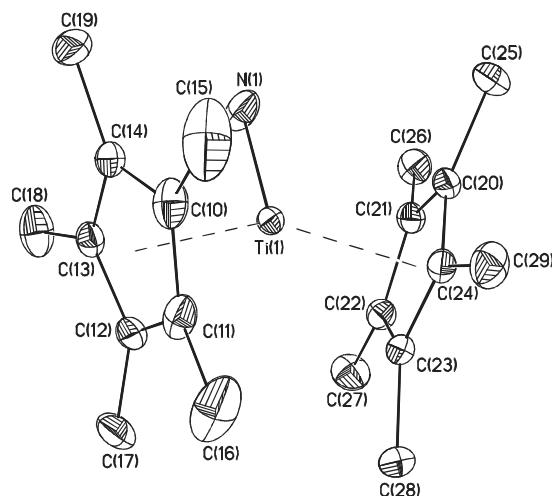
Molecular structure of 11
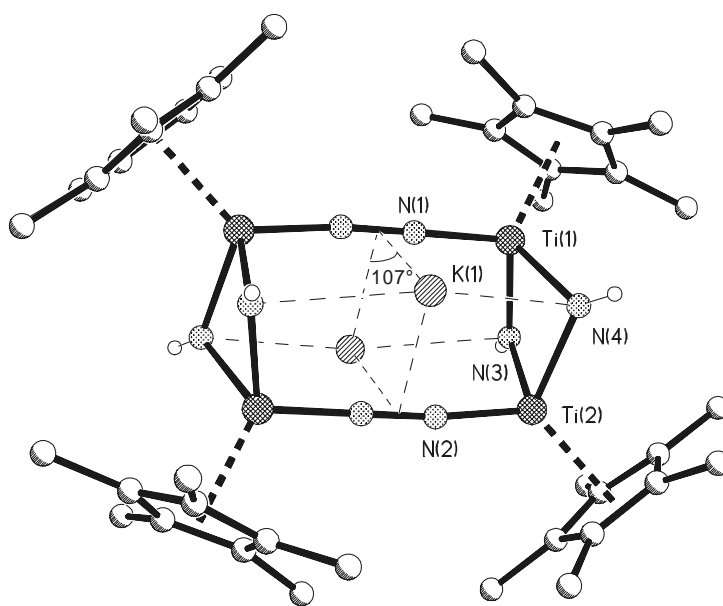
Molecular Structure of 12

It has been shown for the first time that the alkali metal ammonia solutions can be used to prepare dinitrogen metal complexes. Treatment of Cp^*_2TiCl with K in liquid ammonia and toluene yields the imido Ti(II)/Ti(III) potassium dinitrogen complex $[(Cp^*Ti)_4(\mu_3-NH)_4(\mu_4-\eta^1:\eta^1:\eta^2:\eta^2-N_2)_2K_2]$ (**12**). The molecular structure of **12** consists of two distorted four-membered $(Cp^*Ti)_2(NH)_2$ rings which are bridged by a slightly distorted octahedral $K_2(N_2)_2$ moiety placed on the symmetric center of **12** with four Ti–$(\mu-\eta^1:\eta^1-N_2)$ and four K–NH bonds. Two of the parallel

dinitrogen ligands further interact with two K^+ in a side-on manner. The long N−N bonds (1.308(13) Å) indicate that the N_2 moieties in **12** are reduced by end-on coordinated titanium atoms and side-on coordinated potassium atoms.
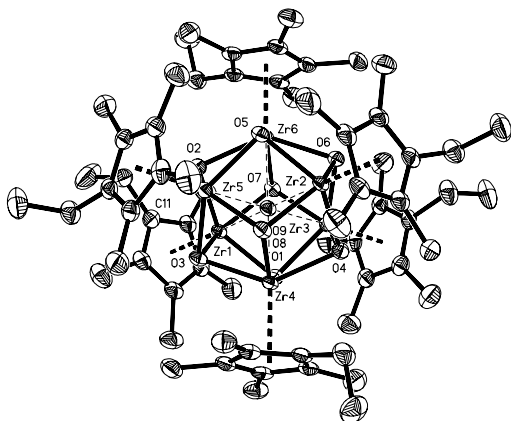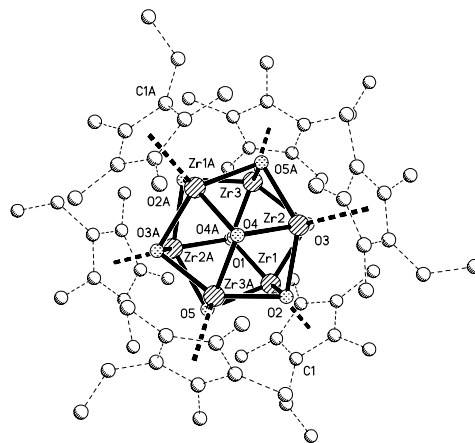
Molecular Structure of 13   **Molecular Structure of 16**

A new method for the preparation of organometal oxides by hydrolysis of an organometal chloride at low temperatures has been developed. Using this method, the organozirconium oxides **13** and **16** have been obtained. In comparison to the traditional preparation of ZrO_2 from $ZrCl_4$ at 1000 °C the new route yields crystalline products below room temperature. It is assumed that the formation of **13** proceeds via zirconium hydroxide and amide intermediates. KH is important for the preparation of **13** in liquid ammonia/toluene. Compounds **13** and **16** contain the largest Zr-O cores so far reported, which can be regarded as dimeric congeners of the previously reported [{(Cp*ZrCl)(μ-OH)}$_3$(μ_3-OH)(μ_3-O)·2THF] cluster[76] without six HCl, four THF, and one H_2O molecules.

So far the largest Brönsted acidic organozirconium oxide/hydroxide cluster **17** has been prepared by hydrolysis of an organometal chloride at low temperatures. The central inorganic core of **17** (overlooking the disordering of the interstitial oxygen atom) can be regarded as a derivative of **13**, in which the μ-O and μ-OH species replace the μ_3-O units. The ab-initio results indicate that the interstitial oxygen atom possesses a floppy nature and the stability of the μ_6-O core is comparable to that of the off-center one. The organic ligands and the acidic OH groups due to the Zr(IV) centers on the cluster surface render **17** soluble and reactive to a variety of metal

compounds in solution. Therefore further reactions might take place preferentially at the metal oxide surface.
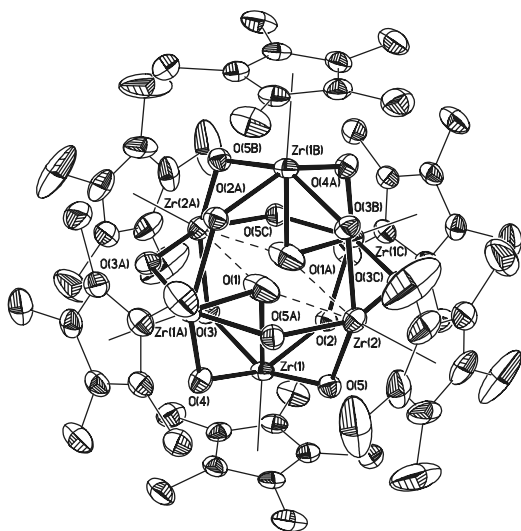
Molecular structure of 17
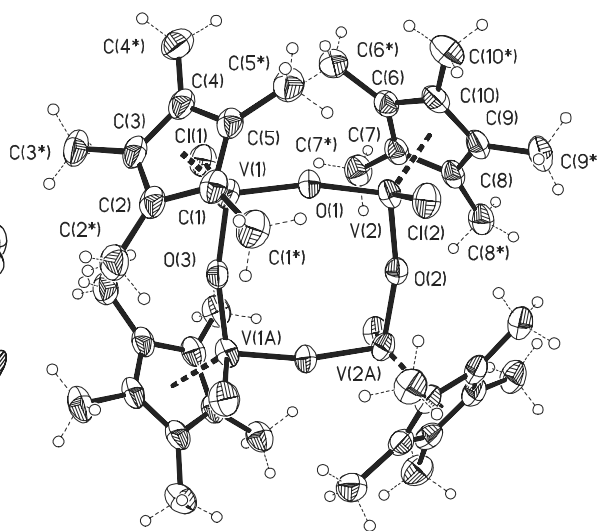
Molecular structure of 18

Upon treatment of $[Cp^*V(\mu\text{-}Cl)_2]_3$ with $NaNH_2$ in THF at 40 °C no chlorine free amido, imido or nitrido vanadium compound was isolable. Controlled oxidation of the resulting THF solution generated tetraoxovanadium(IV) chloride $[Cp^*VCl(\mu\text{-}O)]_4 \cdot THF$ (**18**).
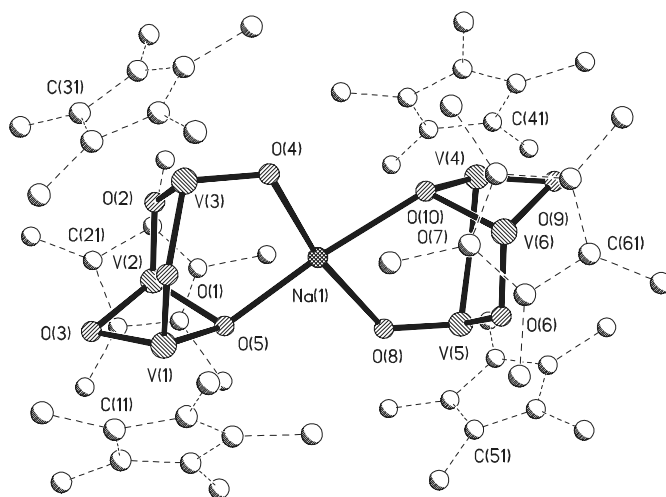
Molecular structure of 19

The reaction of $[Cp^*V(\mu\text{-}Cl)_2]_3$ with O_2 in toluene at room temperature with successive treatment by $NaNH_2$ in liquid ammonia/toluene at -78 °C results in the complete removal of chloride and the formation of the organic V(IV)/V(V) sodium oxide $(Cp^*V)_6(\mu\text{-}O)_8(\mu_3\text{-}O)_2Na$ (**19**). **19** can be regarded as a V(IV) anion $[(Cp^*V)_3O_5]^-$ and a V(IV)/V(V) unit $[(Cp^*V)_3O_5]$ linked together by a sodium cation.

It has been shown for the first time that the alkali metal ammonia solutions can be used to prepare a zirconium dihydride via an intramolecular reaction with simultaneous coupling of two silicon chloride substituted cyclopentadienyl rings. The first imido-*ansa*-zirconocene dihydride **20** is accessible when $(ClMe_2SiC_5H_4)_2ZrCl_2$ is treated with K (Na) in liquid ammonia/toluene. Appearingly, the Si–NH–Si unit is crucial for forming and stabilizing the zirconium hydride.
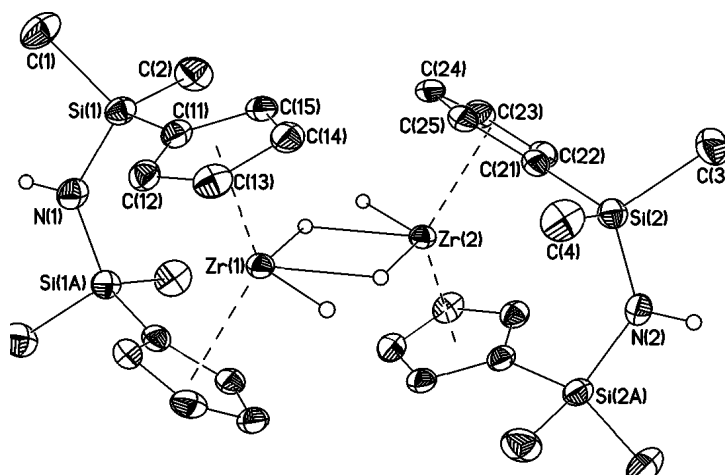
Molecular structure of 20

The two phase system ammonia/toluene increases the solubility of the organic and inorganic components, so that the reaction preferentially occurs at the interface. Therefore we assume that the liquid ammonia and toluene two phase system is important for the above reactions.

The reaction of methylcyclopentadienyl titanium trichloride with lithiated trimethylsilyl diazomethane leads to the imido bridged dinuclear titanium complex **22**. This is an interesting example of a migration of a trimethylsilyl group when a diazo derivative is reacted with a transition metal compound. Obviously, during the reaction an elimination of a CN group occurs. Moreover, the less sterically hindered and strong Lewis acidic titanium center is important for the formation of **22**. The direct reaction of Cp_2ZrHCl with Me_3SiCHN_2 in toluene at room

temperature produces the η^2-hydrazonato complex **23** in high yield. In compound **23** an electronic delocalization over the C–N–N unit leads to an easy interconversion of the isomer (N=CHSiMe$_3$) from *cis* to *trans* in solution in agreement with two resonances for SiMe$_3$, Cp and NH protons, respectively, in the ^{1}H NMR spectrum.
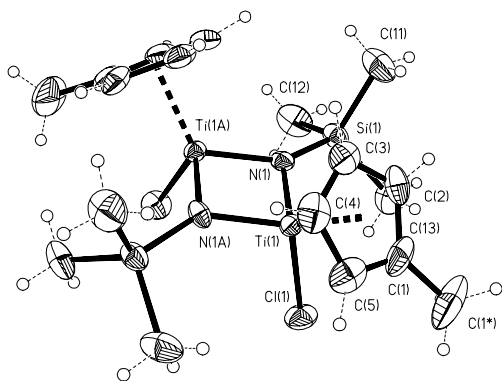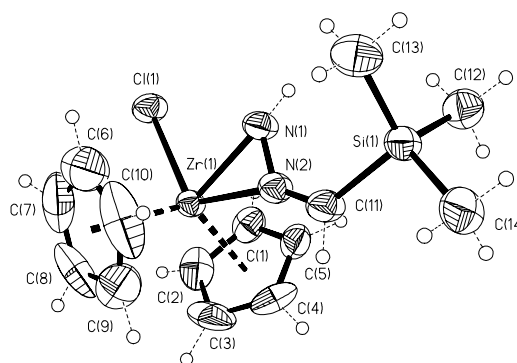
Molecular structure of 22   **Molecular structure of 23**

Treatment of ZrCl$_4$ with PhNH$_2$ and K generates imido bridged dinuclear compound **24**. The significantly different Cl–Zr–Cl angles and slightly different Cl–Zr bond lengths result from the different coordination spheres at the Zr atoms in **24**.
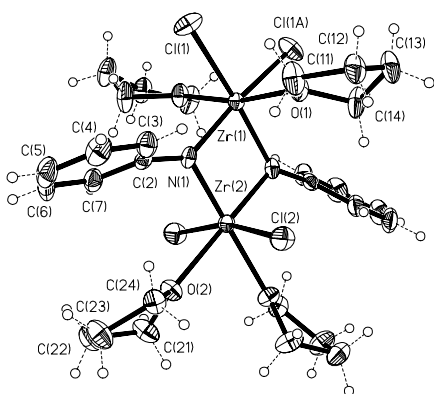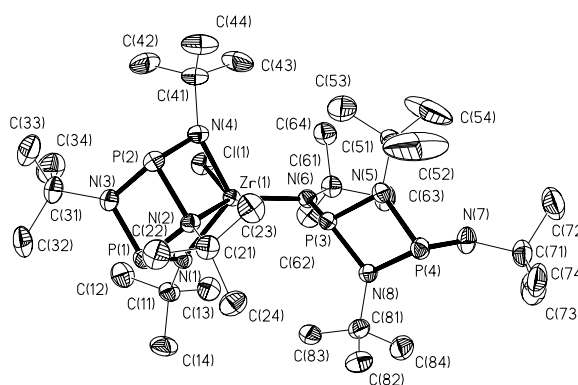
Molecular structure of 24   **Molecular structure of 26**

Treatment of ZrCl$_4$ with lithiated bis(*tert*-butylamido)cyclodiphosph(III)azane yields LZrCl$_2$ (**25**). Reaction of ZrCl$_4$ with LH$_2$ and *n*BuLi results in the formation of the η^3/η^1-bis(*tert*-butylamido)cyclodiphosph(III)azane zirconium chloride **26**.

Further reaction of **26** with K/Na alloy in toluene leads to the cleavage of two P–N bonds of the η^3-L ligand and the formation of a Zr=N double bond, a P–P single bond, and K–N bonds. It is assumed that the bulky η^1-L, imido and η^2-amido ligands on zirconium are important for forming and furthermore stabilizing the imido zirconium monomer **27,** while the interactions between K and amido moieties, η^6-C$_7$H$_8$ as well as agostic interaction with two methyl groups are important to stabilize the potassium ion in **27**. Furthermore, compound **27** should be a good precursor for the synthesis of homo- and heterometallic complexes.
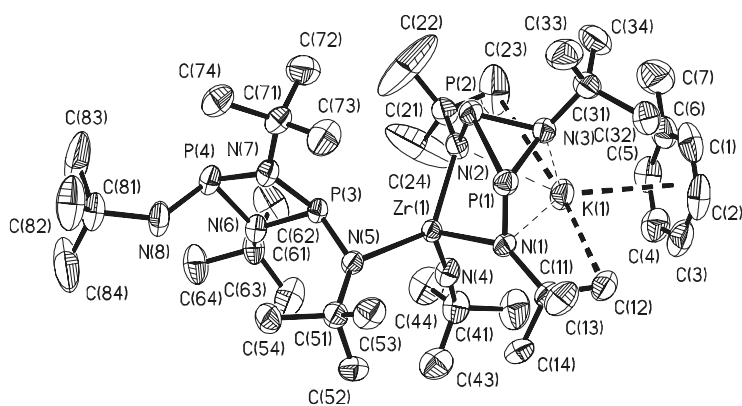
Molecular Structure of 27

Three different coordination modes (η^1-, η^2- and η^3-) of the bis(*tert*-butylamido)cyclodiphosph(III)azane ligand (L) to a zirconium center have been found in **9**, **25**, **26**, and **27**, respectively.

3.2. Outlook

This work has been focused on the strong base assisted ammonolysis and hydrolysis of organometallic chlorides in liquid ammonia/toluene two phase system, which resulted in several polynuclear transition metal nitrogen-containing complexes and organometallic oxides.

A burgeoning discipline of transition metal inorganic and organometallic chemistry involves the preparation of solid-state materials via solution methods using molecular precursors. The development of solution synthesis for M$_x$N$_y$ solids via inorganic and organometallic precursors

represents an intriguing challenge in the materials science field. The metal nitrogen-containing complexes are promising precursors to solid-state metal nitride materials via solution methods. This work describes a new method for the preparation of polyamido, imido and/or nitrido metal complexes from metal halides. Using this method, some larger interesting nitrogen-containing metal clusters, such as $[(RZr)_6(\mu_6\text{-N})(\mu_3\text{-NH})_8]^-$ should be prepared. Hoffmann and co-workers[21] indicated that the hypothetical cluster anion has a large HOMO-LUMO gap and therefore should be electronically stable. Consequently they predicted that it should be possible to prepare the polyimidonitrido zirconium cluster anion. As seen from EI-MS spectrum, $[(Cp^*Zr)_6(\mu_6\text{-N})(\mu_3\text{-NH})_6(\mu_3\text{-O})_2]$ or $[(Cp^*Zr)_6(\mu_6\text{-O})(\mu_3\text{-NH})_7(\mu_3\text{-O})]$ has been prepared successfully in the liquid ammonia/toluene two phase system.

Metal oxides have long been used extensively as very useful catalysts for a variety of inorganic and organic reactions and used directly in the chemical industry. The polyoxo organometallic aggregates can be used as model systems for molecular metal oxides in solution and as catalysts in homogeneous systems. A new method has been developed in this work for the preparation of metal oxides which are difficult or very expensive to be synthesized by other methods. A great variety of metal and nonmetal oxides could be easily prepared by these methods.

Polyoxometalate-supported transition metal catalysts which can be fully investigated at the atomic level both structurally and mechanistically represent a new development of oxide-supported catalysts. Organic polyoxozirconium-supported metal complexes are very rare. A new method has been developed in this work for the preparation of metal oxides/hydroxides which are Brönsted acidic due to the the metal centers and soluble in solution. These metal oxides/hydroxides can be used as homogeneous catalysts and for the preparations of homo- or heterometallic clusters. Metal compounds or other functional groups can be anchored on the surfaces of the clusters. Furthermore, the sizes of the oxide cores are in the nanometer range, these metal oxides/hydroxides may be a good precursors for the preparation of nanometer size metal oxides.

Metal hydride complexes provide valuable catalysts and reagents for the selective synthesis of various organic derivatives. This work has shown that alkali metal ammonia solutions can be used to prepare metal hydrides which may have special properties, such as stereo- or chemoselectivity for functional organic groups.

From these fundamental studies, we anticipate that some new convenient and cheap methods for the preparations of nitrogen- and oxygen-containing metal and nonmetal compounds, such as

M–N (e.g Al–N, Si–N, Ti–N, Zr–N) and M–O (e.g. Al–O (MAO), Si–O, Ti–O, Zr–O), and polyoxometal-supported metal catalysts suitable for industrial applications can be developed.

NH_3 is a stronger ligand for metals than N_2. Interestingly, a dinitrogen complex **12** was isolated from a liquid ammonia solution. This result may provide some new ideas for dinitrogen-fixation studies.

Furthermore, the formation of nitrogen- and oxygen-containing compounds such as **3**, **9**, **13**, **17**, **19**, **20**, **24**, **25**, **26,** and **27** may allow further reactions or catalysis studies with these compounds.

4. Experimental Section

4.1. General Procedures

All experimental manipulations, unless otherwise specified, were carried out under an atmosphere of purified nitrogen using standard Schlenk techniques. Samples prepared for spectral measurements as well as for reactions were manipulated in a glove-box where the O_2 and H_2O levels were normally maintained below 1 ppm. The glassware used in all the manipulations was oven-dried at 150 °C, assembled hot and cooled under high vacuum before use. Solvents were dried using conventional procedures,[200] distilled under nitrogen and degassed prior to use.

4.2. Physical Measurements

The *melting points* of all new compounds were measured on a BÜCHI Melting Point B-540 instrument.

The *NMR spectra* were recorded on Bruker AM 200, AM 250, MSL 400 or MSL 500 NMR spectrometers with $SiMe_4$ as external standard for ^1H, and ^{13}C, 85 % H_3PO_4 for ^{31}P. The heteroatom NMR spectra were measured ^1H decoupled. The chemical shifts are reported in ppm. Downfield shifts from the reference are quoted positive and upfield shifts are reported as negative values. The multiplicities are assigned as follows: s (singlet), d (doublet), t (triplet), q (quartet), and m (multiplet). The deuterated solvents THF-d_8 and C_6D_6 were dried over Na/K alloy, and $CDCl_3$ was refluxed with CaH_2 and then trap-to-trap distilled.

Mass spectra were recorded on a Finnigan MAT 8230 or Varian MAT CH 5 mass spectrometer by EI-MS methods. The most intensive peak of an isotope distribution is tabulated.

IR spectra were recorded on Bio-Rad FTS-7 spectrometer as nujol mulls between KBr plates. Intensities are estimated as follows: w (weak), m (medium), s (strong), and vs (very strong). Only very strong, strong and characteristic absorptions are given.

Elemental analyses were performed at the Analytical Laboratory of the Institute of Inorganic Chemistry, University of Göttingen.

Crystal structure determination: The crystals were removed from the flask under argon or nitrogen gas and mounted on a glass fiber in a rapidly cooled perfluoropolyether[201] and then flash-cooled in a cold nitrogen stream.[202] Intensity data for compounds **9**, **12**, **13**, **16**, **18**, **19**, **21**, **22**, **23**, **24**, **26**, and **27** were collected on a STOE-AED2 four-circle diffractometer. The diffraction data for the compounds **3**, **4**, **10**, **11**, and **20** were measured on a STOE-Siemens-Huber four-circle-diffractometer coupled to a Siemens CCD area-detector. Data for the structure of **17** were collected on a STOE IPDS II diffractometer. The data for all compounds were collected at low temperatures (listed for individual compounds in the tables in Section 6) with graphite monochromated Mo-Kα radiation ($\lambda = 0.71073$ Å), performing φ and ω scans. The structures were solved by direct methods using either SHELXS-90[203] or SHELXS-97[204] programs and refined against F^2 on all data by full-matrix least-squares with SHELXL-97.[205] All non-hydrogen atoms were refined anisotropically with similarity and rigid bond restraints. All hydrogen atoms bonded to carbon were included in the models at geometrically calculated positions and refined using a riding model. The other hydrogen atoms were located in difference Fourier synthesis and refined freely and − in the case of N−H bonds − with the help of distance restraints. The crystal data for all the compounds related to data collection, structure solution, and refinement are listed in Section 6 in tabular form.

4.3. Starting Materials

The starting materials (PNtBu)$_2$(tBuNLi·THF)$_2$,[206] (MeC$_5$H$_4$)$_2$ZrCl$_2$,[207] Cp*ZrCl$_3$,[208] (MeC$_5$H$_4$)TiCl$_3$,[208] (EtMe$_4$C$_5$)ZrCl$_3$,[209] Cp$_2$ZrHCl,[210] (ClMe$_2$SiC$_5$H$_4$)$_2$ZrCl$_2$,[211] Cp*$_2$TiCl,[212] [Cp*V(μ-Cl)$_2$]$_3$[159] were prepared following literature procedures. NaNH$_2$, KH, KOH, and Me$_3$SiCl were used as received. K and Na were cut in a glove-box and NH$_3$ was condensed at -78 °C and dried over Na prior to use.

4.4. Syntheses of Amido (NH$_2^-$), Imido (NH^{2-}), and Nitrido(N^{3-}) Group 4 Metal Compounds in a Liquid Ammonia/Toluene Two Phase System

4.4.1. Syntheses of [{(MeC$_5$H$_4$)Zr}$_5$(μ_5-N)(μ_3-NH)$_4$(μ-NH$_2$)$_4$] (3) and (MeC$_5$H$_4$K)$_n$ (4)

Method A: Ammonia (80 mL) was condensed onto a suspension of (MeC$_5$H$_4$)$_2$ZrCl$_2$ (2.56 g, 8.0 mmol) and potassium (0.94 g, 24 mmol) in toluene (80 mL) at -78 °C and stirred for 1 h. Then excess ammonia was allowed to evaporate from the reaction mixture under stirring over 4 h.

During this period the mixture warmed slowly to room temperature. The reaction mixture was filtered and the light yellow solution was kept at room temperature for four weeks. Colorless crystals of **3** were obtained in 25 % yield (0.40 g). The residue was extracted with THF (30 mL). After filtration and concentration to 10 mL, the resulting light yellow solution was kept at room temperature for four weeks. Colorless crystals of **4** formed in 40 % yield (0.38 g). Method B: In a procedure similar to method A, ammonia (50 mL) was condensed onto a solution of $(MeC_5H_4)_2ZrCl_2$ (1.61 g, 5.0 mmol) in toluene (60 mL) at -78 ^{o}C. $NaNH_2$ (0.59 g, 15.1 mmol) was added to the resulting mixture. **3** and **4** were obtained in 53 % (0.52 g) and 47 % (0.28 g) yields, respectively. Method C: THF (50 mL) was added to a mixture of $(MeC_5H_4)_2ZrCl_2$ (1.61 g, 5.0 mmol) and $NaNH_2$ (0.59 g, 15.1 mmol) at room temperature. The mixture was stirred for 4 h at room temperature. After filtration and concentration *in vacuo* to about 20 mL, the pale yellow solution was kept at room temperature for 2 weeks. Colorless crystals of **3** were obtained in 28 % yield (0.28 g). After concentration of the filtrate, a mixture of **3** and **4** was formed.

3:

Mp: 302 °C.

IR (Nujol): $\tilde{\nu}$ = 3371 (w), 3299 (w), 1718 (w), 1557 (s), 1039 (s), 1033 (s), 933 (m), 841 (s), 787 (vs), 722 (vs), 669 (vs), 519 (vs), 452 (s), 364 (s), 346 (s) cm^{-1}.

EI-MS: *m/z* (%) 989 (62) [M^+], 910 (100) [$M^+ - MeC_5H_4$].

^{1}H NMR (250 MHz, THF-d_8): δ 6.56 (br s, 4 H, N*H*), 5.73 − 5.56 (m, 20 H, C_5H_4), 2.13/2.11 (s, 15 H, C*H*$_3$), 0.69 (br d, ^2J(H,H) = 8.3 Hz, 4 H, N*H*H′), 0.14 (br d, ^2J (H,H) = 8.3 Hz, 4 H, NH*H*′).

^{13}C NMR (100 MHz, THF-d_8): δ 110.50, 109.80, 109.20, 108.18 (C_5H_4), 15.58, 15.42 (*Me*).

Elemental analysis for $C_{30}H_{47}N_9Zr_5$ (989.87):

	C	H	N
calcd:	36.4	4.8	12.7 %,
found:	37.1	5.0	12.3 %.

4:

Mp: 250 °C.

IR (Nujol): $\tilde{\nu}$ 3047 (m), 1615 (w), 1555 (w), 1261 (m), 1234 (w), 1037 (s), 1025 (s), 966 (w), 927 (m), 891 (m), 852 (m), 782 (vs), 723 (vs), 638 (s) cm^{-1}.

EI-MS: m/z (%) 79 (100) [MeC$_5$H$_4^+$], 39 (20) [K$^+$].

^{1}H NMR (250 MHz, toluene-d$_8$, 100 °C): δ 5.47 – 5.40 (m, 4 H, C$_5$*H*$_4$), 2.17 (s, 3 H, *Me*C$_5$).

Elemental analysis for (C$_6$H$_7$K)$_n$ (118.23 × n):

	C	H
calcd:	61.0	6.0 %,
found:	60.2	6.5 %.

4.4.2. Synthesis of [(η^3-L)Zr(μ-NH)]$_2$ (9)

In a procedure similar to method A for the preparation of **3** ammonia (50 mL) was condensed onto a suspension of LZrCl$_2$ (**25**, 1.02 g, 2.0 mmol) and KH (0.17 g, 4.2 mmol) in toluene (80 mL) at -78 °C with stirring. The resulting colorless solution was concentrated to 15 mL *in vacuo* and stored at 0 °C for one week. Colorless crystals of **9** (0.10 g) were obtained. After concentration of the filtrate to 5 mL, the solution was kept at -20 °C for three days. An additional crop of **9** (0.15 g) was formed. Total yield 0.25 g (28 %).

Dec: 220 °C.

IR (Nujol): $\tilde{\nu}$ = 3378 (w), 1589 (w), 1360 (s), 1192 (vs), 1135 (w), 1079 (w), 1032 (m), 997 (s), 956 (m), 859 (s), 813 (s), 775 (s), 678 (w), 641 (w), 580 (vs), 517 (s), 477 (m), 431 (m) cm^{-1}.

^{1}H NMR (500 MHz, C$_6$D$_6$): δ 8.84, 7.99, 7.72 (br s, N*H*), 1.58, 1.45, 1.40, 1.23 (s, *tBu*).

EI-MS: m/z (%): 904 (38) [M$^+$], 847 (46) [M$^+$ – *t*Bu], 832 (83) [M$^+$ – *t*Bu – Me], 58 (100) [*t*BuH$^+$].

Elemental analysis for C$_{32}$H$_{74}$N$_{10}$P$_4$Zr$_2$ (905.4):

	C	H	N
calcd:	42.5	8.2	15.5 %,
found:	42.3	8.4	15.5 %.

4.4.3. Synthesis of [(L′Ti)$_6$(μ_3-NH)$_6$(μ_3-N)$_2$·6(C$_7$H$_8$)] (10)

In a procedure similar to method B for the preparation of **3** ammonia (40 mL) was condensed onto a solution of L′$_2$TiCl$_2$ (1.35 g, 2.01 mmol) in toluene (60 mL) with stirring at -78 °C. NaNH$_2$ (0.16 g, 4.10 mmol) was added to the resulting mixture. After filtration and partial removal of the solvent *in vacuo* the resulting reddish-brown solution was kept at room temperature for 3 weeks. Yellow single crystals of **10** were obtained in 6 % yield (0.05 g). After concentration of the filtrate

to ca 10 mL and addition of hexane (15 mL) the solution was kept at -20 °C for 2 weeks. Yellow solid of impure **10** (0.21 g) was formed.

Dec: 300-330 °C.

IR (Nujol): $\tilde{\nu}$ = 3381 (m), 1612 (m), 1248 (s), 1166 (m), 1111 (w), 1025 (m), 994 (s), 845 (vs), 763 (m), 728 (s), 648 (m), 633 (m), 576 (m), 464 (s) cm^{-1}.

EI-MS: *m/z*: 2536 [M$^+$ − NSiMe$_3$].

Elemental analysis for C$_{126}$H$_{204}$N$_{20}$Si$_{12}$Ti$_6$ (2623.6):

	N	Ti
calcd:	10.7	11.0 %,
found:	10.7	11.7 %.

4.4.4. Synthesis of Cp$^*_2$TiNH$_2$ (11)

In a procedure similar to method A for the preparation of **3** ammonia (40 mL) was condensed onto a suspension of Cp$^*_2$TiCl (1.06 g, 3.0 mmol) and KH (0.12 g, 3.0 mmol) in toluene (60 mL) under stirring at -78 °C. After filtration and partial removal of the solvent *in vacuo*, the resulting deep brown solution was kept at 0 °C for 3 weeks. Black crystals of **11** were obtained in a 27 % yield (0.27 g).

Mp: 202 °C.

IR (Nujol) $\tilde{\nu}$ = 3437 (w), 1653 (w), 1536 (m), 1262 (w), 1155 (w), 1064 (m), 1024 (s), 970 (m), 800 (m), 722 (s), 617 (s), 599 (s), 571 (m), 491 (s), 428 (s) cm^{-1}.

^{1}H NMR (200 MHz, C$_6$D$_6$): δ 2.50 − 1.97 (br m), 1.82, 1.79, 1.76, 1.66, 1.15 (br s).

EI-MS: *m/z* (%): 334 (53) [M$^+$], 317 (100) [M$^+$ − NH$_3$].

Elemental analysis for C$_{20}$H$_{32}$NTi (334.4):

	C	H	N
calcd:	71.8	9.6	4.2 %,
found:	70.9	9.4	3.6 %.

4.5. Synthesis of [(Cp*Ti)$_4$(μ_3-NH)$_4$(μ_3-η^1:η^1:η^2:η^2-N$_2$)$_2$K] (12) in a Liquid/Ammonia/Toluene Two Phase System

In a procedure similar to method A for the preparation of **3** ammonia (40 mL) was condensed onto a suspension of Cp*$_2$TiCl (1.41g, 4.0 mmol) and K (0.31 g, 8.0 mmol) in toluene (60 mL) with stirring at -78 °C. After filtration and partial removal of the solvent *in vacuo* the resulting deep brown solution was kept at 0 °C for 2 months. Black crystals of **12** (0.01 g) were obtained. After concentration of the filtrate to 10 mL and addition of hexane (5 mL), the solution was stored at -20 °C for 2 weeks. Black crystals of **12** (0.15 g) are formed. Total yield 0.16 g (17 %).

Mp: > 340 °C.

IR (Nujol): $\tilde{\nu}$ = 3353 (br w), 2046 (br w), 1797 (w), 1652 (w), 1601 (w), 1260 (s), 1092 (br s), 1066 (br s), 1023 (br s), 975 (br s), 796 (br s), 723 (br s), 623 (w), 489 (w) cm^{-1}.

^{1}H NMR (200 MHz, C$_6$D$_6$): δ 2.50 − 1.98 (br m), 1.79, 1.73, 1.35, 1.00, 0.96 (s), -0.18 (br s).

EI-MS: *m/z* (%): 803 (9) [M$^+$ − 2 K − 3 NH], 789 (16) [M$^+$ − 2 K − 2 NH − N$_2$ − H], 654 (28) [M$^+$ − 2 K − 2 NH − N$_2$ − H − Cp*], 119 (100) [Cp*$^+$ − CH$_4$].

4.6. Syntheses of Organometallic Oxides and Hydroxides in a Liquid Ammonia/Toluene Two Phase System

4.6.1. Synthesis of [{(EtMe$_4$C$_5$)Zr}$_6$(μ_6-O)(μ_3-O)$_8$·(C$_7$H$_8$)] (13)

H$_2$O (0.08 g, 4.5 mmol) was added to a solution of (EtMe$_4$C$_5$)ZrCl$_3$ (1.04 g, 3.0 mmol) in toluene (80 mL) at room temperature. The solution turned to light yellow and was stirred for 2 h at this temperature. KH (0.37 g, 9.2 mmol) was added to the solution and then ammonia (50 mL) was condensed onto the resulting suspension at -78 °C with stirring. Using the same procedure described for the preparation of **3**, the resulting solution was filtered and the remaining yellowish brown precipitate was extracted with warm toluene (50 °C, 2 × 20 mL). The combined light yellow solutions were concentrated *in vacuo* to 15 mL and kept at 0 °C for one week. Colorless crystals of **13** (0.10 g) were obtained. After concentrating the filtrate to 5 mL the solution was kept at -20 °C for one week. Colorless crystals of **13** (0.11 g) were formed. Total yield 0.21 g (25 %).

Mp: >410 °C.

IR (Nujol): $\tilde{\nu}$ = 1580 (br s), 1309 (m), 1261 (m), 1097 (s), 1050 (s), 1023 (s), 779 (m), 727 (m), 659 (s), 562 (s), 506 (vs), 454 (m) cm^{-1}.

^{1}H NMR (200 MHz, C$_6$D$_6$, 60 °C): δ 2.74 (q, ^3J = 7.5 Hz, 12 H, CH_2Me$_3$), 2.23, 2.17 (s, 72 H, C$_5Me_4$), 1.08 (t, ^3J = 7.5 Hz, 18 H, CH$_2Me_3$).

EI-MS: *m/z* (%): 1586 (4) [M$^+$ – C$_7$H$_8$], 1437 (100%) [M$^+$ – C$_7$H$_8$ – EtMe$_4$C$_5$].

Elemental analysis for C$_{73}$H$_{110}$O$_9$Zr$_6$ (1679.0):

	C	H
calcd:	52.2	6.6 %,
found:	52.7	6.7 %.

4.6.2. Synthesis of [{(EtMe$_4$C$_5$)Zr}$_6$(μ_6-O)(μ_3-O)$_8$·(C$_9$H$_{12}$)] (16)

Crystals of **13** (0.05 g) were dissolved in warm mesitylene (80 °C; 8 mL). The resulting colorless solution was kept at 0 °C for one week. A quantitative yield of colorless crystals of **16** was obtained.

Mp >410 °C.

EI-MS: *m/z* (%): 1586 (12) [M$^+$ – C$_9$H$_{12}$], 1437 (100%) [M$^+$ – C$_9$H$_{12}$ – EtMe$_4$C$_5$].

4.6.3. Synthesis of [(Cp*Zr)$_6$(μ_6-O)(μ_3-O)$_4$(μ_3-OH)$_8$·2(C$_7$H$_8$)] (17)

In a procedure similar to method A for the preparation of **3** ammonia (40 mL) was condensed onto the suspension of Cp*ZrCl$_3$ (0.665 g, 2.0 mmol) and KOH (KOH > 84 %, H$_2$O 10 – 15 %; 0.20 g, 3.0 mmol) in toluene (80 mL) at -78 °C with stirring. The resulting solution was filtered and the remaining colorless precipitate was extracted with warm toluene (50 °C, 2 × 10 mL). The combined light yellow solutions were concentrated *in vacuo* to 10 mL and kept at room temperature for one month. Colorless crystals of **17** (0.06 g, 10 %) were obtained.

Mp: >410 °C.

IR (Nujol): $\tilde{\nu}$ = 3689 (br w), 1654 (br w), 1306 (w), 1261 (s), 1093 (s), 1022 (s), 799 (s), 730 (s), 657 (m), 610 (m), 535 (m) cm^{-1}.

^{1}H NMR (200 MHz, C$_6$D$_6$): δ 2.05 (C$_5Me_5$).

EI-MS: *m/z* (%): 1512 (18) [M$^+$ – C$_7$H$_8$ – Cp* – 2 H$_2$O], 1437 (56) [M$^+$ – 2 C$_7$H$_8$ – Cp* – 5 H$_2$O].

Elemental analysis for C$_{74}$H$_{114}$O$_{13}$Zr$_6$ (1759.0):

	C	H	N
calcd:	50.5	6.5	0 %,
found:	50.1	6.5	0 %.

4.6.4. Syntheses of [Cp*VCl(μ-O)]$_4$·OC$_4$H$_8$ (18) and (Cp*V)$_6$(μ-O)$_8$(μ_3-O)$_2$Na (19)

A suspension of [Cp*V(μ-Cl)$_2$]$_3$ (0.38 g, 0.5 mmol) and NaNH$_2$ (0.20 g, 5.1 mmol) in THF (50 mL) was stirred at 40 °C for 24 h. After filtration and concentration *in vacuo* to 10 mL the resulting deep green solution was stored at -20 °C for one week. No chlorine free amido, imido or nitrido vanadium compound was isolated. The solution was warmed to room temperature and exposed to air for a short time, and then stored at -20 °C for 2 weeks. Deep green crystals of **18** were obtained in 16 % yield (0.06 g). After further concentration of the filtrate to 5 mL the solution was kept at -20 °C for one week. Deep green crystals (0.08 g) were obtained, which contain **18** and chlorine-containing vanadium compounds as seen from EI mass spectrum.

Dioxygen was led into the solution of [Cp*V(μ-Cl)$_2$]$_3$ (0.77 g, 1.0 mmol) in toluene (60 mL) under stirring at room temperature for 2 h. After degassing *in vacuo* NaNH$_2$ (0.47 g, 12.0 mmol) was added to the resulting deep green solution. In a procedure similar to method A for the preparation of **3** ammonia (40 mL) was condensed onto the resulting suspension with stirring at -78 °C. After filtration and partial removal of the solvent the resulting deep green solution was kept at room temperature for one month. Few green crystals of **19** suitable for X-ray determination were deposited on the wall of the flask and at the surface of the solution. The solid product obtained by concentration of the resulting solution was not pure enough to do further characterization of **19**.

4.7. Synthesis of [{HN(SiMe$_2$C$_5$H$_4$)$_2$ZrH(μ-H)}$_2$·C$_7$H$_8$] (20) in a Liquid Ammonia/Toluene Two Phase System

In a procedure similar to method A for the preparation of **3** ammonia (50 mL) was condensed onto a suspension of (ClMe$_2$SiC$_5$H$_4$)$_2$ZrCl$_2$ (1.43 g, 3.0 mmol) and K (0.47 g, 12.0 mmol) in toluene (80 mL) at -78 °C with stirring. The resulting solution was filtered and the remaining brown precipitate was extracted with warm toluene (50 °C, 2 × 30 mL). The combined pale yellow solutions were concentrated to 30 mL and kept at -20 °C for 2 weeks. Pale yellow crystals of **20** (0.12 g) were obtained. After further concentration of the filtrate to 5 mL and addition of hexane

(20 mL) the solution was kept at -20 °C overnight. Slightly impure microcrystalline **20** (0.60 g) thus could be isolated. Total yield: 0.72 g (60.2 %).

Dec: 200-228 °C.

IR (Nujol): $\tilde{v}$ = 1612 (br s), 1586 (br s), 1316 (s), 1260 (m), 1251 (s), 1186 (s), 1163 (m), 1096 (br m), 1046 (s), 929 (s), 904 (m), 828 (m), 804 (s), 789 (s), 731 (s), 693 (m), 650 (m), cm^{-1}.

EI-MS: *m/z* (%) 795 (1) [M$^+$ − H], 348 (100) [M$^+$ − C$_7$H$_8$ − HN(SiMe$_2$C$_5$H$_4$)$_2$ − C$_5$H$_4$ − 2Me − H)].

^{1}H NMR (500 MHz, THF-d$_8$): δ 6.41, 6.03, 5.86, 5.33 (m, 16 H, C$_5$*H*$_4$), 3.03 (t, ^2J(H, H) = 7.5 Hz, 2 H, *H*$_t$), 1.33 (s, 2 H, N*H*), 0.28 (s, 12 H, Si*Me*Me′), 0.23 (s, 12 H, SiMe*Me*′), -3.94 (t, ^2J(H, H) = 7.5 Hz, 2 H, *H*$_b$).

^{13}C NMR (125 MHz, THF-d$_8$): δ 113.99 (substituted C, *C*C$_4$H$_4$), 108.45, 106.47, 105.80, 105.76 (C*C*$_4$H$_4$), 2.37 (Si*Me*Me′), 2.18 (SiMe*Me*′).

Elemental analysis for C$_{35}$H$_{54}$N$_2$Si$_4$Zr$_2$ (797.60):

	C	H	N
calcd:	52.7	6.8	3.5 %,
found:	52.5	6.9	3.9 %.

4.8. Synthesis of L′$_3$Ti (21) by the Reduction of L′$_2$TiCl$_2$ with Alkali Metal Ammonia Solutions in Toluene

In a procedure similar to method A for the preparation of **3** ammonia (50 mL) was condensed onto a suspension of L′$_2$TiCl$_2$ (2.02 g, 3.0 mmol) and K (0.24 g, 6.0 mmol) in toluene (80 mL) at -78 °C with stirring. After filtration and concentration to about 15 mL *in vacuo* the dark green solution was kept at -20 °C for 2 weeks. Green crystals of **21** were obtained in 33 % yield (0.87 g).

Mp: 301 °C.

IR (Nujol): $\tilde{v}$ = 1613 (m), 1244 (s), 1162 (m), 1111 (m), 981 (s), 844 (vs), 758 (s), 717 (m), 644 (m), 632 (m), 603 (w), 466 (s) cm^{-1}.

^{1}H NMR (200 MHz, C$_6$D$_6$): δ 8.58 − 8.62 (m, 6 H, C$_6$*H*$_2$H′$_2$), 8.31 − 8.34 (m, 6 H, C$_6$H$_2$*H*′$_2$), 2.16 (s, 9 H), 0.21 (br s, 54 H, Si*Me*$_3$).

EI-MS: *m/z* (%): 879 (62) [M$^+$], 190 (100) [MeC$_6$H$_4$CNSiMe$_3$$^+$]

Elemental analysis for C$_{42}$H$_{75}$N$_6$Si$_6$Ti (880.52):

	C	H	N	Ti
calcd:	57.3	8.6	9.5	5.4 %,
found:	58.0	8.8	9.9	5.2 %.

4.9. Syntheses of Nitrogen Containing Titanium and Zirconium Compounds via the Reactions of Corresponding Metal Compounds with Diazo Derivatives and Aniline

4.9.1. Synthesis of [(MeC$_5$H$_4$)TiCl(μ-NSiMe$_3$)]$_2$ (22)

(MeC$_5$H$_4$)TiCl$_3$ (0.93 g, 4.0 mmol) in THF (20 mL) was added dropwise to freshly prepared Me$_3$SiCLiN$_2$ (4 mmol) in THF (20 mL) at -78 °C. The reaction mixture turned to reddish-brown immediately. Stirring was continued for 1 h at this temperature. The reaction mixture slowly warmed to room temperature and was stirred for additional 12 h. Removal of the solvent *in vacuo* gave a deep brown solid, which was extracted with toluene (20 mL). After filtration and concentration to 8 mL the deep brown solution was kept at -20 °C for two weeks. Reddish brown crystals of **22** (0.08 g) were obtained. After concentration of the filtrate to 5 mL and addition of hexane (10 mL) the solution was kept at -20 °C for 2 days. An additional crop of **22** (0.14 g) was obtained. Total yield 0.22 g (22 %).

Mp: 242 °C.

IR (Nujol): $\tilde{\nu}$ = 1589 (s), 1406 (m), 1261 (s), 1094 (vs), 1022 (vs), 802 (vs), 658 (m), 451 (m) cm^{-1}.

EI-MS: *m/z* (%) 498 (32) [M$^+$], 483 (100) [M$^+$ − Me].

^{1}H NMR (250 MHz, C$_6$D$_6$): δ 6.40 − 6.37, 5.55 − 5.53 (m, 8 H, C$_5$*H$_4$*), 2.17 (s, 6 H, *Me*C$_5$), 0.04(s, 18 H, Si*Me$_3$*).

^{13}C NMR (100 MHz, C$_6$D$_6$): δ 114.45, 112.47 (*C$_5$*H$_4$), 15.86 (*Me*C$_5$), 3.81 (Si*Me$_3$*).

Elemental analysis for C$_{18}$H$_{32}$Cl$_2$N$_2$Si$_2$Ti$_2$ (499.4):

	C	H	N
calcd:	43.3	6.5	5.6 %,
found:	43.7	6.5	5.8 %.

4.9.2. Synthesis of Cp$_2$ZrCl(η^2-NHNCHSiMe$_3$)·C$_7$H$_9$ (23)

Me$_3$SiCHN$_2$ (2 M in hexane, 1.0 mL, 2.0 mmol) was added to a suspension of Cp$_2$ZrHCl (0.52 g, 2.0 mmol) in toluene (40 mL) at room temperature. After the solid dissolved the solution turned

into a light yellow within ten min. Stirring was continued overnight. After concentration *in vacuo* to 5 mL, the light yellow solution was kept at -20 °C for one week. Colorless crystals of **23** were obtained. The crystals were dried *in vacuo*, colorless solid of $Cp_2ZrCl(\eta^2\text{-NHNCHSiMe}_3)$ was obtained in 93 % yield (0.69 g).

Dec: 143 °C.

IR (Nujol): $\tilde{\nu}$ = 3310 (m), 3080 (m), 1535 (s), 1247 (s), 1046 (s), 1025 (m), 1012 (s), 830 (vs), 800 (vs), 750 (m), 692 (m), 657 (m), 589 (m), 482 (s), 372 (s) cm^{-1}.

^{1}H NMR (200 MHz, C$_6$D$_6$): δ 6.84, 6.82 (s, 1 H, NH), 6.01, 5.87 (s, 10 H, C$_5H_5$), 1.06 (s, 1 H, CH), 0.13, 0.67 (s, 9 H, SiMe_3).

Elemental analysis for C$_{14}$H$_{21}$ClN$_2$SiZr (372.10, the lattice toluene was removed *in vacuo*.):

	C	H
calcd:	45.2	5.7 %,
found:	45.2	5.6 %.

4.9.3. Synthesis of [Cl$_2$Zr(μ-NPh)·2THF]$_2$ (24)

A suspension of ZrCl$_4$ (1.40 g, 6.0 mmol), PhNH$_2$ (0.56 g, 6.0 mmol) and K (0.49 g, 12.5 mmol) in toluene (100 mL) was refluxed for 72 h. After cooling to room temperature and filtration, the black residue was extracted with warm THF (50 °C, 3 × 40 mL). The combined deep brown filtrate was concentrated (to 30 mL) *in vacuo* and kept at 0 °C. Light yellow crystals of **24** (0.36 g) were obtained. After concentration of the filtrate to 10 mL the solution was kept at -20 °C and another batch of **24** (0.14 g) was obtained. Total yield 0.50 g (21 %).

Mp: 249 °C.

IR (Nujol): $\tilde{\nu}$ = 1583 (s), 1236 (vs), 1167 (w), 1070 (w), 1041 (w), 1007 (s), 852 (vs), 756 (s), 693 (s), 618 (m), 580 (vs), 501 (s), 472 (m), 445 (w) cm^{-1}.

^{1}H NMR (250 MHz, THF-d$_8$): δ 7.15 − 6.94 (m, 6 H, C$_6H_5$), 6.56 − 6.47 (m, 4 H, C$_6H_5$).

Elemental analysis:

	C	H	N
calcd for C$_{28}$H$_{42}$Cl$_4$N$_2$O$_4$Zr$_2$ (794.9):	42.5	5.3	3.5 %,
calcd for C$_{25.6}$H$_{37.2}$Cl$_4$N$_2$O$_{3.4}$Zr$_2$ (751.6, M − 0.6 THF):	40.9	5.0	3.7 %,
found:	40.9	5.1	3.8 %.

4.10. Syntheses of Bis(*tert*-butylamido)cyclodiphosph(III)azane Zirconium Complexes

4.10.1. Synthesis of LZrCl$_2$ (25)

A suspension of ZrCl$_4$ (3.26 g, 14.0 mmol) and (PN*t*Bu)$_2$(*t*BuNLi·THF)$_2$ (7.0 g, 13.9 mmol) in toluene (100 mL) was stirred for 48 h at 80 °C. After filtration and concentration *in vacuo* to 20 mL the resulting light yellow solution was kept at 0 °C for one week. Colorless crystals of **25** (3.9 g) were obtained. After concentration of the filtrate to 10 mL storage at -20 °C for three days gave an additional crop of **25** (0.8 g). Total yield 4.7 g (66 %).

Mp: 170 °C.

IR (Nujol): $\tilde{\nu}$ = 1392 (m), 1220 (m), 1186 (vs), 1084 (w), 1027 (s), 1003 (m), 946 (s), 868 (s), 824 (vs), 781 (s), 724 (w), 584 (m), 538 (w), 479 (m), 395 (m) cm^{-1}.

^{1}H NMR (500 MHz, C$_6$D$_6$): δ 1.41 (s, 18 H, *tBu*), 1.27 (s, 18 H, *tBu*).

^{13}C NMR (126 MHz, C$_6$D$_6$): δ 59.39, 59.28 (*C*Me$_3$), 55.02, 54.92, 54.83 (*C*Me$_3$), 33.47, 33.49 (C*Me$_3$*), 29.85, 29.80, 29.75 (C*Me$_3$*).

^{31}P NMR (202 MHz, C$_6$D$_6$): δ 103.43.

EI-MS: *m/z* (%): 508 (7) [M$^+$], 493 (100) [M$^+$ − Me].

Elemental analysis for C$_{16}$H$_{36}$Cl$_2$N$_4$P$_2$Zr (508.6):

	C	H	N
calcd:	37.8	7.1	11.0 %,
found:	38.5	7.4	11.0 %.

4.10.2. Synthesis of (η^3-L)(η^1-LH)ZrCl (26)

*n*BuLi (2.5 M in hexane, 14.6 mL, 36.5 mmol) was added to a suspension of ZrCl$_4$ (2.83 g, 12.1 mmol) and LH$_2$ (8.45 g, 24.3 mmol) in toluene (150 mL) at 0 °C. The mixture was warmed to room temperature and then stirred for 48 h at 80 °C. After filtration and concentration *in vacuo* to 40 mL the resulting yellow solution was stored at −20 °C. Yellow crystals were obtained. Recrystallization of the resulting crystals in toluene, pale yellow crystals of **26** were obtained. Yield 3.80 g (48 %).

Mp: 288 °C (dec.).

IR (Nujol): $\tilde{\nu}$ = 3378 (w), 3130 (br w), 1625 (br. m), 1261 (m), 1219 (s), 1192 (s), 1070 (s), 1014

(s), 989 (m), 928 (m), 877 (s), 850 (m), 819 (s), 724 (s), 592 (m), 505 (w), 467 (w) cm^{-1}.

^{1}H NMR (500 MHz, C$_6$D$_6$): δ 3.20, 3.28 (br s, 1 H, N*H*), 1.94 (s, 9 H, *tBu*), 1.68 (s, 18 H, *tBu*), 1.54 (s, 9 H, *tBu*), 1.51 (s, 18 H, *tBu*), 1.31 (s, 9 H, *tBu*), 1.19 (s, 18 H, *tBu*).

^{31}P NMR (202 MHz, C$_6$D$_6$): δ 124.59, 91.60, 91.52, 34.27, 34.20.

EI-MS: *m/e* (%): 818 (8) [M$^+$], 471 (100) [M$^+$ − LH].

Elemental analysis for C$_{32}$H$_{73}$ClN$_8$P$_4$Zr (820.5):

	C	H	N
calcd:	46.8	9.0	13.7 %,
found:	46.1	8.8	13.0 %.

4.10.3. Synthesis of [(η^1-LH)Zr(N*t*Bu){(N*t*Bu)$_2$PPN*t*Bu}{K·(η^6-C$_7$H$_8$)}·0.5C$_7$H$_8$] (27)

The suspension of **26** (1.64 g, 2.0 mmol) and K/Na alloy (K 0.11 g, 2.8 mmol; Na 0.03 g, 1.3 mmol) in toluene (80 mL) was stirred for 48 h at room temperature and then refluxed for 24 h with stirring. After filtration and concentration *in vacuo* to 10 mL the resulting brown solution was kept at -20 °C for one week. Colorless crystals of **27** were obtained in 28% yield (0.54 g).

Mp: 273 °C.

IR (Nujol): $\tilde{\nu}$ = 3377 (m), 3334 (m), 3243 (br w), 1605 (m), 1361 (s), 1220 (vs), 1120 (s), 1087 (s), 1057 (s), 1029 (s), 998 (s), 920 (m), 876 (m), 822 (m), 804 (m), 727 (m), 694 (m), 661 (m), 625 (m) cm^{-1}.

^{1}H NMR (500 MHz, C$_6$D$_6$): δ 3.38, 3.34 (s, 1 H, N*H*), 1.94 (s, 9 H, *tBu*), 1.69 (s, 18 H, *tBu*), 1.60 (s, 18 H, *tBu*), 1.40 (s, 9 H, *tBu*), 1.28, 1.27 (s, 9 H, *tBu*), 1.11 (s, 9 H, *tBu*).

^{31}P NMR (202 MHz, C$_6$D$_6$): δ 90.08, 85.58, −52.28, −52.54, −103.63.

EI-MS: *m/z* (%): 915 (0.2) [M$^+$ − 0.5 C$_7$H$_8$], 784 (9) [M$^+$ − K − 1.5 C$_7$H$_8$ + H], 727 (11) [M$^+$ − K − 1.5 C$_7$H$_8$ − *t*Bu + H], 276 (100) [L$^+$ − N*t*Bu].

Elemental analysis for C$_{42.5}$H$_{85}$KN$_8$P$_4$Zr (962.4):

	C	H	N
calcd:	53.0	8.9	11.6 %,
found:	51.7	8.7	11.3 %.

5. Handling and Disposal of Solvents and Residual Waste

1. The recovered solvents were distilled or condensed into cold-traps under vacuum, and collected in halogen-free or halogen-containing solvent containers, and stored for disposal.

2. Used NMR solvents were classified into halogen-free or halogen-containing solvents and were disposed as heavy metal wastes and halogen-containing wastes, respectively.

3. The heavy metal residues were dissolved in nitric acid and after neutralization were stored in the containers for heavy metal wastes.

4. Drying agents such as KOH, $CaCl_2$, and P_4O_{10} were hydrolyzed and disposed as acid or base wastes.

5. Whenever possible, sodium metal used for drying solvents was collected for recycling.[213] The non-reusable sodium metal was carefully hydrolyzed in cold ethanol and poured into the base-bath used for cleaning glassware.

6. Ethanol and acetone used for solid CO_2 cold-baths were subsequently used for cleaning glassware.

7. The acid-bath used for cleaning glassware was neutralized with Na_2CO_3 and the resulting NaCl solution was washed-off in the water drainage system.

8. The residue of the base-bath used for glassware cleaning was poured into the container for base wastes.

Amounts of disposable wastes generated during the work:

Metal containing wastes	10 L
Halogen-containing solvent wastes	6 L
Halogen-free solvent wastes	38 L
Acid wastes	10 L
Base wastes	20 L

6. **Crystal Data and Refinement Details**

Table 18. Crystal data and structure refinement for 3

Empirical formula	$C_{30}H_{47}N_9Zr_5$
Formula weight	989.87
Temperature	133(2) K
Wavelength	0.71073 Å
Crystal system	Tetragonal
Space group	*I*4
Unit cell dimensions	$a = b = 13.1878(19)$ Å
	$c = \quad 9.5223(19)$ Å
Volume	1656.1(5) Å^3
Z	2
Density (calculated)	1.985 Mg/m^3
Absorption coefficient	1.558 mm^{-1}
F(000)	980
Crystal size	$0.4 \times 0.3 \times 0.3$ mm^3
θ range for data collection	2.18 – 27.98°
Index ranges	$-11 \le h \le 12, 0 \le k \le 17, -12 \le l \le 12$
Reflections collected	20345
Independent reflections	2012 [R(int) = 0.0252]
Refinement method	Full-matrix least-squares on F^2
Data / restraints / parameters	2012 / 281 / 152
Goodness-of-fit on F^2	1.035
Final R indices [$I>2\sigma(I)$]	$R1 = 0.0443, wR2 = 0.1085$
R indices (all data)	$R1 = 0.0458, wR2 = 0.1099$
Largest difference peak and hole	1.417 and -1.983 e Å^{-3}

Table 19. Crystal data and structure refinement for 4

Empirical formula	C_6H_7K
Formula weight	118.22
Temperature	133(2) K
Wavelength	0.71073 Å
Crystal system	Monoclinic
Space group	*C*2/*c*
Unit cell dimensions	$a = 33.959(7)$
	$b = 10.607(2)$ Å $\beta = 120.65(3)°$
	$c = 17.998(4)$ Å
Volume	5577.3(19) Å^3
Z	36
Density (calculated)	1.267 Mg/m^3
Absorption coefficient	0.725 mm^{-1}
F(000)	2232
Crystal size	$0.3 \times 0.3 \times 0.2$ mm^3
θ range for data collection	2.04 – 24.71°
Index ranges	$-39 \leq h \leq 34, 0 \leq k \leq 12, 0 \leq l \leq 21$
Reflections collected	33764
Independent reflections	4657 [R(int) = 0.0563]
Refinement method	Full-matrix least-squares on F^2
Data / restraints / parameters	4657 / 255 / 312
Goodness-of-fit on F^2	1.062
Final R indices [$I>2\sigma(I)$]	$R1 = 0.0531, wR2 = 0.1397$
R indices (all data)	$R1 = 0.0631, wR2 = 0.1473$
Largest difference peak and hole	1.093 and −0.590 e Å^{-3}

Table 20. Crystal data and structure refinement for 9

Empirical formula	$C_{32}H_{74}N_{10}P_4Zr_2$
Formula weight	905.33
Temperature	203(2) K
Wavelength	0.71073 Å
Crystal system	Monoclinic
Space group	$P2_1/c$
Unit cell dimensions	$a = 13.618(7)$ Å
	$b = 18.426(7)$ Å $\beta = 90.25(3)°$
	$c = 18.479(8)$ Å
Volume	4637(3) $Å^3$
Z	4
Density (calculated)	1.297 Mg/m^3
Absorption coefficient	0.620 mm^{-1}
F(000)	1904
Crystal size	$0.9 \times 0.9 \times 0.6$ mm^3
θ range for data collection	3.64 – 23.75°
Index ranges	$-15 \leq h \leq 15, -20 \leq k \leq 0, -19 \leq l \leq 20$
Reflections collected	6971
Independent reflections	6913 [R(int) = 0.0614]
Refinement method	Full-matrix least-squares on F^2
Data / restraints / parameters	6913 / 0 / 457
Goodness-of-fit on F^2	1.107
Final R indices [$I>2\sigma(I)$]	$R1 = 0.0859$, $wR2 = 0.2027$
R indices (all data)	$R1 = 0.1078$, $wR2 = 0.2203$
Largest difference peak and hole	1.418 and -1.109 e $Å^{-3}$

Table 21. Crystal data and structure refinement for 10

Empirical formula	$C_{126}H_{204}N_{20}Si_{12}Ti_6$
Formula weight	2623.57
Temperature	133(2) K
Wavelength	0.71073 Å
Crystal system	Rhombohedral
Space group	$R\overline{3}$
Unit cell dimensions	$a = b = 24.519(4)$ Å
	$c = \quad 18.127(4)$ Å
Volume	9438(3) Å^3
Z	3
Density (calculated)	1.385 Mg/m^3
Absorption coefficient	0.536 mm^{-1}
F(000)	4200
Crystal size	$0.4 \times 0.4 \times 0.4$ mm^3
θ range for data collection	$2.22 - 27.52°$
Index ranges	$-31 \leq h \leq 15, 0 \leq k \leq 31, 0 \leq l \leq 23$
Reflections collected	147127
Independent reflections	4811 [R(int) = 0.091]
Refinement method	Full-matrix least-squares on F^2
Data / restraints / parameters	4808 / 174 / 235
Goodness-of-fit on F^2	1.090
Final R indices [$I>2\sigma(I)$]	$R1 = 0.0892$, $wR2 = 0.2312$
R indices (all data)	$R1 = 0.1302$, $wR2 = 0.2734$
Largest difference peak and hole	1.421 and -0.658 e Å^{-3}

Table 22. Crystal data and structure refinement for 12

Empirical formula	$C_{40}H_{64}K_2N_8Ti_4$
Formula weight	926.79
Temperature	200(2) K
Wavelength	0.71073 Å
Crystal system	Tetragonal
Space group	$I4_1/a$
Unit cell dimensions	$a = b = 24.791(4)$ Å
	$c = \quad 14.556(3)$ Å
Volume	8946(3) Å^3
Z	8
Density (calculated)	1.376 Mg/m^3
Absorption coefficient	0.912 mm^{-1}
F(000)	3888
Crystal size	$0.3 \times 0.2 \times 0.2$ mm^3
θ range for data collection	3.64 – 22.54°
Index ranges	$-26 \le h \le 26, -15 \le k \le 26, 0 \le l \le 15$
Reflections collected	3020
Independent reflections	2925 [R(int) = 0.0558]
Refinement method	Full-matrix least-squares on F^2
Data / restraints / parameters	2925 / 521 / 292
Goodness-of-fit on F^2	1.023
Final R indices [$I > 2\sigma(I)$]	$R1 = 0.1040, wR2 = 0.2186$
R indices (all data)	$R1 = 0.1992, wR2 = 0.2784$
Largest difference peak and hole	0.737 and -0.505 e Å^{-3}

Table 23. Crystal data and structure refinement for 13

Empirical formula	$C_{73}H_{110}O_9Zr_6$
Formula weight	1678.93
Temperature	200(2) K
Wavelength	0.71073 Å
Crystal system	Triclinic
Space group	$P\bar{1}$
Unit cell dimensions	$a = 12.959(3)$ Å $\alpha = 82.85(3)°$
	$b = 14.341(4)$ Å $\beta = 84.562(17)°$
	$c = 19.189(5)$ Å $\gamma = 83.767(13)°$
Volume	3505.7(15) Å^3
Z	2
Density (calculated)	1.591 Mg/m^3
Absorption coefficient	0.914 mm^{-1}
F(000)	1720
Crystal size	$1.0 \times 0.6 \times 0.4$ mm^3
θ range for data collection	$3.52 - 25.05°$
Index ranges	$-15 \leq h \leq 15, -15 \leq k \leq 17, -21 \leq l \leq 22$
Reflections collected	15669
Independent reflections	12318 [R(int) = 0.0787]
Refinement method	Full-matrix least-squares on F^2
Data / restraints / parameters	12318 / 0 / 824
Goodness-of-fit on F^2	1.042
Final R indices [$I>2\sigma(I)$]	$R1 = 0.0408, wR2 = 0.1101$
R indices (all data)	$R1 = 0.0497, wR2 = 0.1187$
Largest difference peak and hole	0.891 and -1.173 e Å^{-3}

Table 24. Crystal data and structure refinement for 16

Empirical formula	$C_{75}H_{114}O_9Zr_6$
Formula weight	1706.98
Temperature	200(2) K
Wavelength	0.71073 Å
Crystal system	Monoclinic
Space group	*C*2/*c*
Unit cell dimensions	$a = 22.641(5)$ Å
	$b = 13.0808(11)$ Å $\beta = 93.196(12)°$
	$c = 24.550(6)$ Å
Volume	7259(2) Å^3
Z	4
Density (calculated)	1.562 Mg/m^3
Absorption coefficient	0.884 mm^{-1}
F(000)	3504
Crystal size	$0.6 \times 0.6 \times 0.4$ mm^3
θ range for data collection	$3.53 - 25.02°$
Index ranges	$-26 \le h \le 26, -13 \le k \le 15, -27 \le l \le 29$
Reflections collected	7944
Independent reflections	6365 [*R*(int) = 0.0330]
Refinement method	Full-matrix least-squares on F^2
Data / restraints / parameters	6365 / 832 / 427
Goodness-of-fit on F^2	1.103
Final R indices [$I>2\sigma(I)$]	$R1 = 0.0307, wR2 = 0.0614$
R indices (all data)	$R1 = 0.0422, wR2 = 0.0683$
Largest difference peak and hole	0.756 and -0.476 e Å^{-3}

Table 25. Crystal data and structure refinement for 17

Empirical formula	$C_{74}H_{106}O_{13}Zr_6$
Formula weight	1750.91
Temperature	133(2) K
Wavelength	0.71073 Å
Crystal system	Monoclinic
Space group	*C2/m*
Unit cell dimensions	$a = 19.530(4)$ Å
	$b = 17.214(3)$ Å $\beta = 123.13(3)$
	$c = 12.985(3)$ Å
Volume	3655.9(13) Å3
Z	2
Density (calculated)	1.591 Mg/m^3
Absorption coefficient	0.884 mm^{-1}
F(000)	1788
θ range for data collection	$3.44 - 49.42°$
Index ranges	$-22 \le h \le 22, -19 \le k \le 20, -15 \le l \le 15$
Reflections collected	11334
Independent reflections	3222 [R(int) = 0.0502]
Refinement method	Full-matrix least-squares on F^2
Data / restraints / parameters	3222 / 62 / 225
Goodness-of-fit on F^2	1.090
Final R indices [$I>2\sigma(I)$]	$R1 = 0.0305$, $wR2 = 0.0831$
R indices (all data)	$R1 = 0.0356$, $wR2 = 0.0848$
Largest diff. peak and hole	0.611 and -0.499 e.Å^{-3}

Table 26. Crystal data and structure refinement for 18

Empirical formula	$C_{44}H_{68}Cl_4O_5V_4$
Formula weight	1022.54
Temperature	200(2) K
Wavelength	0.71073 Å
Crystal system	Orthorhombic
Space group	*Pbcn*
Unit cell dimensions	a = 14.973(3) Å
	b = 18.506(4) Å
	c = 17.441(4) Å
Volume	4832.7(17) Å3
Z	4
Density (calculated)	1.405 Mg/m^3
Absorption coefficient	1.012 mm^{-1}
F(000)	2128
Crystal size	0.5 x 0.5 x 0.4 mm^3
θ range for data collection	3.50 − 22.49°.
Index ranges	$0 \leq h \leq 16$, $-19 \leq k \leq 19$, $-1 \leq l \leq 18$
Reflections collected	3161
Independent reflections	3146 [R(int) = 0.0514]
Refinement method	Full-matrix least-squares on F^2
Data / restraints / parameters	3146 / 515 / 294
Goodness-of-fit on F^2	1.051
Final R indices [$I>2\sigma(I)$]	$R1$ = 0.0369, $wR2$ = 0.0879
R indices (all data)	$R1$ = 0.0465, $wR2$ = 0.0950
Largest diff. peak and hole	0.412 and −0.217 e.Å^{-3}

Crystal Data and Refinement Details

Table 27. Crystal data and structure refinement for 19

Empirical formula	$C_{60}H_{90}NaO_{10}V_6$
Formula weight	1299.95
Temperature	200(2) K
Wavelength	0.71073 Å
Crystal system	Triclinic
Space group	$P\bar{1}$
Unit cell dimensions	$a = 12.912(3)$ Å $\quad \alpha = 88.38(3)°$
	$b = 14.170(3)$ Å $\quad \beta = 89.00(3)°$
	$c = 18.474(4)$ Å $\quad \gamma = 67.42(3)°$
Volume	3119.6(11) Å^3
Z	2
Density (calculated)	1.384 Mg/m^3
Absorption coefficient	0.922 mm^{-1}
F(000)	1358
Crystal size	$0.7 \times 0.2 \times 0.1$ mm^3
θ range for data collection	$3.52 - 20.05°$
Index ranges	$-12 \leq h \leq 12, -13 \leq k \leq 13, -16 \leq l \leq 17$
Reflections collected	7508
Independent reflections	5824 [R(int) = 0.1132]
Refinement method	Full-matrix least-squares on F^2
Data / restraints / parameters	5824 / 985 / 724
Goodness-of-fit on F^2	1.044
Final R indices [$I>2\sigma(I)$]	$R1 = 0.0731$, $wR2 = 0.1768$
R indices (all data)	$R1 = 0.1161$, $wR2 = 0.2088$
Largest difference peak and hole	1.065 and -0.476 e Å^{-3}

Table 28. Crystal data and structure refinement for 20

Empirical formula	$C_{35}H_{54}N_2Si_4Zr_2$
Formula weight	797.60
Temperature	133(2) K
Wavelength	0.71073 Å
Crystal system	Monoclinic
Space group	$P2_1/m$
Unit cell dimensions	$a = 8.1380(16)$ Å
	$b = 15.444(3)$ Å $\quad \beta = 97.43(3)°$
	$c = 15.132(3)$ Å
Volume	1878.9(6) Å^3
Z	2
Density (calculated)	1.410 Mg/m^3
Absorption coefficient	0.708 mm^{-1}
F(000)	828
Crystal size	$0.4 \times 0.2 \times 0.1$ mm^3
θ range for data collection	2.64 – 26.00°
Index ranges	$-10 \leq h \leq 9, 0 \leq k \leq 19, 0 \leq l \leq 18$
Reflections collected	47659
Independent reflections	3839 [R(int) = 0.0516]
Refinement method	Full-matrix least-squares on F^2
Data / restraints / parameters	3839 / 412 / 256
Goodness-of-fit on F^2	1.222
Final R indices [$I>2\sigma(I)$]	$R1 = 0.0397, wR2 = 0.1022$
R indices (all data)	$R1 = 0.0455, wR2 = 0.1049$
Largest difference peak and hole	1.658 and -0.855 e Å^{-3}

Table 29. Crystal data and structure refinement for 21

Empirical formula	$C_{42}H_{75}N_6Si_6Ti$
Formula weight	880.52
Temperature	200(2) K
Wavelength	0.71073 Å
Crystal system	Triclinic
Space group	$P\bar{1}$
Unit cell dimensions	$a = 14.635(7)$ Å $\quad \alpha = 90.41(4)°$
	$b = 18.261(10)$ Å $\quad \beta = 97.43(3)°$
	$c = 19.417(8)$ Å $\quad \gamma = 90.78(5)°$
Volume	5145(4) Å^3
Z	4
Density (calculated)	1.137 Mg/m^3
Absorption coefficient	0.340 mm^{-1}
F(000)	1900
Crystal size	$1.0 \times 0.6 \times 0.6$ mm^3
θ range for data collection	$3.52 - 22.55°$
Index ranges	$-15 \leq h \leq 6, -19 \leq k \leq 19, 0 \leq l \leq 20$
Reflections collected	14439
Independent reflections	10162 [R(int) = 0.0395]
Refinement method	Full-matrix least-squares on F^2
Data / restraints / parameters	10145 / 0 / 1033
Goodness-of-fit on F^2	1.128
Final R indices [$I>2\sigma(I)$]	$R1 = 0.0676, wR2 = 0.1757$
R indices (all data)	$R1 = 0.0782, wR2 = 0.1886$
Largest difference peak and hole	0.657 and -0.342 e Å^{-3}

Table 30. Crystal data and structure refinement for 22

Empirical formula	$C_{18}H_{32}Cl_2N_2Si_2Ti_2$
Formula weight	499.34
Temperature	203(2) K
Wavelength	0.71073 Å
Crystal system	Tetragonal
Space group	$P\bar{4}2_1/c$
Unit cell dimensions	$a = b = 13.4571(15)$ Å
	$c = \quad 13.724(2)$ Å
Volume	2485.4(6) Å^3
Z	4
Density (calculated)	1.334 Mg/m^3
Absorption coefficient	0.960 mm^{-1}
F(000)	1040
Crystal size	$0.8 \times 0.4 \times 0.4$ mm^3
θ range for data collection	3.66 – 22.46°
Index ranges	$-14 \leq h \leq 14, -11 \leq k \leq 14, -12 \leq l \leq 14$
Reflections collected	3699
Independent reflections	1622 [R(int) = 0.0256]
Refinement method	Full-matrix least-squares on F^2
Data / restraints / parameters	1621 / 0 / 122
Goodness-of-fit on F^2	1.123
Final R indices [$I>2\sigma(I)$]	$R1 = 0.0304$, $wR2 = 0.0779$
R indices (all data)	$R1 = 0.0312$, $wR2 = 0.0804$
Largest difference peak and hole	0.529 and -0.251 e Å^{-3}

Table 31. Crystal data and structure refinement for 23

Empirical formula	$C_{21}H_{29}ClN_2SiZr$
Formula weight	464.22
Temperature	203(2) K
Wavelength	0.71073 Å
Crystal system	Monoclinic
Space group	$P2_1/c$
Unit cell dimensions	$a = 13.0530(13)$ Å
	$b = 17.627(3)$ Å $\beta = 109.425(12)°$
	$c = 10.477(2)$ Å
Volume	2273.3(7) Å^3
Z	4
Density (calculated)	1.356 Mg/m^3
Absorption coefficient	0.661 mm^{-1}
F(000)	960
Crystal size	$0.6 \times 0.5 \times 0.4$ mm^3
θ range for data collection	$3.51 - 22.52°$
Index ranges	$-10 \leq h \leq 14, -18 \leq k \leq 0, -11 \leq l \leq 11$
Reflections collected	2966
Independent reflections	2956 [R(int) = 0.0699]
Refinement method	Full-matrix least-squares on F^2
Data / restraints / parameters	2949 / 0 / 247
Goodness-of-fit on F^2	1.052
Final R indices [$I>2\sigma(I)$]	$R1 = 0.0305, wR2 = 0.0772$
R indices (all data)	$R1 = 0.0334, wR2 = 0.0820$
Largest difference peak and hole	0.692 and -0.372 e· Å^{-3}

Table 32. Crystal data and structure refinement for 24

Empirical formula	$C_{28}H_{42}Cl_4N_2O_4Zr_2$
Formula weight	794.88
Temperature	150(2) K
Wavelength	0.71073 Å
Crystal system	Monoclinic
Space group	*P2/c*
Unit cell dimensions	$a = 9.445(2)$ Å
	$b = 11.151(2)$ Å $\quad \beta = 91.17(3)°$
	$c = 15.720(3)$ Å
Volume	1655.2(6) Å^3
Z	2
Density (calculated)	1.595 Mg/m^3
Absorption coefficient	0.987 mm^{-1}
F(000)	808
Crystal size	$0.8 \times 0.7 \times 0.3$ mm^3
θ range for data collection	$3.65 - 25.02°$
Index ranges	$-11 \le h \le 11, -13 \le k \le 13, -18 \le l \le 18$
Reflections collected	5848
Independent reflections	2924 [R(int) = 0.0418]
Refinement method	Full-matrix least-squares on F^2
Data / restraints / parameters	2924 / 0 / 182
Goodness-of-fit on F^2	1.056
Final R indices [$I>2\sigma(I)$]	$R1 = 0.0319, wR2 = 0.0845$
R indices (all data)	$R1 = 0.0350, wR2 = 0.0876$
Largest difference peak and hole	0.550 and -0.632 e Å^{-3}

Table 33. Crystal data and structure refinement for 26

Empirical formula	$C_{32}H_{73}ClN_8P_4Zr$
Formula weight	820.53
Temperature	203(2) K
Wavelength	0.71073 Å
Crystal system	Monoclinic
Space group	$P2_1/n$
Unit cell dimensions	$a = 14.7679(16)$ Å
	$b = 19.227(3)$ Å $\quad \beta = 91.732(12)°$
	$c = 15.448(2)$ Å
Volume	4384.4(10) Å^3
Z	4
Density (calculated)	1.243 Mg/m^3
Absorption coefficient	0.489 mm^{-1}
F(000)	1752
Crystal size	$0.4 \times 0.4 \times 0.4$ mm^3
θ range for data collection	$3.63 - 25.02°$
Index ranges	$-17 \leq h \leq 17, 0 \leq k \leq 22, 0 \leq l \leq 18$
Reflections collected	7716
Independent reflections	7716 [R(int) = 0.0]
Refinement method	Full-matrix least-squares on F^2
Data / restraints / parameters	7716 / 0 / 439
Goodness-of-fit on F^2	1.076
Final R indices [$I>2\sigma(I)$]	$R1 = 0.0372, wR2 = 0.0792$
R indices (all data)	$R1 = 0.0495, wR2 = 0.0873$
Largest difference peak and hole	0.504 and -0.424 e Å^{-3}

Table 34. Crystal data and structure refinement for 27

Empirical formula	$C_{42.5}H_{85}KN_8P_4Zr$
Formula weight	962.39
Temperature	200(2) K
Wavelength	0.71073 Å
Crystal system	Triclinic
Space group	$P\bar{1}$
Unit cell dimensions	$a = 11.070(6)$ Å $\quad \alpha = 72.35(6)°$
	$b = 13.937(12)$ Å $\quad \beta = 85.56(5)°$
	$c = 18.628(15)$ Å $\quad \gamma = 82.79(6)°$
Volume	2715(3) Å^3
Z	2
Density (calculated)	1.177 Mg/m^3
Absorption coefficient	0.432 mm^{-1}
F(000)	1030
Crystal size	$1.2 \times 0.3 \times 0.2$ mm^3
θ range for data collection	3.53 – 25.00°
Index ranges	$-13 \leq h \leq 13, -16 \leq k \leq 16, -22 \leq l \leq 22$
Reflections collected	16403
Independent reflections	9538 [R(int) = 0.0511]
Refinement method	Full-matrix least-squares on F^2
Data / restraints / parameters	9538 / 624 / 546
Goodness-of-fit on F^2	1.061
Final R indices [$I > 2\sigma(I)$]	$R1 = 0.0453$, $wR2 = 0.1018$
R indices (all data)	$R1 = 0.0647$, $wR2 = 0.1135$
Largest difference peak and hole	0.661 and -0.568 e Å^{-3}

7. References

[1]   W. Weyl, *Pogg. Ann. Chem.* **1864**, *121*, 601.

[2]   C. A. Kraus, *J. Am. Chem. Soc.* **1908**, *30*, 1323.

[3]   J. L. Dye, *Prog. Inorg. Chem.* **1984**, *32*, 327.

[4]   a) K.-L. Tsai, J. L. Dye, *J. Am. Chem. Soc.* **1991**, *113*, 1650; b) A. J. Birch, H. Smith, *Rev. Chem.Soc.* **1991**, *113*, 1650; c) M. Fieser, *Reagents for Organic Synthesis*, Vol. 15, Willey, New York, **1990**; d) I. Schön, *Chem. Rev.* **1984**, *84*, 289.

[5]   E. Zintl, J. Goubeau, W. Dullenkopf, *Z. Phys. Chem.* **1931**, *154A*, 1.

[6]   G. W. Watt, J. L. Hall, G. R. Choppin, *J. Phys. Chem.* **1953**, *57*, 567.

[7]   G. W. Watt, W. C. Keenan, *J. Am. Chem. Soc.* **1949**, *71*, 3833.

[8]   G. W. Watt, G. R. Choppin, J. L. Hall, *J. Electrochem. Soc.* **1954**, *101*, 229.

[9]   G. W. Watt, P. J. Mayfield, *J. Am. Chem. Soc.* **1953**, *75*, 6178.

[10]   C. A. Kraus, H. F. Kurtz, *J. Am. Chem. Soc.* **1925**, *47*, 43.

[11]   G. W. Watt, D. D. Davies, *J. Am. Chem. Soc.* **1953**, *75*, 1760.

[12]   G. W. Watt, W. A. Jenkins, *J. Am. Chem. Soc.* **1951**, *73*, 3275.

[13]   a) C. M. Loane, *J. Phys. Chem.* **1933**, *37*, 615; b) W. M. Burgess, E. H. Smoker, *Chem. Rev.* **1931**, *31*, 265.

[14]   G. W. Watt, R. J. Thompson, *J. Inorg. Nucl. Chem.* **1947**, *9*, 311.

[15]   D. Nicholls, *J. Inorg. Nucl. Chem.* **1962**, *24*, 1001.

[16]   T. J. Swift, H. H. Lo, *J. Am. Chem. Soc.* **1967**, *89*, 3988.

[17]   W. L. Taylor, E. Griswold, J. Kleinberg, *J. Am. Chem. Soc.* **1955**, *77*, 294.

[18]   A. K. Holliday, G. Pass, *J. Chem. Soc.* **1958**, 3485.

[19]   G. W. Watt, L. J. Baye, *J. Inorg. Nucl. Chem.* **1964**, *26*, 2099.

[20]   K. H. Whitmire, *Adv. Organomet. Chem.* **1998**, *42*, 1.

[21]   K. A. Lawler, R. Hoffmann, M. M. Banaszak Holl, P. T. Wolczanski, *Z. Anorg. Allg. Chem.* **1996**, *622*, 392.

[22]   F. Bottomley, L. Sutin, *Adv. Organomet. Chem.* **1988**, *28*, 339.

[23]   S. Martinengo, G. Ciani, A. Sironi, B. T. Heaton, J. Mason, *J. Am. Chem. Soc.* **1979**, *101*, 7095.

[24]   W. L. Gladfelter, *Adv. Organomet. Chem.* **1985**, *24*, 41.

[25] T. S. Haddad, A. Aistars, J. W. Ziller, N. M. Doherty, *Organometallics* **1993**, *12*, 2420.

[26] D. B. Sable, W. H. Armstrong, *Inorg. Chem.* **1992**, *31*, 161.

[27] K. L. Sorensen, M. E. Lerchen, J. W. Ziller, N. M. Doherty, *Inorg. Chem.* **1992**, *31*, 2678.

[28] C. D. Abernethy, F. Bottomley, A. Decken, T. S. Cameron, *Organometallics* **1996**, *15*, 1758.

[29] N. M. Doherty, S. C. Critchlow, *J. Am. Chem. Soc.* **1987**, *109*, 7906.

[30] N. W. Hoffman, N. Prokopuk, M. J. Robbins, C. M. Jones, N. M. Doherty, *Inorg. Chem.* **1991**, *30*, 4177.

[31] S. C. Critchlow, M. E. Lerchen, R. C. Smith, N. M. Doherty, *J. Am. Chem. Soc.* **1988**, *110*, 8071.

[32] H. Plenio, H. W. Roesky, M. Noltemeyer, G. M. Sheldrick, *Angew. Chem.* **1988**, *100*, 1377; *Angew. Chem., Int. Ed. Engl.* **1988**, *27*, 1330.

[33] R. A. Wheeler, R. Hoffmann, J. Strähle, *J. Am. Chem. Soc.* **1986**, *108*, 5381.

[34] H. W. Roesky, M. Lücke, *J. Chem. Soc., Chem. Commun.* **1989**, 748.

[35] M. M. Banaszak Holl, M. Kersting, B. D. Pendley, P. T. Wolczanski, *Inorg. Chem.* **1990**, *29*, 1518.

[36] L. E. Toth, *Transition Metal Carbides and Nitrides*, Vol. 7, Academic Press, New York, **1971**.

[37] a) M. K. Wahlstrom, E. Johansson, E. Veszelei, P. Bennich, M. Olsson, S. Hogmark, *Thin Solid Films* **1992**, *220*, 315; b) M. Veszelei, E. Veszelei, *Thin Solid Films* **1993**, *236*, 46; c) M. Wittmer, H. Melchor, *Thin Solid Films* **1982**, *93*, 397; d) R. S. Nowicki, M. A. Nicolet, *Thin Solid Films* **1982**, *96*, 317; e) R. Fix, R. G. Gordon, D. M. Hoffman, *Chem. Mater.* **1991**, *3*, 1138; f) R. Fix, R. G. Gordon, D. M. Hoffman, *Chem. Mater.* **1993**, *5*, 614.

[38] a) L. H. Dubois, *Polyhedron* **1994**, *13*, 1329; b) R. Fix, R. G. Gordon, D. M. Hoffman, *J. Am. Chem. Soc.* **1990**, *112*, 7833.

[39] W. Schintlmeister, O. Pacher, K. Pfaffinger, *J. Electrochem. Soc.* **1976**, *123*, 924.

[40] S. R. Kurtz, G. R. Gordon, *Thin Solid Films* **1986**, *140*, 277.

[41] N. Yokoyama, K. Hinode, Y. Homma, *J. Electrochem. Soc.* **1991**, *138*, 190.

[42] B. H. Weiller, *J. Am. Chem. Soc.* **1996**, *118*, 4975.

[43] G. M. Brown, L. Maya, *J. Am. Ceram. Soc.* **1988**, *71*, 78.

[44] a) A. L. Robinson, *Science* **1986**, *233*, 25; b) G. W. Parshall, *Organometallics* **1987**, *6*, 867.

[45]   M. M. Banaszak Holl, P. T. Wolczanski, G. D. Van Duyne, *J. Am. Chem. Soc.* **1990**, *112*, 7989.

[46]   M. M. Banaszak Holl, P. T. Wolczanski, *J. Am. Chem. Soc.* **1992**, *114*, 3854.

[47]   a) P. J. Walsh, F. J. Hollander, R. G. Bergman, *J. Am. Chem. Soc.* **1988**, *110*, 8729; b) C. C. Cummins, S. M. Baxter, P. T. Wolczanski, *J. Am. Chem. Soc.* **1988**, *110*, 8731.

[48]   a) C. C. Cummins, C. P. Schaller, G. D. Van Duyne, P. T. Wolczanski, A. W. E. Chan, R. Hoffmann, *J. Am. Chem. Soc.* **1991**, *113*, 2985; b) J. L. Bennett, P. T. Wolczanski, *J. Am. Chem. Soc.* **1994**, *116*, 2179; c) S. Y. Lee, R. G. Bergman, *J. Am. Chem. Soc.* **1995**, *117*, 5877.

[49]   a) A. M. Baranger, P. J. Walsh, R. G. Bergman, *J. Am. Chem. Soc.* **1993**, *115*, 2753; b) P. J. Walsh, A. M. Baranger, R. G. Bergman, *J. Am. Chem. Soc.* **1992**, *114*, 1708.

[50]   C. C. Cummins, G. D. Van Duyne, C. P. Schaller, P. T. Wolczanski, *Organometallics* **1991**, *10*, 164.

[51]   a) J. L. Thorman, I. A. Guzei, V. G. Young, Jr., L. K. Woo, *Inorg. Chem.* **1999**, *38*, 3814; b) K. E. Meyer, P. J. Walsh, R. G. Bergman, *J. Am. Chem. Soc.* **1994**, *116*, 2669; c) P. L. McGrane, M. Jensen, T. Livinghouse, *J. Am. Chem. Soc.* **1992**, *114*, 5459; d) K. M. Doxsee, J. B. Farahi, H. Hope, *J. Am. Chem. Soc.* **1991**, *113*, 8889; e) R. L. Zuckerman, R. G. Bergman, *Organometallics* **2000**, *19*, 4795; f) A. Bashall, P. E. Collier, L. H. Gade, M. McPartlin, P. Mountford, S. M. Pugh, S. Radojevic, M. Schubart, I. J. Scowen, D. J. M. Trösch, *Organometallics* **2000**, *19*, 4784.

[52]   a) J. L. Thorman, I. A. Guzei, V. G. Young, Jr., L. K. Woo, *Inorg. Chem.* **2000**, *39*, 2344; b) P. J. Walsh, F. J. Hollander, R. G. Bergman, *Organometallics* **1993**, *12*, 3705; c) S. Y. Lee, R. G. Bergman, *J. Am. Chem. Soc.* **1996**, *118*, 6396.

[53]   a) P. L. Holland, R. A. Andersen, R. G. Bergman, *Organometallics* **1998**, *17*, 433; b) J. R. Fulton, T. A. Hanna, R. G. Bergman, *Organometallics* **2000**, *19*, 602; c) A. M. Baranger, F. J. Hollander, R. G. Bergman, *J. Am. Chem. Soc.* **1993**, *115*, 7890; d) A. M. Baranger, R. G. Bergman, *J. Am. Chem. Soc.* **1994**, *116*, 3822; e) T. A. Hanna, A. M. Baranger, R. G. Bergman, *Angew. Chem.* **1996**, *108,* 693; *Angew. Chem., Int. Ed. Engl.* **1996**, *35*, 653.

[54]   C. H. Winter, P. H. Sheridan, T. S. Lewkebandara, M. J. Heeg, J. W. Proscia, *J. Am. Chem. Soc.* **1992**, *114*, 1095.

[55] a) K. E. Meyer, P. J. Walsh, R. G. Bergman, *J. Am. Chem. Soc.* **1995**, *117*, 974; b) P. J. Stewart, A. J. Blake, P. Mountford, *Inorg. Chem.* **1997**, *36*, 3616; c) D. L. Thorn, W. A. Nugent, R. L. Harlow, *J. Am. Chem. Soc.* **1981**, *103*, 357; d) Y. E. Ovchinnikov, M. V. Ustinov, V. A. Igonin, Y. T. Struchkov, I. D. Kalikhman, M. G. Voronkov, *J. Organomet. Chem.* **1993**, *461*, 75; e) A. J. Blake, P. E. Collier, S. C. Dunn, W.-S. Li, P. Mountford, O. V. Shishkin, *J. Chem. Soc., Dalton Trans.* **1997**, 1549; f) N. W. Alcock, M. Pierce-Butler, G. R. Willey, *J. Chem. Soc., Dalton Trans.* **1976**, 707; g) R. D. Profilet, C. H. Zambrano, P. E. Fanwick, J. J. Nash, I. P. Rothwell, *Inorg. Chem.* **1990**, *29*, 4362; h) C. H. Zambrano, R. D. Profilet, J. E. Hill, P. E. Fanwick, I. P. Rothwell, *Polyhedron* **1993**, *12*, 689.

[56] W. A. Nugent, R. L. Harlow, *Inorg. Chem.* **1979**, *18*, 2030.

[57] W. J. Grigsby, M. M. Olmstead, P. P. Power, *J. Organomet. Chem.* **1996**, *513*, 173.

[58] D. J. Arney, M. A. Bruck, S. R. Huber, D. E. Wigley, *Inorg. Chem.* **1992**, *31*, 3749.

[59] A. J. Blake, P. Mountford, G. I. Nikonov, D. Swallow, *Chem. Commun.* **1996**, 1835.

[60] M. D. Fryzuk, J. B. Love, S. J. Rettig, *Organometallics* **1998**, *17*, 846.

[61] A. Abarca, P. Gómez-Sal, A. Martín, M. Mena, J. M. Poblet, C. Yélamos, *Inorg. Chem.* **2000**, *39*, 642.

[62] H. W. Roesky, H. Voelker, M. Witt, M. Noltemeyer, *Angew. Chem.* **1990**, *102*, 712; *Angew. Chem., Int. Ed. Engl.* **1990**, *29*, 669.

[63] M. Witt, D. Stalke, T. Henkel, H. W. Roesky, G. M. Sheldrick, *J. Chem. Soc., Dalton Trans.* **1991**, 663.

[64] H. W. Roesky, T. Raubold, M. Witt, R. Bohra, M. Noltemeyer, *Chem. Ber.* **1991**, *124*, 1521.

[65] Y. Bai, H. W. Roesky, H.-G. Schmidt, M. Noltemeyer, *Z. Naturforsch* **1992**, *47B*, 603.

[66] Y. Bai, M. Noltemeyer, H. W. Roesky, *Z. Naturforsch* **1991**, *46B*, 1357.

[67] F.-Q. Liu, A. Herzog, H. W. Roesky, I. Usón, *Inorg. Chem.* **1996**, *35*, 741.

[68] Y. Bai, H. W. Roesky, M. Noltemeyer, M. Witt, *Chem. Ber.* **1992**, *125*, 825.

[69] a) X. Yin, H. Han, A. Miyamoto, *Phys. Chem. Chem. Phys.* **2000**, *2*, 4243; b) J. L. Burton, R. L. Garten, *Advanced Materials in Catalysis*, Academic Press, New York, **1977**; c) K. Krohn, I. Vinke, H. Adam, *J. Org. Chem.* **1996**, *61*, 1467; d) H. Ogawa, H. Fujinami, K. Taya, S. Teratani, *J. Chem. Soc., Chem. Commun.* **1981**, 1274; e) S. F. Davison, B. E. Mann, P. M. Maitlis, *J. Chem. Soc., Dalton Trans.* **1984**, 1223.

[70]   a) V. W. Day, W. G. Klemperer, *Science* **1985**, *228*, 533; b) M. T. Pope, A. Müller, *Angew. Chem.* **1991**, *103*, 56; *Angew. Chem., Int. Ed. Engl.* **1991**, *30*, 34; c) F. Bottomley, *Polyhedron* **1992**, *11*, 1707; d) F. Bottomley, L. Sutin, *Adv. Organomet. Chem.* **1988**, *28*, 339.

[71]   a) S. A. Giddings, *Inorg. Chem.* **1964**, *3*, 684; b) J. F. Clarke, M. G. B. Drew, *Acta Crystallogr.* **1974**, *B30*, 2267; c) W. E. Hunter, D. C. Hrncir, R. Vann Bynum, R. A. Penttila, J. L. Atwood, *Organometallics* **1983**, *2*, 750; d) F. R. Fronczek, E. C. Baker, P. R. Sharp, K. N. Raymond, H. G. Alt, M. D. Rausch, *Inorg. Chem.* **1976**, *15*, 2284.

[72]   a) M. Björgvinsson, S. Halldorsson, I. Arnason, J. Magull, D. Fenske, *J. Organomet. Chem.* **1997**, *544*, 207; b) U. Thewalt, D. Schomburg, *J. Organomet. Chem.* **1977**, *127*, 169.

[73]   G. L. Hillhouse, J. E. Bercaw, *J. Am. Chem. Soc.* **1984**, *106*, 5472.

[74]   a) R. Andrés, M. Galakhov, M. P. Gómez-Sal, A. Martín, M. Mena, C. Santamaría, *J. Organomet. Chem.* **1996**, *526*, 135; b) A. Martín, M. Mena, C. Yélamos, R. Serrano, P. R. Raithby, *J. Organomet. Chem.* **1994**, *467*, 79; c) R. Andrés, M. V. Galakhov, A. Martín, M. Mena, C. Santamaría, *Organometallics* **1994**, *13*, 2159.

[75]   H.-P. Klein, U. Thewalt, K. Döppert, R. Sanchez-Delgado, *J. Organomet. Chem.* **1982**, *236*, 189.

[76]   L. M. Babcock, V. W. Day, W. G. Klemperer, *J. Chem. Soc., Chem. Commun.* **1988**, 519.

[77]   L. M. Babcock, V. W. Day, W. G. Klemperer, *Inorg. Chem.* **1989**, *28*, 806.

[78]   L. M. Babcock, V. W. Day, W. G. Klemperer, *J. Chem. Soc., Chem. Commun.* **1987**, 858.

[79]   a) F. Palacios, P. Royo, R. Serrano, J. L. Balcázar, I. Fonseca, F. Florencio, *J. Organomet. Chem.* **1989**, *375*, 51; b) A. C. Skapski, P. G. H. Troughton, *Acta Crystallosr.* **1970**, *B26*, 716.

[80]   A. Roth, C. Floriani, A. Chiesi-Villa, C. Guastini, *J. Am. Chem. Soc.* **1986**, *108*, 6823.

[81]   F. Bottomley, D. F. Drummond, G. O. Egharevba, P. S. White, *Organometallics* **1986**, *5*, 1620.

[82]   G. Fachinetti, C. Floriani, A. Chiesi-Villa, C. Guastini, *J. Am. Chem. Soc.* **1979**, *101*, 1767.

[83]   G. Kickelbick, U. Schubert, *Chem. Ber.* **1997**, *130*, 473.

[84]   G. Kickelbick, P. Wiede, U. Schubert, *Inorg. Chim. Acta* **1999**, *284*, 1.

[85]   G. Kickelbick, U. Schubert, *J. Chem. Soc., Dalton Trans.* **1999**, 1301.

[86] a) T. Aoyama, M. Kabeya, A. Fukushima, T. Shioiri, *Heterocycles* **1985**, *23*, 2363; b) T. Aoyama, M. Kabeya, A. Fukushima, T. Shioiri, *Heterocycles* **1985**, *23*, 2367; c) T. Aoyama, M. Kabeya, T. Shioiri, *Heterocycles* **1985**, *23*, 2371; d) K. H. Dötz, *Angew. Chem.* **1984**, *96*, 573; *Angew. Chem., Int. Ed. Engl.* **1984**, *23*, 587; e) W. A. Herrmann, *Angew. Chem.* **1978**, *90*, 855; *Angew. Chem., Int. Ed. Engl.* **1978**, *17*, 800.

[87] a) H. Siebald, M. Dartiguenave, Y. Dartiguenave, *J. Organomet. Chem.* **1992**, *438*, 83; b) M. J. Menu, P. Desrosiers, M. Dartiguenave, Y. Dartiguenave, G. Bertrand, *Organometallics* **1987**, *6*, 1822; c) S.-I. Murahashi, Y. Kitani, T. Hosokawa, *J. Chem. Soc., Chem. Commun.* **1979**, 450; d) S.-I. Murahashi, Y. Kitani, T. Uno, T. Hosokawa, K. Miki, T. Yonezawa, N. Kasai, *Organometallics* **1986**, *5*, 356; e) H. König, M. J. Menu, M. Dartiguenave, Y. Dartiguenave, H. F. Klein, *J. Am. Chem. Soc.* **1990**, *112*, 5351.

[88] a) W. A. Herrmann, *Adv. Organomet. Chem.* **1982**, *20*, 159; b) W. A. Herrmann, M. L. Ziegler, O. Serhadi, *Organometallics* **1983**, *2*, 958; c) M. A. Gallop, T. C. Jones, C. E. F. Rickard, W. R. Roper, *J. Chem. Soc., Chem. Commun.* **1984**, 1002.

[89] P. C. Wailes, R. S. P. Coutts, H. Weigold, *Organometallic Chemistry of Titanium, Zirconium, and Hafnium*, Academic Press, New York, **1974**.

[90] a) K. D. Schramm, J. A. Ibers, *Inorg. Chem.* **1980**, *19*, 2441; b) W. A. Herrmann, B. Menjón, E. Herdtweck, *Organometallics* **1991**, *10*, 2134; c) M. J. Menu, G. Crocco, M. Dartiguenave, Y. Dartiguenave, G. Bertrand, *J. Chem. Soc., Chem. Commun.* **1988**, 1598; d) M. J. Menu, G. Crocco, M. Dartiguenave, Y. Dartiguenave, *Organometallics* **1988**, *7*, 2231; e) K. D. Schramm, J. A. Ibers, *Inorg. Chem.* **1980**, *19*, 1231; f) R. Ben-Shoshan, J. Chatt, G. J. Leigh, W. Hussain, *J. Chem. Soc., Dalton Trans.* **1980**, 771; g) M. D. Curtis, L. Messerle, J. J. D'Errico, W. M. Butler, M. S. Hay, *Organometallics* **1986**, *5*, 2283; h) L. Messerle, M. D. Curtis, *J. Am. Chem. Soc.* **1982**, *104*, 889.

[91] a) L. Messerle, M. D. Curtis, *J. Am. Chem. Soc.* **1980**, *102*, 7789; b) G. M. Arvanitis, J. Schwartz, D. van Engen, *Organometallics* **1986**, *5*, 2157.

[92] G. Boche, J. C. W. Lohrenz, F. Schubert, *Tetrahedron* **1994**, *50*, 5889.

[93] G. Boche, K. Harms, M. Marsch, F. Schubert, *Chem. Ber.* **1994**, *127*, 2193.

[94] N. Feeder, M. A. Hendy, P. R. Raithby, R. Snaith, A. E. H. Wheatley, *Eur. J. Org. Chem.* **1998**, 861.

[95]   a) T. Kottarathil, G. Lepoutre, *J. Chim. Phys.* **1976**, *73*, 849; b) G. W. A. Fowles, D. Nicholls, *J. Chem. Soc.* **1959**, 990; c) A. Anagnostopoulos, D. Nicholls, *J. Inorg. Nucl. Chem.* **1965**, *27*, 339; d) G. W. A. Fowles, D. Nicholls, *J. Chem. Soc.* **1961**, 95; e) R. Juza, W. Klose, *Z. Anorg. Allg. Chem.* **1964**, *327*, 207; f) R. Juza, A. Rabenau, I. Nitschke, *Z. Anorg. Allg. Chem.* **1964**, *332*, 1; g) D. Nicholls, *J. Inorg. Nucl. Chem.* **1962**, *24*, 1001; h) G. W. A. Fowles, D. Nicholls, *J. Chem. Soc.* **1958**, 1687; i) G. W. A. Fowles, F. H. Pollard, *J. Chem. Soc.* **1952**, 4938; j) H. Moreau, C. Hamblett, *J. Am. Chem. Soc.* **1937**, *59*, 33; k) P. J. H. Carnell, G. W. A. Fowles, *J. Chem. Soc.* **1959**, 4113; l) G. W. A. Fowles, B. P. Osborne, *J. Chem. Soc.* **1959**, 2275.

[96]   C. H. Winter, T. S. Lewkebandara, J. W. Proscia, A. L. Rheingold, *Inorg. Chem.* **1994**, *33*, 1227.

[97]   T. Kottarathil, G. Lepoutre, *J. Chim. Phys.* **1976**, *73*, 849.

[98]   O. Ruff, O. Treidel, *Chem. Ber.* **1912**, *45*, 1364.

[99]   M. Allbutt, G. W. A. Fowles, *J. Inorg. Nucl. Chem.* **1963**, *25*, 67.

[100]   H. Blunk, R. Juza, *Z. Anorg. Allg. Chem.* **1974**, *406*, 145.

[101]   P. W. Schenk, K. Huste, E. Tulhoff, *Angew. Chem.* **1963**, *75*, 683.

[102]   R. Lavine, W. C. Fernelius, *Chem. Rev.* **1954**, *54*, 452.

[103]   F. W. Bergstrom, *J. Am. Chem. Soc.* **1925**, *47*, 2317.

[104]   H. W. Roesky, Y. Bai, M. Noltemeyer, *Angew. Chem.* **1989**, *101*, 788; *Angew. Chem., Int. Ed. Engl.* **1989**, *28*, 754.

[105]   Ammonia was passed through a solution of Cp*TiMe$_3$ in THF at -30 °C resulting in the formation of [Cp*TiMe(μ-NH)]$_2$.

[106]   G. Bai, P. Müller, H. W. Roesky, I. Usón, *Organometallics* **2000**, *19*, 4675.

[107]   G. Bai, H. W. Roesky, P. Müller, *Bull. Pol. Acad. Sc. Chem.*, in the press.

[108]   J. C. Huffman, J. G. Stone, W. C. Krusell, K. G. Caulton, *J. Am. Chem. Soc.* **1977**, *99*, 5829.

[109]   F. Bottomley, G. O. Egharevba, P. S. White, *J. Am. Chem. Soc.* **1985**, *107*, 4353.

[110]   D. E. Gindelberger, *Acta Crystallogr.* **1996**, *C52*, 2493.

[111]   a) M. D. Fryzuk, T. S. Haddad, M. Mylvaganam, D. H. McConville, S. J. Rettig, *J. Am. Chem. Soc.* **1993**, *115*, 2782; b) J. D. Cohen, M. D. Fryzuk, T. M. Lochr, M. Mylvaganam, S. J. Rettig, *Inorg. Chem.* **1998**, *37*, 112.

[112] P. Jutzi, W. Leffer, B. Hampel, S. Pohl, W. Saak, *Angew. Chem.* **1987**, *99*, 563; *Angew. Chem., Int. Ed. Engl.* **1987**, *26*, 583.

[113] G. Bai, H. W. Roesky, H.-G. Schmidt, M. Noltemeyer, *Organometallics* **2001**, *20*, 2962.

[114] D. Nicholls, *Inorganic Chemistry in Liquid Ammonia*, Monograph 17, New York, **1979**, 7.

[115] G. L. Hillhouse, J. E. Bercaw, *J. Am. Chem. Soc.* **1984**, *106*, 5472.

[116] L. Grocholl, V. Huch, L. Stahl, R. J. Staples, P. Steinhart, A. Johnson, *Inorg. Chem.* **1997**, *36*, 4451.

[117] L. Grocholl, I. Schranz, L. Stahl, R. J. Staples, *Inorg. Chem.* **1998**, *37*, 2496.

[118] G. I. Nikonov, A. J. Blake, P. Mountford, *Inorg. Chem.* **1997**, *36*, 1107.

[119] P. Gómez-Sal, A. Martín, M. Mena, C. Yélamos, *J. Chem. Soc., Chem. Commun.* **1995**, 2185.

[120] G. Bai, H. W. Roesky, M. Noltemeyer, H. Hao, H.-G. Schmidt, *Organometallics* **2000**, *19*, 2823.

[121] P. G. Eller, D. C. Bradley, M. B. Hursthouse, D. W. Meek, *Coord. Chem. Rev.* **1977**, *24*, 1.

[122] F. Cimpoesu, H. W. Roesky, G. Bai, N. C. Mösch-Zanetti, M. Ferbinteanu, *Challenges for Coordination Chemistry in the New Century*, edited by M. Melnik, A. Sirota, Slovak Technical University Press, Bratislava, **2001**, 127.

[123] E. Brady, J. R. Telford, G. Mitchell, W. Lukens, *Acta Crystallogr.* **1995**, *C51*, 558.

[124] a) S. Gambarotta, *J. Organomet. Chem.* **1995**, *500*, 117; b) M. Hidai, Y. Mizobe, *Chem. Rev.* **1995**, *95*, 1115; c) J. Chatt, J. R. Dilworth, R. L. Richards, *Chem. Rev.* **1978**, *78*, 589.

[125] A. D. Allen, C. V. Senoff, *J. Chem. Soc., Chem. Commun.* **1965**, 621.

[126] R. D. Sanner, J. M. Manriquez, R. E. Marsh, J. E. Bercaw, *J. Am. Chem. Soc.* **1976**, *98*, 8352.

[127] Y. Mizobe, Y. Yokoayashi, H. Oshita, T. Takahashi, M. Hidai, *Organometallics* **1994**, *13*, 3764.

[128] J. D. Cohen, M. Mylvaganam, M. D. Fryzuk, T. M. Loehr, *J. Am. Chem. Soc.* **1994**, *116*, 9529.

[129] R. Duchateau, S. Gambarotta, N. Beydoun, C. Bensimon, *J. Am. Chem. Soc.* **1991**, *113*, 8986.

[130] M. D. Fryzuk, J. B. Love, S. J. Rettig, V. G. Young, *Science* **1997**, *275*, 1445.

[131] G. P. Pez, P. Apgar, R. K. Crissey, *J. Am. Chem. Soc.* **1982**, *104*, 482.

[132] J. Jeffery, M. F. Lappert, P. I. Riley, *J. Organomet. Chem.* **1979**, *181*, 25.

[133] R. Ferguson, E. Solari, C. Floriani, A. Chiesi-Villa, C. Rizzoli, *Angew. Chem.* **1993**, *105*, 453; *Angew. Chem., Int. Ed. Engl.* **1993**, *32*, 396.

[134] K. Jonas, D. J. Brauer, C. Krüger, P. J. Roberts, Y.-H. Tsay, *J. Am. Chem. Soc.* **1976**, *98*, 76.

[135] J. Jubb, S. Gambarotta, *J. Am. Chem. Soc.* **1994**, *116*, 4477.

[136] J. R. Hagadorn, J. Arnold, *Organometallics* **1998**, *17*, 1355.

[137] J. R. Hagadorn, J. Arnold, *J. Am. Chem. Soc.* **1996**, *118*, 893.

[138] R. D. Sanner, D. M. Duggan, T. C. McKenzie, R. E. Marsh, J. E. Bercaw, *J. Am. Chem. Soc.* **1976**, *98*, 8358.

[139] K. F. Tesh, T. P. Hanusa, J. C. Huffman, *Inorg. Chem.* **1990**, *29*, 1584.

[140] a) M. Anpo, T. Nomura, *Res. Chem. Intermed.* **1990**, *13*, 195; b) S. C. Tseng, N. B. Jackson, J. G. Ekerdt, *J. Catal.* **1988**, *109*, 284; c) N. B. Jackson, J. G. Ekerdt, *J. Catal.* **1986**, *101*, 90; d) M.-Y. He, J. G. Ekerdt, *J. Catal.* **1984**, *87*, 238; e) M.-Y. He, J. G. Ekerdt, *J. Catal.* **1984**, *87*, 381; f) M.-Y. He, J. G. Ekerdt, *J. Catal.* **1984**, *90*, 17; g) H. Abe, K.-I. Maruya, K. Domen, T. Onishi, *Chem. Lett.* **1984**, 1875; h) Z. Feng, W. S. Postula, C. Erkey, C. V. Philip, A. Akgerman, R. G. Anthony, *J. Catal.* **1994**, *148*, 84; i) T. Maehashi, K.-I. Maruya, K. Domen, K.-I. Aika, T. Onishi, *Chem. Lett.* **1984**, 747.

[141] a) J. Kondo, K. Domen, T. Onishi, *Res. Chem. Intermed.* **1993**, *19*, 521; b) S.-C. Moon, K. Tsuji, T. Nomura, M. Anpo, *Chem. Lett.* **1994**, 2241.

[142] a) T. Yamaguchi, H. Sasaki, K. Tanabe, *Chem. Lett.* **1973**, 1017; b) S.-C. Moon, M. Fujino, H. Yamashita, M. Anpo, *J. Phys. Chem. B* **1997**, *101*, 369; c) A. Satoh, H. Hattori, K. Tanabe, *Chem. Lett.* **1983**, 497.

[143] K. Kaneda, Y. Kawanishi, S. Teranishi, *Chem. Lett.* **1984**, 1481.

[144] A. W. Henderson, K. B. Higbie, *J. Am. Chem. Soc.* **1954**, *76*, 5878.

[145] G. Bai, H. W. Roesky, P. Lobinger, M. Noltemeyer, H.-G. Schmidt, *Angew. Chem.* **2001**, *113*, 2214; *Angew. Chem., Int. Ed. Engl.* **2001**, *40*, 2156.

[146] a) G. W. A. Fowles, F. H. Pollard, *J. Chem. Soc.* **1953**, 4128; b) G. W. A. Fowles, F. H. Pollard, *J. Chem. Soc.* **1953**, 2588.

[147] U. Thewalt, K. Döppert, W. Lasser, *J. Organomet. Chem.* **1986**, *308*, 303.

[148] R. P. Ziebarth, J. D. Corbett, *J. Am. Chem. Soc.* **1987**, *109*, 4844.

[149] J. D. Smith, J. D. Corbett, *J. Am. Chem. Soc.* **1985**, *107*, 5704.

[150] H. Imoto, J. D. Corbett, A. Cisar, *Inorg. Chem.* **1981**, *20*, 145.

[151] R. P. Ziebarth, J. D. Corbett, *J. Solid State Chem.* **1989**, *80*, 56.

[152] D. K. Smith, H. W. Newkirk, *Acta Crystallogr.* **1965**, *18*, 983.

[153] a) M. Pohl, D. K. Lyon, N. Mizuno, K. Nomiya, R. G. Finke, *Inorg. Chem.* **1995**, *34*, 1413 and references therein; b) V. W. Day, C. W. Earley, W. G. Klemperer, D. J. Maltbie, *J. Am. Chem. Soc.* **1985**, *107*, 8261.

[154] G. Bai, H. W. Roesky, F. Cimpoesu, J. Magull, T. Labahn, Q. Ma, *Angew. Chem.*, submitted for publication.

[155] a) The RHF (Restricted Hartree-Fock) and B3LYP-DFT (Density Functional Theory) calculations were performed with 3-21G basis sets using the GAMESS package: M. W. Schmidt, K. K. Baldridge, J. A. Boatz, S. T. Elbert, M. S. Gordon, J. H. Jensen, S. Koseki, N. Matsunaga, K. A. Nguyen, S. J. Su, T. L. Windus, M. Dupuis, J. A. Montgomery, *J. Comput. Chem.* **1993**, *14*, 1347; b) For sake of simplicity, the terminal ligands were taken as Cp.

[156] W. J. A. Maaskant, I. B. Bersuker, *J. Phys. Condens. Mat.* **1991**, *3*, 37.

[157] a) I. B. Bersuker, *Ferroelectrics* **198**9, *95*, 51; b) I. B. Bersuker, *Chem. Rev.* **2001,** *101,* 1067.

[158] a) J. S. O. Evans, T. A. Mary, T. Vogt, M. A. Subramanian, A. W. Sleight, *Chem. Mater.* **1996**, *8*, 2809; b) J. S. O. Evans, *J. Chem. Soc., Dalton Tran*s. **1999**, 3317; c) G. Ernst, C. Broholm, G. R. Kowach, A. P. Ramirez, *Nature* **1998**, *396*, 147.

[159] C. D. Abernethy, F. Bottomley, R. W. Day, A. Decken, D. A. Summers, R. C. Thompson, *Organometallics* **1999**, *18*, 870.

[160] F. Bottomley, J. Darkwa, L. Sutin, P. S. White, *Organometallics* **1986**, *5*, 2165.

[161] S. Yamada, C. Katayama, J. Tanaka, M. Tanaka, *Inorg. Chem.* **1984**, *23*, 253.

[162] K. Kato, E. Takayama-Muromachi, *Acta Crystallogr.* **1985**, *C41*, 647.

[163] A. Giacomelli, C. Floriani, A. O. D. S. Duarte, A. Chiesi-Villa, C. Guastini, *Inorg. Chem.* **1982**, *21*, 3310.

[164] F. A. Cotton, L. Kruczynski, B. A. Frenz, *J. Organomet. Chem.* **1978**, *160*, 93.

[165] T. Greiser, E. Weiss, *Chem. Ber.* **1977**, *110*, 3388.

[166]   a) S. Couturier, G. Tainturier, B. Gautheron, *J. Organomet. Chem.* **1980**, *195*, 291; b) R. Choukroun, M. Basso-Bert, D. Gervais, *J. Chem. Soc., Chem. Commun.* **1986**, 1317; c) A.-M. Larsonneur, R. Choukroun, *Organometallics* **1993**, *12*, 3216; d) A. G. Carr, D. M. Dawson, M. Thornton-Pett, M. Bochmann, *Organometallics* **1999**, *18*, 2933; e) J. Corker, F. Lefebvre, C. Lécuyer, V. Dufaud, F. Quignard, A. Choplin, J. Evans, J.-M. Basset, *Science* **1996**, *271*, 966.

[167]   a) A. Maraval, B. Donnadieu, A. Igau, J.-P. Majoral, *Organometallics* **1999**, *18*, 3138; b) G. Erker, R. Schlund, C. Krüger, *Organometallics* **1989**, *8*, 2349; (c) S. B. Jones, J. L. Petersen, *Organometallics* **1985**, *4*, 966; d) E.-I. Negishi, J. A. Miller, T. Yoshida, *Tetrahedron Lett.* **1984**, *25*, 3407; e) D. B. Carr, J. Schwartz, *J. Am. Chem. Soc.* **1979**, *101*, 3521; f) D. W. Hart, T. F. Blackburn, J. Schwartz, *J. Am. Chem. Soc.* **1975**, *97*, 679.

[168]   a) J. M. Manriquez, D. R. McAlister, R. D. Sanner, J. E. Bercaw, *J. Am. Chem. Soc.* **1976**, *98*, 6733; b) J. M. Manriquez, D. R. McAlister, R. D. Sanner, J. E. Bercaw, *J. Am. Chem. Soc.* **1978**, *100*, 2716; c) P. T. Wolczanski, J. E. Bercaw, *Acc. Chem. Res.* **1980**, *13*, 121.

[169]   a) P. C. Wailes, H. Weigold, *J. Organomet. Chem.* **1970**, *24*, 405; b) P. T. Wolczanski, J. E. Bercaw, *Organometallics* **1982**, *1*, 793; c) W. K. Kot, N. M. Edelstein, A. Zalkin, *Inorg. Chem.* **1987**, *26*, 1339; d) T. Cuenca, M. Galakhov, E. Royo, P. Royo, *J. Organomet. Chem.* **1996**, *515*, 33; e) R. B. Grossman, R. A. Doyle, S. L. Buchwald, *Organometallics* **1991**, *10*, 1501; f) X. Liu, Z. Wu, Z. Peng, Y.-D. Wu, Z. Xue, *J. Am. Chem. Soc.* **1999**, *121*, 5350; g) S. B. Jones, J. L. Petersen, *Inorg. Chem.* **1981**, *20*, 2889; h) R. Choukroun, F. Dahan, A.-M. Larsonneur, E. Samuel, J. Petersen, P. Meunier, C. Sornay, *Organometallics* **1991**, *10*, 374.

[170]   a) P. J. Chirik, M. W. Day, J. E. Bercaw, *Organometallics* **1999**, *18*, 1873; b) H. Lee, P. J. Desrosiers, I. Guzei, A. L. Rheingold, G. Parkin, *J. Am. Chem. Soc.* **1998**, *120*, 3255; c) C. J. Curtis, R. C. Haltiwanger, *Organometallics* **1991**, *10*, 3220; d) L. E. Schock, T. J. Marks, *J. Am. Chem. Soc.* **1988**, *110*, 7701; e) J. E. Bercaw, *Adv. Chem. Ser.* **1978**, *167*, 136.

[171]   G. P. Pez, C. F. Putnik, S. L. Suib, G. D. Stucky, *J. Am. Chem. Soc.* **1979**, *101*, 6933.

[172]   O. W. Lofthus, C. Slebodnick, P. A. Deck, *Organometallics* **1999**, *18*, 3702.

[173]   a) L. Labella, A. Chernega, M. L. H. Green, *J. Organomet. Chem.* **1995**, *485*, C18; b) A. Chernega, J. Cook, M. L. H. Green, L. Labella, S. J. Simpson, J. Souter, A. H. H. Stephens, *J. Chem. Soc., Dalton Trans.* **1997**, 3225.

[174] F. Liu, H. Gornitzka, D. Stalke, H. W. Roesky, *Angew. Chem.* **1993**, *105*, 447; *Angew. Chem., Int. Ed. Engl.* **1993**, *32*, 442.

[175] C. Ribbing, K. Pierloot, A. Ceulemans, *Inorg. Chem.* **1998**, *37*, 5227.

[176] Computed with GAMESS and 6-311G*set (M. W. Schmidt, K. K. Baldridge, J. A. Boatz, S. T. Elbert, M. S. Gordon, J. H. Jensen, S. Koseki, N. Matsunaga, K. A. Nguyen, S. J. Su, T. L. Windus, *J.Comput.Chem.* **1993**, *14*, 1347).

[177] G. Bai, H. W. Roesky, H. Hao, M. Noltemeyer, H.-G. Schmidt, *Inorg. Chem.* **2001**, *40*, 2424.

[178] J. L. Polse, R. A. Andersen, R. G. Bergman, *J. Am. Chem. Soc.* **1996**, *118*, 8737.

[179] S. Gambarotta, C. Floriani, A. Chiesi-Villa, C. Guastini, *J. Am. Chem. Soc.* **1982**, *104*, 1918.

[180] S. Gambarotta, C. Floriani, A. Chiesi-Villa, C. Guastini, *Inorg. Chem.* **1983**, *22*, 2029.

[181] P. J. Walsh, F. J. Hollander, R. G. Bergman, *J. Am. Chem. Soc.* **1990**, *112*, 894.

[182] C. H. Chang, R. F. Porter, S. H. Bauer, *J. Am. Chem. Soc.* **1970**, *92*, 5313.

[183] K. Burgess, B. F. G. Johnson, J. Lewis, P. R. Raithby, *J. Chem. Soc., Dalton Trans.* **1982**, 263.

[184] G. Bai, H. W. Roesky, M. Noltemeyer, H.-G. Schmidt, *Eur. J. Inorg. Chem.*, in preparation.

[185] K. Prout, T. S. Cameron, R. A. Forder, S. R. Critchley, B. Denton, G. V. Rees, *Acta Crystallogr.* **1974**, *B30*, 2290.

[186] R. A. Howie, G. P. McQuillan, D. W. Thompson, G. A. Lock, *J. Organomet. Chem.* **1986**, *303*, 213.

[187] F. A. Cotton, G. Wilkinson, *Advanced Inorganic Chemistry*, 5th ed., Wiley, New York, **1988**.

[188] G. Bai, H. W. Roesky, M. Noltemeyer, H.-G. Schmidt, *J. Chem. Soc., Dalton Trans*, submitted for publication.

[189] G. Bai, H. W. Roesky, M. Noltemeyer, H.-G. Schmidt, *Organometallics*, in the press.

[190] A. Brown, S. Rundquist, *Acta. Crystallogr.* **1965**, *19*, 684.

[191] R. B. King, *Encyclopedia of Inorganic Chemistry*, John Wiley & Sons ltd., West Sussex, **1994**, 3115.

[192] S. Chitsaz, B. Neumüller, K. Dehnicke, *Z. Anorg. Allg. Chem.* **1999**, *625*, 6.

[193] G. R. Fuentes, P. S. Coan, W. E. Streib, K. G. Caulton, *Polyhydron* **1991**, *10*, 2371.

[194] P. B. Hitchcock, M. F. Lappert, A. V. Protchenko, *J. Am. Chem. Soc.* **2001**, *123*, 189.

[195] P. B. Hitchcock, M. F. Lappert, G. A. Lawless, B. Royo, *J. Chem. Soc., Chem. Commun.* **1993**, 554.

[196] C. J. Schaverien, J. B. van Mechelen, *Organometallics* **1991**, *10*, 1704.

[197] J. Sunner, K. Nishizawa, P. Kebarle, *J. Phys. Chem.* **1981**, *85*, 1814.

[198] W. Clegg, S. Kleditzsch, R. E. Mulvey, P. O'Shaughnessy, *J. Organomet. Chem.* **1998**, *558*, 193.

[199] S. S. Al-Juaid, C. Eaborn, S. El-Hamruni, A. Farook, P. B. Hitchcock, M. Hopman, J. D. Smith, W. Clegg, K. Izod, P. O'Shaughnessy, *J. Chem. Soc.*, *Dalton Trans.* **1999**, 3267.

[200] D. D. Perrin, W. L. F. Armarego, *Purification of Laboratory Chemicals*, 3th ed., Pergamon, London, **1988.**

[201] T. Kottke, D. Stalke, *J. Appl. Crystallogr.* **1993,** *26*, 615.

[202] W. Clegg, *Acta Crystallogr.* **1981**, *A37*, 22.

[203] G. M. Sheldrick, *Acta Crystallogr.* **1990**, *A46*, 467.

[204] G. M. Sheldrick, SHELX-93/96/97, *Program for Crystal Structure Refinement*, Göttingen, **1993/1996/1997**.

[205] G. M. Sheldrick, SHELX 97, Universität Göttingen, **1997**.

[206] I. Schranz, L. Stahl, R. J. Staples, *Inorg. Chem.* **1998**, *37*, 1493.

[207] M. F. Lappert, C. J. Pickett, P. I. Riley, P. I. W. Yarrow, *J. Chem. Soc., Dalton. Trans.* **1991**, 805.

[208] C. H. Winter, X. X. Zhou, D. A. Dobbs, M. J. Heeg, *Organometallics* **1991**, *10*, 210.

[209] J. Blenkers, B. Hessen, F. van Bolhuis, A. J. Wagner, J. H. Teuben, *Organometallics* **1987**, *6*, 459.

[210] B. Kautzner, P. C. Wailes, H. Weigold, *J. Chem. Soc., Chem. Commun.* **1969**, 1105.

[211] S. Ciruelos, T. Cuenca, P. Gómez-Sal, A. Manzanero, P. Royo, *Organometallics* **1995**, *14*, 177.

[212] J. W. Pattiasina, H. J. Heeres, F. van Bolhuis, A. Meetsma, J. H. Teuben, A. L. Spek, *Organometallics* **1987**, *6*, 459.

[213] B. Hübler-Blank, M. Witt, H. W. Roesky, *J. Chem. Educ.* **1993**, *70*, 408.

CURRICULUM VITAE

Personal Information

Name, first name	Bai, Guangcai
Data of Birth	30. 05. 1962
Place of Birth	Guangdong, P. R. China
Sex	Male
Parents	Yueen Bai (Father)
	Guilan Zhao (Mother)
Marital Status	Married, one son
Nationality	P. R. China

Education

09. 1970 – 07. 1976	Primary School, Jinzhou, Liaoning, P. R. China
09. 1976 – 07. 1981	Middle and High School, Jinzhou, Liaoning, P. R. China
09. 1981 – 07. 1985	**B. A. Student** (majored in organic chemistry), Nankai University, Tianjin, P. R. China
09. 1985 – 07. 1988	**M. Sc. Student** (majored in organic chemistry), Nankai University, Tianjin, P. R. China
01. 1997 – 04. 2001	**Ph. D. Student**, Institute für Anorganische Chemie der Georg-August Universität, Göttingen, Germany

Research and working experence

09. 1984 – 07. 1985	Synthesis of organometallic compounds and hydrozirconation of C=O and N=N containing organic compounds
09. 1985 – 07. 1988	Synthesis of organometallic compounds and organic epoxides, hydrozirconation of epoxides and their applications in organic synthesis
08. 1988 – 1990	**Assistant Engineer** in chemical engineering. Research on the formulations and manufacture of powder coatings in the Research Institute of Engineering Technology of China National Petroleum and Natural Gas Corporation

1991 – 1996	**Engineer** in chemical engineering. Research on the new polymers, curing agents and catalysts of powder coatings for the pipelines of oil fields and the auto parts as well as the manufacture of the new powder coatings as leader of a research group, being responsible for the research and development of the Anti-Corrosion and Insulation Department as vice-director in the Research Institute of Engineering Technology of China National Petroleum and Natural Gas Corporation
1997 – 2001	**Research Associate** in the new methods for the synthesis of amido, imido, nitrido and dinitrogen metallic compounds and organometallic hydrides and oxides and their applications as catalysts in the Institute für Anorganische Chemie der Georg-August Universität, Göttingen, Germany